Spectroscopic studies of the internal modes of amino-aromatics by fluorescence excitation and dispersed emission in supersonic jet
by Shuxin Yan

A thesis submitted in partial fulfillment of the requirements for the degree of Doctor of Philosophy in Chemistry
Montana State University

Abstract:
A systematic study for the NH2 inversional mode in aniline and para substituted anilines has been performed using the techniques of the fluorescence excitation and dispersed emission in supersonic jet. The transitions of the nitrogen inversion mode in aniline and para substituted anilines have been assigned in both the fluorescence excitation and dispersed emission spectra, which are strongly supported by the evidence of a large deuterium shift, the presence of a strong hot band, and the intense second overtone transition of the amino inversion in the excitation spectra of all the aniline molecules. The potential surface of each aniline has been fit using the observed inversional levels in both the ground and excited states. The molecular structure of each aniline has been investigated based on the experimental results.

The NH2 torsional transition is assigned in the excitation spectrum of each aniline molecule for the first time. The absence of a torsional hot band and no observable tunneling splitting in the NH2 torsional mode indicates that the NH2 torsion mode in the anilines must have a very high first quanta in the ground state.

The mechanism of I20 and T20 splittings in the excitation spectrum of p-toluidine has been explained by using molecular symmetry. The splittings are caused by the torsion - torsion coupling between the NH2 and CH3 groups.

The structure of p-amino-p'-methyl-trans-stilbene (PPTS) has been studied by spectroscopic methods and X-ray diffraction. The nearly planar geometry of the proton donor in the PPTS crystal dimer provides important evidence that the structure of gas phase PPTS is planar in the ground state. The absence of the hot band and I20 in the excitation spectrum of PPTS indicates that the potential surface of PPTS must be a single well in both states, which is consistent with the X-ray result. The methyl torsional transition frequencies are significantly reduced by the para substitution of the NH2 group in PPTS (as compared to p-methyl-trans-stilbene) which is attributed to the electron donating nature of the NH2 group and the lone pair in the amino group involved in the π-cloud of PPTS changing the methyl hyperconjugation with the πsystem.

SPECTROSCOPIC STUDIES OF THE INTERNAL MODES OF AMINO-AROMATICS BY FLUORESCENCE EXCITATION AND DISPERSED EMISSION IN SUPERSONIC JET

by

Shuxin Yan

A thesis submitted in partial fulfillment
of the requirements for the degree

of

Doctor of Philosophy

in

Chemistry

MONTANA STATE UNIVERSITY
Bozeman, Montana
November 1992

APPROVAL

of a thesis submitted by

Shuxin Yan

This thesis has been read by each member of the thesis committee and has been found to be satisfactory regarding content, English usage, format, citations, bibliographic style, and consistency, and is ready for submission to the College of Graduate Studies.

12/7/92
Date

Lee F Spangler
Chairperson, Graduate Committee

Approved for the Major Department

12/7/92
Date

John R Causard
Head, Major Department

Approved for the College of Graduate Studies

12/15/92
Date

R L Brown
Graduate Dean

STATEMENT OF PERMISSION TO USE

In presenting this thesis in partial fulfillment of the requirements for a doctoral degree at Montana State University, I agree that the Library shall make it available to borrowers under rules of the Library. I further agree that copying of this thesis is allowable only for scholarly purposes, consistent with "fair use" as prescribed in the U.S. Copyright Law. Requests for extensive copying or reproduction of this thesis should be referred to University Microfilms International, 300 North Zeeb Road, Ann Arbor, Michigan 48106, to whom I have granted "the exclusive right to reproduce and distribute copies of the dissertation in and from microfilm and the right to reproduce and distribute by abstract in any format."

Signature Zhuxin Yan

Date 12/10/92

ACKNOWLEDGMENTS

I wish to faithfully thank Professor Lee Spangler for his guidance and instruction in my graduate education. I would like to thank Matthew Rees for his help in my organic synthesis. I also appreciate Ray Larsen for the X-ray experiment in PPTS.

TABLE OF CONTENTS

TABLE OF CONTENTS (Continued)

LIST OF TABLES

LIST OF FIGURES

LIST OF FIGURES (continued)

LIST OF FIGURES (continued)

ABSTRACT

A systematic study for the NH_2 inversional mode in aniline and para substituted anilines has been performed using the techniques of the fluorescence excitation and dispersed emission in supersonic jet. The transitions of the nitrogen inversion mode in aniline and para substituted anilines have been assigned in both the fluorescence excitation and dispersed emission spectra, which are strongly supported by the evidence of a large deuterium shift, the presence of a strong hot band, and the intense second overtone transition of the amino inversion in the excitation spectra of all the aniline molecules. The potential surface of each aniline has been fit using the observed inversional levels in both the ground and excited states. The molecular structure of each aniline has been investigated based on the experimental results.

The NH_2 torsional transition is assigned in the excitation spectrum of each aniline molecule for the first time. The absence of a torsional hot band and no observable tunneling splitting in the NH_2 torsional mode indicates that the NH_2 torsion mode in the anilines must have a very high first quanta in the ground state.

The mechanism of I^2_0 and T^2_0 splittings in the excitation spectrum of p-toluidine has been explained by using molecular symmetry. The splittings are caused by the torsion - torsion coupling between the NH_2 and CH_3 groups.

The structure of p-amino-p′-methyl-trans-stilbene (PPTS) has been studied by spectroscopic methods and X-ray diffraction. The nearly planar geometry of the proton donor in the PPTS crystal dimer provides important evidence that the structure of gas phase PPTS is planar in the ground state. The absence of the hot band and I^2_0 in the excitation spectrum of PPTS indicates that the potential surface of PPTS must be a single well in both states, which is consistent with the X-ray result. The methyl torsional transition frequencies are significantly reduced by the para substitution of the NH_2 group in PPTS (as compared to p-methyl-trans-stilbene) which is attributed to the electron donating nature of the NH_2 group and the lone pair in the amino group involved in the π-cloud of PPTS changing the methyl hyperconjugation with the π system.

INTRODUCTION

Internal modes in molecules have intrinsic interest for chemists due to several special features compared to skeletal modes. First of all, internal modes do not conform to the harmonic approximation. The anharmonicities can make the spectral analysis more difficult. Also most internal modes are nonrigid vibrations for which the point group will not work properly. The correct symmetry description for nonrigid molecules is molecular symmetry groups which is constructed from nuclear permutations which reflect the motions of the nonrigid modes[1-3] Additionally, the potential surfaces of many internal modes have multiple minima and tunneling often occurs between the wells which causes vibrational level splitting. Lastly, internal modes usually are large amplitude motions which are easily perturbed by other substituents. In the multiply substituted aromatics, the interaction between the groups can be easily achieved through the conjugated π system even with significant separation.

Aniline and para substituted anilines, such as p-methyl-aniline and p-fluoroaniline, have been studied for many years,[4-24] Brand et al assigned the transitions of aniline and deuterated aniline in the room temperature gas phase spectrum, however, the large rotational broadening and congestion from

hot bands prevented them from discerning close lying transitions, such as the three peaks around 550 cm^{-1} in the deuterated aniline spectrum. The significant difference of the fluorescence excitation spectrum of p-toluidine in a supersonic expansion and at room temperature can be seen in Figure 1. The very broad band widths and a large number of congestions cannot give rise to the correct transitional frequencies in the room temperature spectrum. Meanwhile, the weak transitions cannot be seen in the spectrum. However, the spectrum taken in a supersonic jet has no congestions and provides very accurate transition frequencies. The weak transitions appear obviously in the jet-cooled spectrum. Other workers have used a supersonic expansion to cool the molecules thereby reducing line widths and congestion due to hot bands but they didn't use other powerful techniques to support their assignments. This thesis presents a symmetric study of aniline, and some substituted aniline using the techniques of expansion cooling under different conditions to reveal hot bands, fluorescence excitation, dispersed emission, and isotopic substitution.

Nitrogen Inversion and NH_2 Torsion

The structure of aniline in the ground state has the equilibrium position of the two NH_2 protons out of the ring plane and the angle between the ring plane and the plane formed by NH_2 was estimated to be around 42°.[6,12] The motion of the two protons up and down about the ring plane is called the

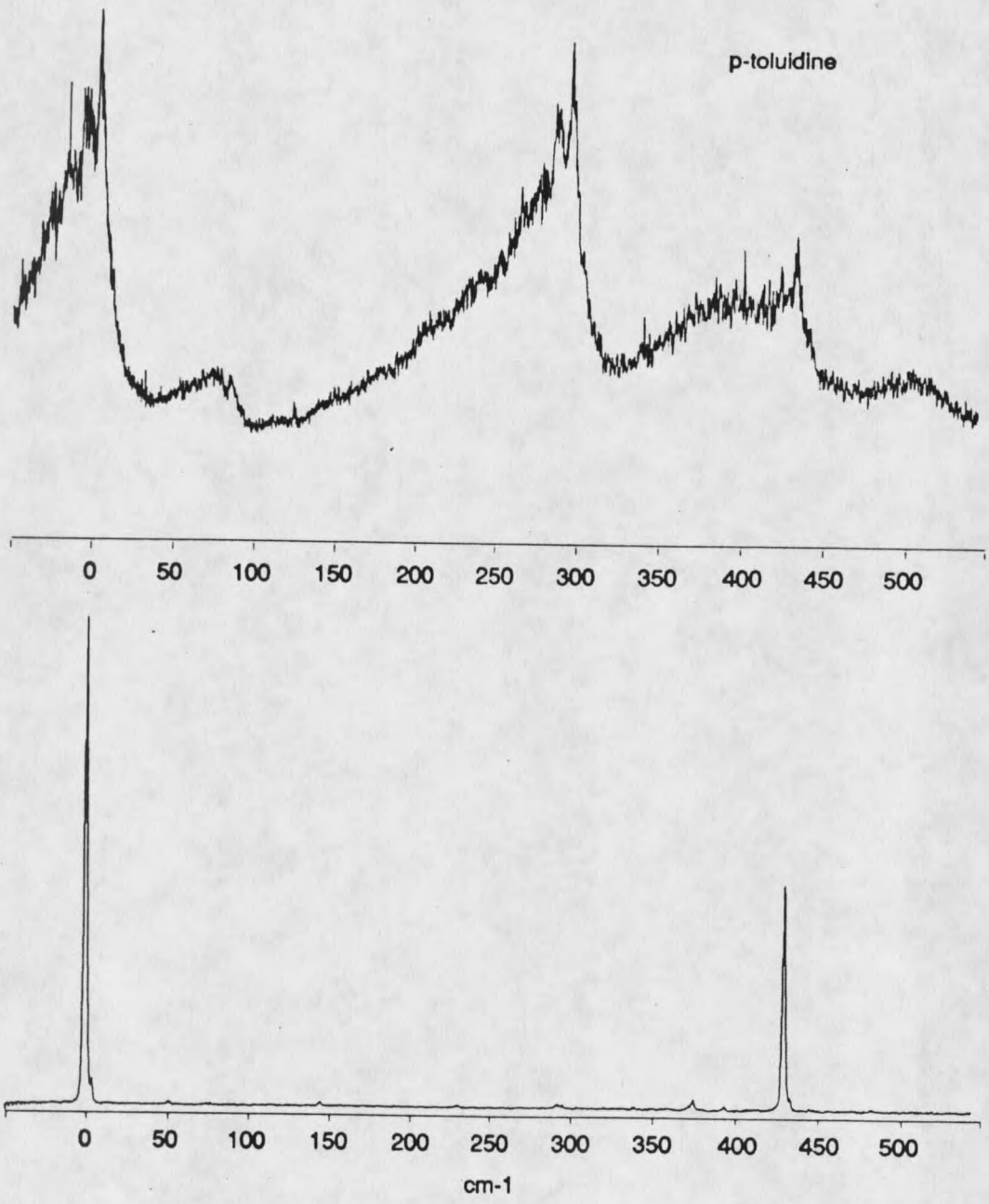

Figure 1. Comparison of the excitation spectrum of aniline (top trace) at room temperature with the one (bottom trace) in a supersonic jet (7 bar backing pressure).

nitrogen inversion mode which is analogous to the "umbrella" motion in ammonia. The nitrogen inversion is a large amplitude motion and has a double minimum potential in aniline.

Kydd and Krueger[6] fit the barrier height to nitrogen inversion as 526 cm^{-1} based on far-infrared results. The first inversion quanta of aniline and deuterated aniline in the ground state were measured at 40.8 cm^{-1} and 13.4 cm^{-1} respectively.[6] The large deuterium shift is very convincing evidence for their assignment. The second quanta of nitrogen inversion in aniline and deuterated aniline were assigned as 423.8 and 337.5 cm^{-1} respectively.[6]

The barrier height and the inversion levels of aniline in the excited state were studied by several groups.[4,8,13-15] Although there were some differences in calculated barriers (Brand et al[4] fit the barrier with 24 cm^{-1} and Hollas et al[8] fit it to be zero), the results indicate that the barrier for inversion in the excited state should be extremely low. Our result for the inversional barrier height in the excited state is in good agreement with the fit by Hollas et al. Thus, the structure of the amino group in the excited state is expected to be planar. Hollas and co-workers rejected Ito's assignment[13] for the transitions around 352 cm^{-1} as I_0^1 in the excitation spectrum of aniline because this transition is restricted by the even quanta selection rules of nitrogen inversion. In the deuterated aniline, the deuterium shift for the inversion transitions are significant. The I_1^1 and I_0^2 were measured at 239.3 and 546.8 cm^{-1} respectively.[8] The peaks around 352 cm^{-1} in the excitation spectrum of deuterated aniline do

not have significant shifts. This indicates that the peaks around 352 cm^{-1} do not contribute to the NH_2 group. Later, Bacon and Hollas[16] proved the doublet splitting for the transitions around 352 cm^{-1} to be a Darling-Dennison resonance and assigned them as $10b_0^2$ and $16a_0^2$ for the low and high wavenumber components, respectively. The first and second quanta of nitrogen inversion in the excited state were measured at 333.4 and 760.2 cm^{-1} for aniline and 246.7 and 545.4 cm^{-1} for deuterated aniline.[8]

The nitrogen inversion has also been studied in some para substituted anilines, such as p-fluoroaniline,[12] p-toluidine,[17-19] and p-trifluoromethyl-aniline.[20] The inversion levels and potential in p-fluoroaniline and p-toluidine are very similar to those in aniline. This is expected because the inversion mode is relatively independent of the other modes in the molecule. However, the first quanta and barrier height of nitrogen inversion in p-trifluoromethyl-aniline were measured to be 72.0 cm^{-1} and 373 cm^{-1} in the ground state, respectively.[20] Compared with 40.8 cm^{-1} of the first quanta and 525 cm^{-1} of the barrier in aniline, this change is rather large. This may perhaps be due to the highly electron withdrawing nature of the CF_3 group. The resonance enhanced two photon ionization spectra of p-fluoroaniline and p-toluidine were reported by Lubman and co-workers,[21] but they did not assign the inversion transitions. The peak at 775 cm^{-1} in the p-fluoroaniline spectrum and the peak at 707 cm^{-1} in the p-toluidine spectrum were assigned as 12_0^1. We disagree with this assignment because both of these transitions can be attributed to internal

modes of NH_2 group. The peak at 775 cm^{-1} in the p-fluoroaniline spectrum is very similar to the I_0^2 transition in aniline and should be assigned that way. Further evidence for this assignment will be provided later in this thesis. However, we also observe a different frequency for this transition, 759.6 cm^{-1} instead of 775 cm^{-1}. We question the assignment for the 707 cm^{-1} peak in Ref. 21 on the basis of our deuterated p-toluidine work presented in detail later. This peak is shifted in our deuterated p-toluidine spectrum by more than 140 cm^{-1} so it cannot be a transition from a skeleton mode and must be due to an internal motion of the NH_2 group. Smalley and co-workers[19] assigned the peak at 734 cm^{-1} in the excitation spectrum of p-toluidine as I_0^2. This peak, however, is only one member of a quartet that appears around this frequency. The observed inversion levels are listed in Table 1.

Table 1. The Inversion Levels of Nitrogen Inversion in Aniline and Para-Substituted Anilines.(cm^{-1})

State	Assignment	aniline	aniline-ND_2	p-Fluoroaniline	p-Toluidine
Ground					
I_1	40.8[6]	13.4[6]	31.7[12]	33.2[17]	
I_2	423.8	337.5	437.9	434.1	
I_3	700.1	457.0	708.4	684.2	
	Barrier	525.9	543.4	596.4	588
Excited					
I^1	333.4[8]	252.7[8]	---	---	
I^2	760.2	546.8	---	737.3[19]	
	I^3	1224.6	873.8	---	---
Barrier	0	0	---	---	

It is clear that the inversional levels have very different spacings. Thus, the

nitrogen inversion mode is very anharmonic in both states.

NH_2 torsion, where the two hydrogens bonded to nitrogen twist around N-C bond, is another internal motion of the amino group in the anilines. The NH_2 torsional transition in the ground state was claimed by Fateley and coworkers[22] to be at 285 cm^{-1} but was assigned as 277.3 cm^{-1} by Nicolaison et al.[12] The NH_2 torsional barrier was estimated to be 2005 cm^{-1} which seems to be acceptable.[12] To our knowledge, no NH_2 torsional transitions have been assigned in the excited state. The potential function for NH_2 torsion around the C-N bond is assumed to be of the $\cos 2\alpha$ type and one quanta transitions of the amino torsional mode are forbidden, both in the IR and as vibronic transition. The transition level was observed in the far IR[12] in combination with $(T_1 + I_1)$ and a difference band $(T_1 - I_1)$ In the excitation spectra of aniline and p-toluidine, however, no cross combination transitions T_iI_j (i+j = even number) have ever been found. This is because evaluation of the molecular symmetry shows the two modes are of different symmetry.

Internal Rotation of a Methyl Group

The internal rotation (or torsion) of a methyl group is one of the large-amplitude motions of chemical importance and the studies have been extended from microwave, Raman, and infrared spectroscopies to laser induced fluorescence excitation spectroscopy.[25-29] In the excitation studies, the supersonic expansion cooling technique has provided a powerful tool to study

the hindered internal rotation of methyl groups.[30,31] The internal rotation of a methyl group can show a strong dependence on electronic state. Spangler et al calculated the internal torsion barrier to be 28 cm^{-1} in the ground state and 150 cm^{-1} in the excited state for p-methyl-trans-stilbene by fitting the experiment results.[30]

The potential function for methyl internal rotation can be expressed by

$$V(\alpha) = \frac{1}{2}V_3(1-\cos 3\alpha) + \frac{1}{2}V_6(1-\cos 6\alpha) + \frac{1}{2}V_9(1-\cos\alpha) + \cdots \cdots$$

in which the V_n are potential constants and α is the torsional angle. V_3 and V_6 terms are most often used to express the methyl torsion with higher terms rarely being needed. The first term in the potential function is dependent upon the symmetry, or the number of equivalent conformations. For example, in toluene, the methyl group has three equivalent hydrogens as has three fold symmetry and there is a two fold symmetry from the phenyl ring. Thus the total torsional potential in toluene has six minima.[31] The first no-zero term of the potential function determines the barrier height and higher order terms shape the potential. When the barrier height is zero, the energy levels associated with the torsion coincide with those of one-dimensional free rotor and are given by Bm^2. Here B is the internal rotation constant of the methyl group and m is the rotational angular momentum quantum number. When the torsional barrier is nonzero, the internal torsional levels become split by tunneling. The energy levels of a methyl rotor can be labeled by the internal rotation angular momentum number and the symmetry of the levels. The

levels are $0a_1$, 1e, 2e, $3a_2$, $3a_1$, 4e, 5e, $6a_2$, $6a_1$, ··· in order of increasing energy.[30] The above potential function can be used in the Hamiltonian to fit the observed methyl torsional transition frequencies.

If the methyl torsional transitions can be observed in a spectrum, the methyl rotor can be used as a probe to study electronic features of the molecule since it is very sensitive to the local electronic environment.[32] A "remote" substitution effect can be delivered to the methyl rotor by a conjugated system, which is manifest as a change in torsional harrier with substitution. Dorigo et al[34] found that hyperconjugation, the interaction between the p orbital of the carbon atom in the methyl rotor and the π system, is the dominant influence on methyl behavior. In aliphatic systems, the net hyperconjugation interaction is antibonding in the ground state and bonding in the excited state. Therefore, the conformation of maximum overlap is favored in the excited state but not in the ground state.[30]

Low Frequency Modes of Trans-Stilbenes

A number of groups have been involved in the study of trans-stilbene, however, many of them paid more attention to photoisomerization between trans and cis-stilbenes and the assignments of skeletal modes above 200 cm^{-1} instead of the low frequency ones.[35-40] Warshel calculated the normal modes for C_{2v} symmetry in both the ground and excited states using QCFF-π.[41] Most of the later studies followed his notation to label the trans-stilbene modes. The

observed low frequency modes in trans-stilbene have been assigned as ν_{25} (phenyl in-plane wag), ν_{37} (ring torsion), and ν_{36} (phenyl out-plane flap). The low frequency modes of ν_{25}, ν_{37}, and ν_{36} are a_g, a_u, and a_u respectively. The totally symmetric mode ν_{25} has no restriction for the transitions between the S_0 and S_1 states. The A_u modes, however, are restricted to only even quanta transitions. The transition frequencies of the three modes 25_0^1, 37_0^2, and 36_0^2 in trans-stilbene were observed at 197.8, 95.3, and 69.6 cm^{-1} in the excitation spectrum and at 200, 19.0 and 114 cm^{-1} in the dispersed emission spectra, respectively.[42-44] Mode ν_{25} is harmonic in both ground and excited state but ν_{37} is only harmonic in the excited state. The very low first quanta and anharmonic potential of ν_{37} in the ground state and its strong couplings with other vibrational modes contribute to the acceleration of the intramolecular vibration redistribution rate.[45]

Some trans-stilbene van der Waals complexes and trans-stilbene-H_2/D_2 were studied by Zwier and co-workers.[46-48] They found a strong mode-dependent broadening of the van der Waals complex transitions associated with the low frequency vibration 37_0^2.

Ring Modes in Anilines

The assignments of the ring modes in aniline and its para-substituted analogs are based on the assignments of benzene[49,50] In each of the anilines the origin is prominent in its excitation spectrum. Only three benzene-like

ring modes appear with high intensities in the anilines, ν_{6a}, ν_1, and ν_{12}, based on Wilson's classification for benzene[49]. All the three modes are totally symmetric. The transition frequencies of $6a_0^1$, 1_0^1, and 12_0^1 in the fluorescence excitation spectrum of aniline are at 493, 798, 954[4,10,13] respectively. Some disagreements for the assignments of mode 1_0^1 and 12_0^1 can be found in different publications. Brand, William, and Cook assigned the modes 12_0^1 and 1_0^1 for the peaks at 798 and 953 cm^{-1}, respectively. However the peaks at the above frequencies were assigned as 1_0^1 and 12_0^1 by Reilly and coworkers instead.[51] According to Varsanyi the 1_1 has lower frequency than 12_1 does in ground state.[50]

The absolute frequency of the origin is not certain even though it was shown to be around 34032 ± 10 cm^{-1}.[4,14] In the excitation spectra of para-substituted aniline (p-fluoroaniline and p-toluidine) the origin peaks shift down to 32658 and 33095 cm^{-1} respectively according to Tembreull et al.[21] The ν_{6a} mode shifts down by about 60 cm^{-1} but the other two ring modes ν_1 and ν_{12} show only minor shift. This is because ν_{6a} involves some motion of the substituent.[49] Since all the three ring modes are totally symmetric, the transitions from these modes will have no restriction by the selection rules. All of the three modes in the anilines are nearly harmonic. The overtones should be easily found in the excitation spectra especially for the low frequency overtone $6a_0^2$.

In this thesis, we concentrate on the assignments for the internal modes in aniline and para substituted anilines in the FE and DE spectra.

EXPERIMENTAL

Fluorescence Excitation in a Supersonic Jet

A high power, frequency doubled, pulsed Nd: YAG (Lumonics HY750) was used to pump a tunable dye laser (Lumonics HyperDye 300) in the fluorescence excitation experiments. A 2400 groove/mm grating used at grazing incidence in the dye laser provides 0.07 cm^{-1} resolution. Since all the molecules discussed in this thesis involved $\pi \rightarrow \pi^*$ transitions located in the UV range, a dye laser frequency doubler (Lumonics HyperTrack 1000) was used to double the visible dye laser frequency to the UV.

All the laser dyes were purchased from Exciton. The sample was loaded in a stainless steel sample chamber and heated to increase the vapor pressure. High purity helium was allowed to flow over the sample, through a nozzle orifice (General Valve nozzle series-9 with 0.8 mm diameter), and then was expanded into the vacuum chamber.

The frequency doubled dye laser beam was passed through three apertures, which were used to exclude room light, then crossed the jet expansion at right angles. The intersection of the laser and jet axis was placed at the focal point of an ellipsoidal reflector (Melles Griot REM 014). Any emission was then

reflected to the second focal point where the photocathode of a photomultiplier tube (PMT, EMI 9813QB) was positioned. The resulting signal was measured by the PMT, amplified, and then sent to a boxcar averager (SRS boxcar system), digitized, and stored on an IBM compatible computer. The experimental set up is presented in Figure 2.

The supersonic expansion cooling is a thermodynamic process. The vibrational, rotational, and translational energies in a molecule are called thermoenergies because they are affected by temperature. However, only vibrational and rotational energies have significant effect on spectroscopy. These energies can be transferred by collision between molecules. When the molecules are passed through the nozzle orifice and expanded into the vacuum chamber, the collision between the sample molecules and the He atom will transfer the internal energy between the sample molecule to the atoms. In a gas phase mixture, the diluted sample molecules have much larger probability to collide with the carrier gas atoms than with themselves. Then the vibration and rotation energies will be transferred from the sample molecules to the carrier gas atoms since the collision is nonelastic. Finally the molecule can be cooled significantly. The temperature in the cooled sample molecules in the jet can be below 5 K, which is cold enough to cool all the sample molecules down to the zero quanta level in the ground state. Because the rotational levels are much lower energy than the vibrational levels, rotations cannot be completely cooled out. However, the lower the temperature, the less rotational levels will

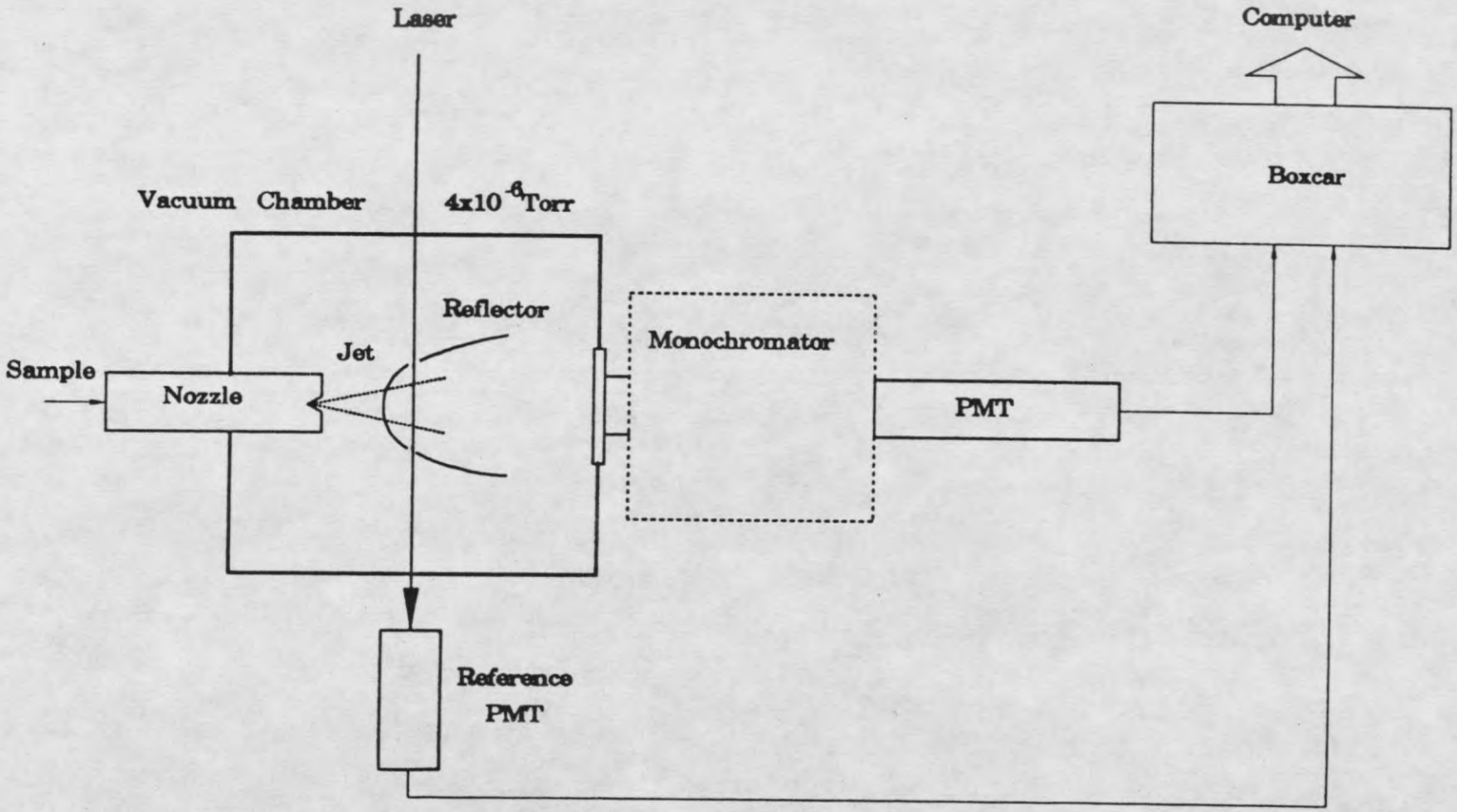

Figure 2. The principle scheme of the experimental set up which is used for fluorescence excitation and dispersed emission experiment in a supersonic jet.

be populated, the narrower the observed band width will be in the excitation spectrum.

The expansion conditions can easily be changed by changing the He backing pressure over a range of 0.2 - 7 bar, gauge. High backing pressure makes the sample more dilute and the molecules have collisions with helium so that they are cooled more efficiently. At low backing pressure, however, the molecules cannot be cooled down to the zero vibrational level completely. Thus, some transitions will originate from the nonzero quanta in S_0 and are called hot bands in the excitation spectrum. Higher temperature will give hot bands more intensity in the spectrum which can aide in identification of same inversional bands. However, very high temperature can greatly complicate the spectrum due to the presence of numerous hot bands. Furthermore, the higher temperature will make the band width broader so that close transitions overlap. The temperatures for protonated and deuterated anilines at 7 bar of the backing pressure are predicted to about 5 K and 10.5 K respectively, according to the jet cooled spectra.

Another technique used in the fluorescence excitation experiment was to saturate the strong transition bands in order to get enough intensity in weak bands. In order to get a saturated spectrum, high laser power was used to excite the molecules which improved the signal to noise for the weak transitions.

Dispersed Emission Technique

A fluorescence excitation spectrum of a cold molecule can provide very important information for the molecular behavior in an excited state. However, complete characterization requires probing the ground state as well. The fluorescence excitation and dispersed emission mechanism in a jet is presented in Figure 3. Assume all the transitions shown in Figure 3 are allowed. The molecules are pumped from the lowest level in the ground state to a single vibrational level in the excited state. When the molecular population is built up in the excited state, spontaneous emission will let the molecules lose energy and go down to the ground state. Fluorescence will be emitted in this process. Actually, not all the molecules will go back to the original level in the ground state. Some of the molecules will emit to different levels in the ground state.

It is equivalent to say that the fluorescence is composed of different frequencies, and if a monochromator is used, a dispersed emission spectrum can be obtained. The frequency difference from a transition to the origin band reveals the difference for the vibration levels.

In the dispersed emission set up, a monochromator is placed between the emitting molecule and the signal detector. At first the molecules were pumped from ground state to a certain level of the excited state. The emission signal, is then dispersed by the monochromator.

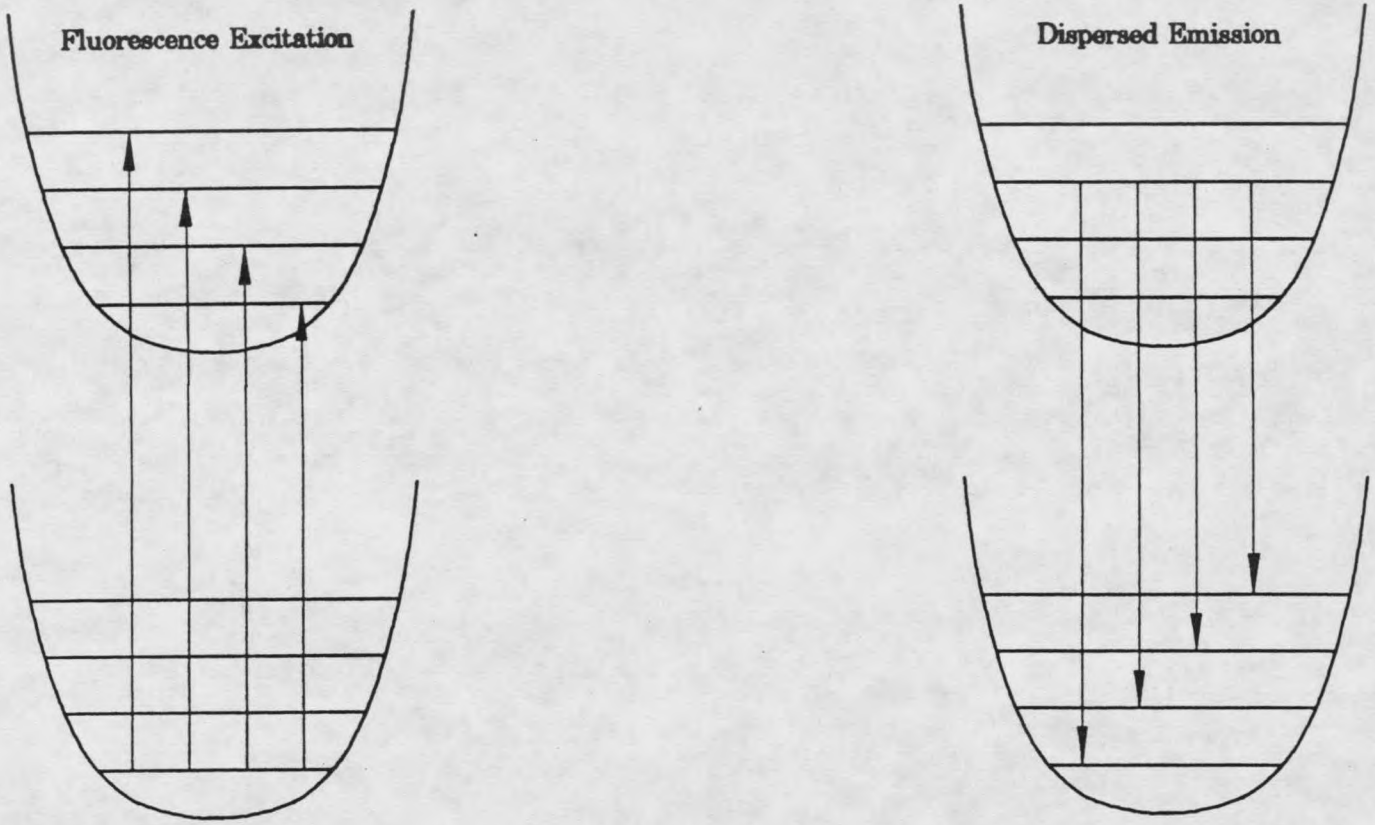

Figure 3. A diagram of the fluorescence excitation and dispersed emission processes. In the cold environment of the jet most absorptions originate in the v=0 level so fluorescence excitation probes the excited state. After pumping a selected level, ground state information can be obtained by dispersing the emission which terminates in multiple S_0 levels (right).

In the experiment, a quarter meter monochromator (ORIEL 77200) was used for the dispersed emission. The monochromator entrance slit was placed at the second focal point of the ellipsoidal reflector. The light was detected by a PMT and processed, digitalized and stored in the same fashion as the fluorescence excitation spectrum. The resolution of the monochromator ranged from 11 cm^{-1} with 0.05 mm slit width to 22 cm^{-1} with 0.1 mm slit width. Most of the dispersed emission spectra shown in this thesis were taken as an average of two scans and smoothed by 11 points.

Materials

Aniline was obtained from Mallinckrodt Chemical Works and was used without further purification. Aniline-ND_2 was purchased from CIL with 99 percent purity claimed by the manufacturer, but both the excitation spectrum and NMR analysis showed the sample to be approximately 75 percent ND_2 and 25 percent NHD species. P-fluoroaniline and p-toluidine were purchased from Aldrich. The purities of p-fluoroaniline and p-toluidine were claimed by the manufacturer to be 99 percent and 99.9 percent, respectively, and were used in the experiments without further purification.

P-toluidine-CD_3 was made by Professor B. P. Mundy at Montana State University. The purity was shown to be about 90 percent by NMR and mass spectroscopy analysis.

P-toluidine-ND_2 was made from commercial p-toluidine by exchanging with

deuterium oxide. Two grams of p-toluidine and 18 grams of D_2O were mixed together in a 100-ml round flask. The mixture was refluxed under helium protection for 20 hours and then cooled in an ice bath for 20 minutes. The mixture was vacuum filtered and the whole exchange procedure was repeated two more times. The final product was then dried under vacuum with slight warming (37°C). There was no evidence of ring exchange under these neutral conditions in either the NMR or FE spectra. The purity of the final product just after preparation was about 96 percent. However, the dry p-toluidine-ND_2 easily absorbs water from the air and back exchanges so the sample used in the experiment was of only about 85 percent purity.

P-amino-p′-methyl-trans-stilbene (PPTS) was synthesized in this lab based on the Wittig reaction[52]. Four reactions were chosen to reach the final product which are shown as follows.

Reaction 1.

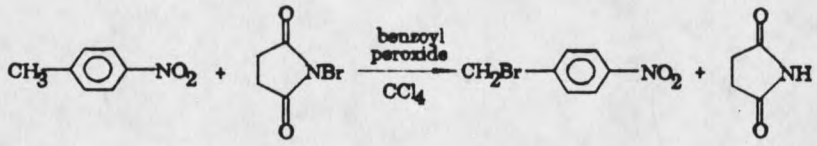

Reaction 2.

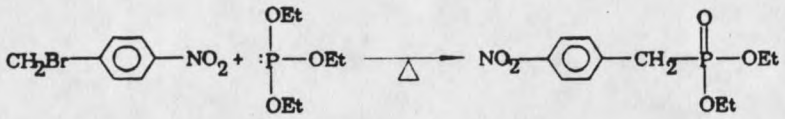

Reaction 3.

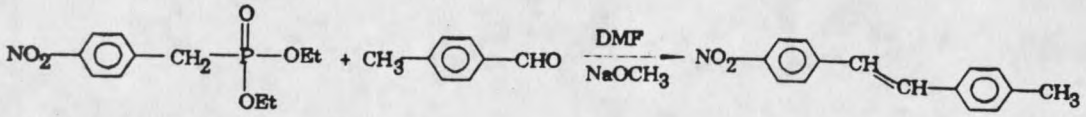

Reaction 4.

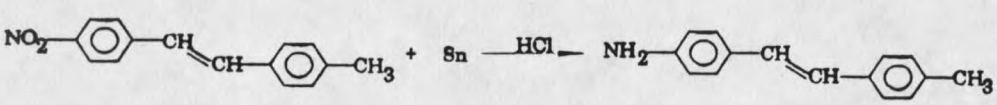

In reaction 1,[53] 5.48 grams (0.040 mol) of p-nitro-toluene and 6.71 grams (0.038 mol) of N-bromosuccinimide were dissolved in 50 ml of carbon tetrachloride with 0.1 grams of benzoyl peroxide as catalyst. This solution was refluxed under nitrogen protection with irradiation from a long wavelength UV lamp for 2 hours. The reaction mixture was cooled and passed through a pad of silica gel on a filter funnel to remove succinimide. The pad was thoroughly washed with ether, and the filtrate was stripped in vacuo to give a brown oil. The desired bromomethyl compound was obtained after the above in 55% yield.

Reaction 2 and 3 constitute a typical Wittig reaction sequence. In reaction 2, 6.48 (0.030 mol) grams of 1-bromomethyl-4-nitro benzene and 5.48 (0.033 mol) grams of triethyl phosphite were mixed and refluxed for one hour. The reaction was run under nitrogen protection. The boiling point of the solution started at 130°C and rose to 200°C at completion of the reaction. Reaction 3. was initiated immediately by adding 1.62 grams (0.03 mol) of sodium methoxide and 24.4 ml of DMF to the above mixture. The flask was swirled in an ice bath to thoroughly chill the contents. And then 2.88 ml 4-methyl-benzaldehyde was added. The mixture was then swirled vigorously in the ice bath for 5 minutes, removed, and allowed to stand at room temperature for 25 minutes. The solid product p-nitro-p'-methyl-trans-stilbene was filtered with a Buchner funnel after addition of 25 ml of distilled water. The product was washed with several 10-ml portions of distilled water.

In the reduction reaction 4, powdered tin (Sn) was used to reduce the nitro

group without affecting the double bond. One gram (0.0042 mol) of the product from reaction 3 and 2.33 g (0.019 mol)tin powder were placed in a 100-ml round flask. Then 11.6 ml of (37%) HCl was added to the flask in 3 portions, each followed by vigorous swirling. After the exothermic reaction had subsided, additional 19.4 ml of ethanol (100%) was added and the mixture was heated in a steam bath for 2 hours with occasional swirling. The mixture was cooled to ice-water bath temperature and then 13 ml of NaOH (30%) was slowly added. The amino compound was extracted with three 100 ml portions of ether which were then combined. The combined ether extract was then washed with a saturated NaCl aqueous solution in order to separate the water soluble chemicals. Eight grams of $MgSO_4$ was added to dry the ether solution, and then separated by filtration. A rotovap was used to concentrate the product. The final product, p-amino-p'-methyl-trans-stilbene (PPTS), was a light yellow solid (about 0.35 g, 40%) which should be stored in dark to keep from possible isomerization caused by UV. The yield of reaction 4 was 40 percent.

A crystal of PPTS was made for X-ray structure analysis. 50 milligrams of PPTS powder was dissolved in methanol in a small vial, covered lightly with aluminum foil and placed in a larger vial which was partially filled with water. The larger vial was sealed and kept in the dark for 15 days at room temperature. This yielded crystals which grew up to about 1 millimeter long and 0.15 millimeter for the shortest dimension on the cross section.

RESULTS AND ASSIGNMENTS

The Assignments of the Nitrogen Inversional Transitions for Aniline and para-Substituted Anilines

The internal mode of nitrogen inversion in aniline is completely analogous to the "umbrella" motion of NH_3. The difference is that aniline has a relative massive phenyl ring plane and the two amino protons flap up and down about the ring plane. In the ground state of aniline, the amino group is pyramidal with an angle of about 42 degrees between the H-N-H plane and the ring plane. There is a second, equivalent geometry with the protons 42° on the opposite side of the ring plane and an energy barrier between the two equilibrium positions. Thus, the potential surface for inversion has a double minimum in the ground state with a barrier height of about 526 cm^{-1}.[6] In contrast with the ground state geometry, the structure of aniline in the excited state is known to be planar.[10] Therefore, the excited state potential surface has a single minimum, or in other words, the excited state inversion barrier is equal to zero. Even though the inversion mode in aniline has been extensively studied, no systematic studies have been performed on the logical analogs. Furthermore, more evidence is desirable to solidify the difficult assignment for the inversion transitions for aniline itself in both ground and

assignment for the inversion transitions for aniline itself in both ground and excited states. In this section the inversion mode is studied for eight aniline and substituted aniline molecules in order to support the inversion assignments for the known transitions and to identify many new inversion assignments.

In the following assignments the inversion transitions are going to be identified in both the fluorescence excitation (FE) and dispersed emission (DE) spectra for each aniline-like molecule. In the excited state the inversion transition is expressed in I_a^b which means the transition from "a" quanta of inversion in the ground state to "b" quanta in the excited state. In the dispersed emission spectra, transitions will often be labeled as I_a which gives only the number of inversion quanta in ground state. This makes comparison of DE spectra resulting from excitation of different vibrational levels in the S_1 state more straightforward.

It is important to consider certain special features of the inversion potential surface and the spectral consequences. Figure 4 presents the even quanta allowed inversional transitions observed in the excitation spectrum. Transitions originating from the zero quantum level in the ground state can only terminate in the even quanta levels in the excited state. The relative frequency shown in each spectrum is taken from the electronic origin. In other words, the transition frequency from zero quanta in the ground state to zero vibrational quanta in the excited state is set to zero. The observed frequency

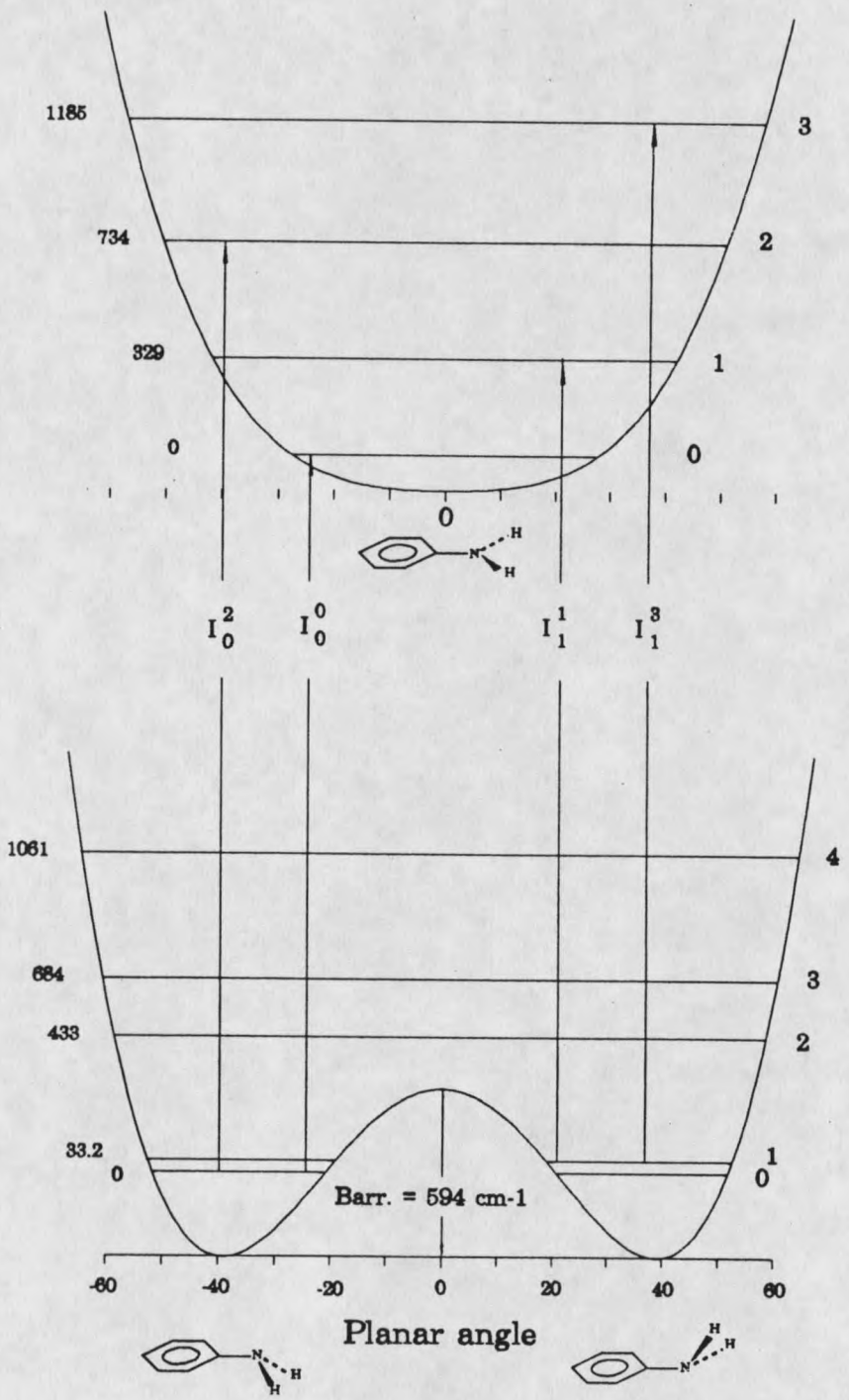

Figure 4. The allowed nitrogen inversion transitions for p-toluidine between ground and excited states. The barrier between the two minima of the potential in ground state is 594 cm^{-1} but the one in the excited state is zero.

in the excitation spectrum gives rise to the exact frequency of a certain vibrational level if the transition is from zero quanta in S_0. However, if the transition begins from a higher quanta in the ground state, the observed frequency in the excitation spectrum is not equal to the frequency of the terminal vibrational level. The level frequency can be obtained by summing the relative transition frequency with the S_0 level frequency. Since all the potentials and the inversional levels are a plot of a computer fit to the experimental data, this diagram nicely demonstrates the real transition mechanism for inversion levels. The very low first quanta in the S_0 indicates that this level will be easily populated by changing the expansion conditions. Thus, strong hot bands due to transitions initiated from I_1 are expected in the excitation spectrum with warmer jet conditions. The double minimum potential in S_0 and the single well in S_1 will be discussed later.

Aniline

The excitation spectrum of aniline taken under two different expansion conditions is shown in Figure 5. The lower trace, recorded using 7 bar of He as the carrier gas, has a vibrational temperature (T_v) of approximately 10 K. The upper trace used 0.2 bar He has $T_v \simeq 28$ K. The relative temperatures are also evident in the rotational line widths. P- and R-branches are evident in the broader bands of the warmer spectrum. The cold spectrum contains narrow, nearly structureless lines. Comparison of the two spectra reveals a prominent line at 292 cm^{-1} in the warmer spectrum that is not evident in the

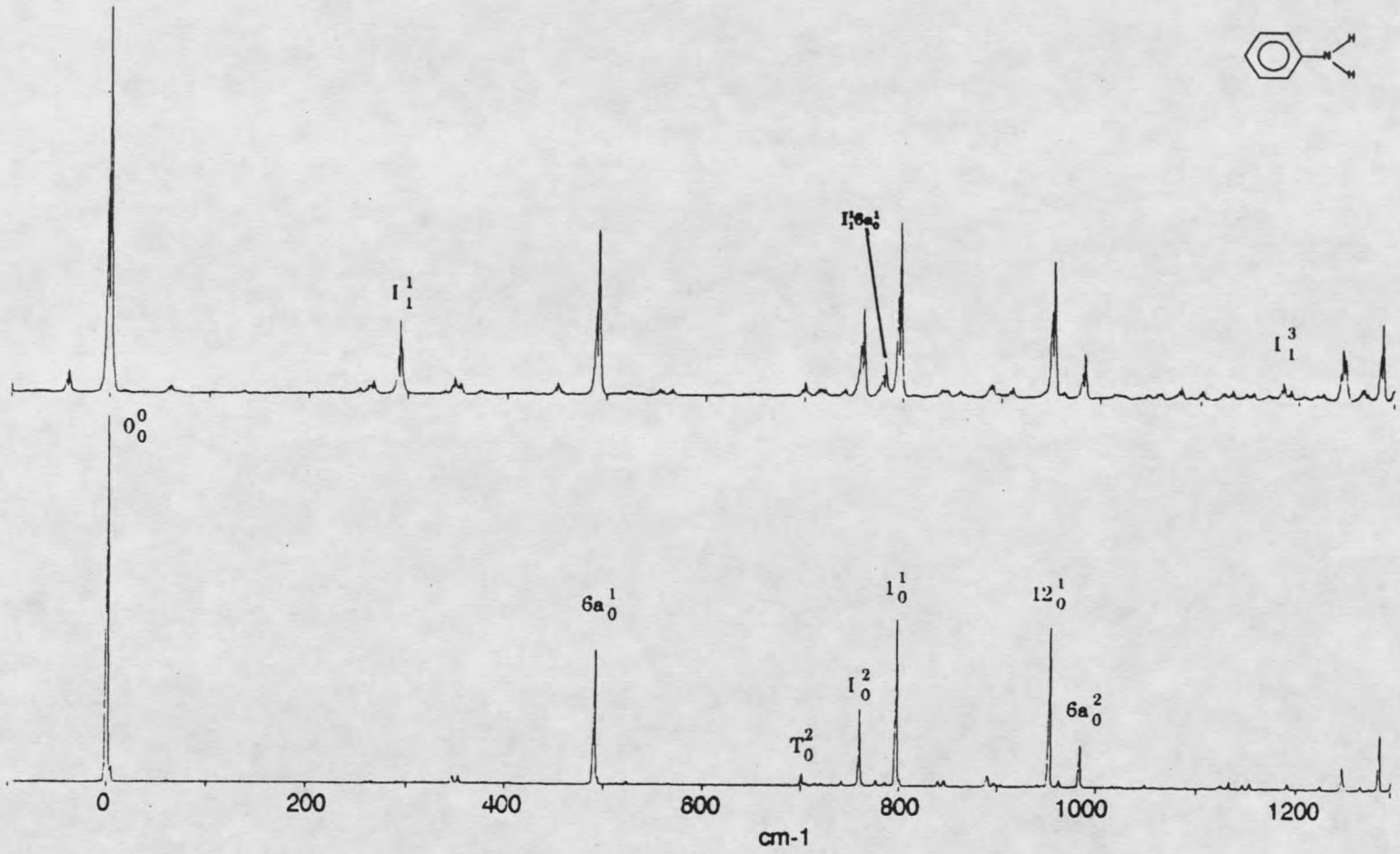

Figure 5. The excitation spectrum of aniline. The spectrum in the top trace was taken at warmer jet conditions (0.2 bar) and the bottom one was taken at 7 bar.

ground state that has at least one quanta in a vibrational mode. Given that there are no strong hot bands that could be found at these temperature in benzene, the hot band must originate from an amine group mode, most likely I_1. Even under the milder expansion conditions the temperatures are very low so the mode causing the hot band must have a very low fundamental frequency. Another hot band was found at 1184 in the same spectrum that can not be attributed to any combination by its frequency. This hot band probably originates from the same level as the one at 292 cm^{-1}. The only mode which fits this description is the inversion and IR experiments place the I_1 frequency at 40.8 cm^{-1}.[6] Further evidence will be provided later to solidify this assignment. Other prominent hot bands can be assigned as combinations involving I_1^1 or the hot band that appears at -40 cm^{-1}.

The next question is to identify the inversion band I_0^2 (only transition causing even quanta changes in I are expected because it is not totally symmetric). Previous work assigned the 760 cm^{-1} transition as I_0^2 based on the room temperature vapor phase absorption spectrum and the dispersed emission from that band. Since seven other transitions appear with ± 60 cm^{-1} of 760 in the cold spectrum it seemed prudent to confirm this assignment under jet conditions where these lines do not overlap.

Figure 6 is an excitation spectra of deuterated aniline. In this molecule the two protons on the amino group are substituted by two deuterium atoms. Because inversion involves almost exclusive motion of the amino hydrogens,

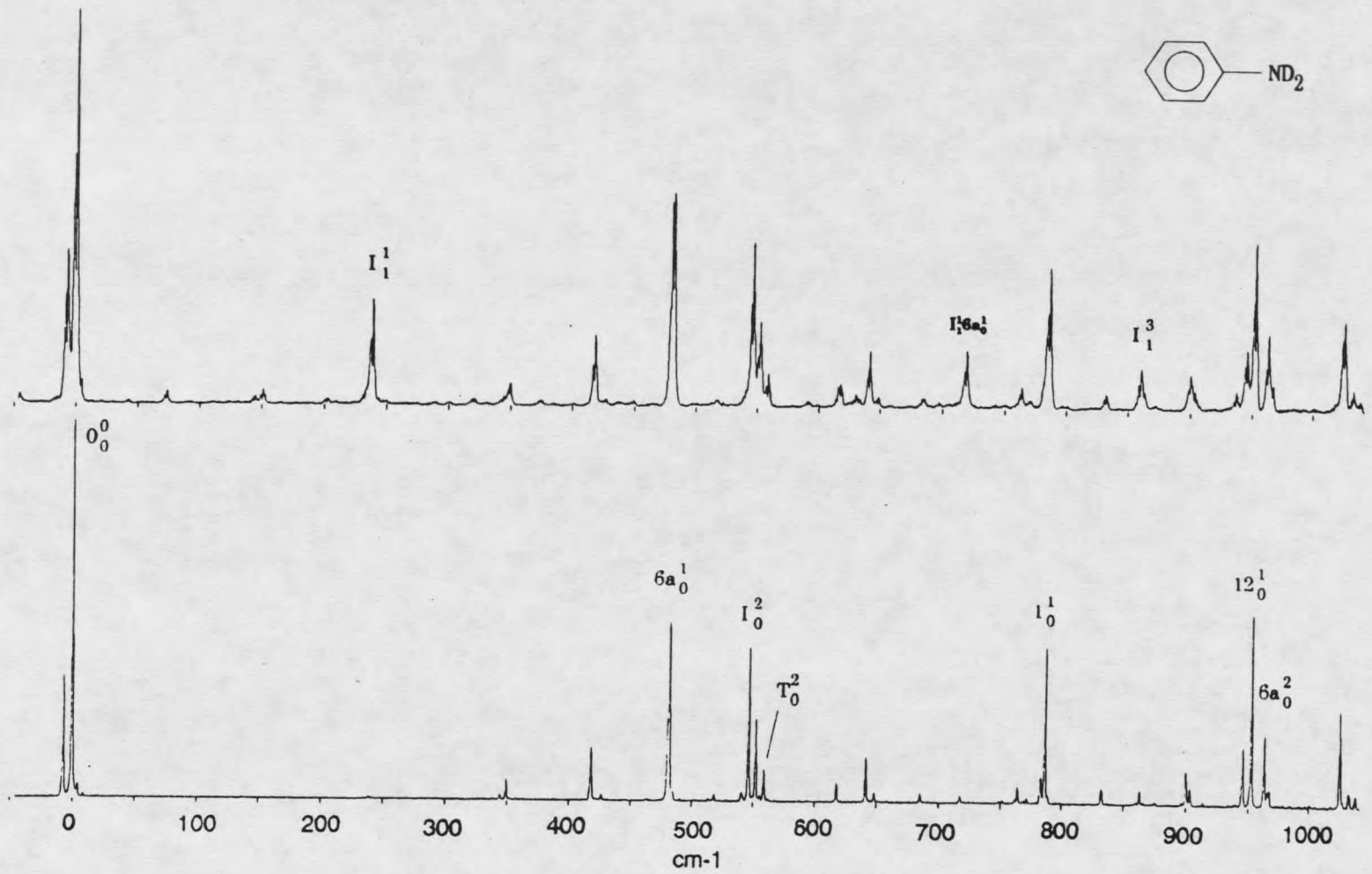

Figure 6. The excitation spectrum of deuterated aniline. The top trace was taken under 0.2 bar backing pressure and the bottom trace under 7 bar.

its frequency should change by a factor of approximately $\sqrt{2}$. For aniline-ND_2 the new peaks are found around 550 cm^{-1} and the 760 cm^{-1} band in the spectra is missing. Such a large deuterium shift is strong evidence supporting the I_0^2 assignment.

In Figure 7 five dispersed emission spectra of aniline are presented. The strongest transition in both the origin and I_0^2 spectra appears at 421 cm^{-1}. It is absent in the dispersed emission from I_1^1 and I_1^3. By contrast, the emission spectra from I^3 and I^1 display a transition at 661 cm^{-1} which is absent in the 0^0_0 and I_0^2 spectra. Given the assignments in the excited state and the even quanta selection rule for the inversion mode, the transition at 421 cm^{-1} can be assigned as I_2 and 661 cm^{-1} as I_3 in the ground state. As mentioned in the introduction chapter we cannot measure the first quanta inversion level because of the even quanta selection rules. The different intensity patterns of I_3 in the emission spectra of I_1^1 and I_1^3 strongly support the assignment of I_1^3 in the excitation spectra of aniline. The two potential surfaces of the inversion mode in ground and excited states have no displacement. In this case the strongest transition in the progression is typically a same quanta transition between two electronic states. Therefore the transition from I^1 to I_1 should be stronger than that of I^1 to I_3 and vice versa.

Further evidence is supplied by combination bands in the DE spectra. When zero or two quanta of the inversion is exited, only even quanta of I should be seen in combination with totally symmetric ring modes. Conversely,

Figure 7. The dispersed emission spectra of aniline. Each of the spectra were taken by setting the laser frequency on the absorption band indicated at the left side of the spectrum. The emission spectrum for the hot bands were taken under 0.2 bar and the others were taken under 7 bar.

when I_1^1 and I_1^3 is exited I_{odd} should appear in combination bands. For instance, in Figure 7, the ring mode $6a_1$ is at 531 cm^{-1} and 1_1 at 818 cm^{-1}. The combination bands, I_26a_1 and I_21_1, are found at 943 cm^{-1} and 1244 cm^{-1}, respectively in the origin and I_0^2 spectra but are missing in the I_1^1 and I_1^3 spectra. Conversely, the combination bands of I_36a_1 and I_31_1 are found at 1183 cm^{-1} and 1493 cm^{-1}, respectively, in the I_1^1 and I_1^3 spectra but are missing in the origin and I_0^2 DE spectra.

The assigned frequencies of the inversion mode in both ground and excited states can be very well fit by computer calculation. The inversion barrier and the potential parameters were calculated by using the VNCOS program[54] to fit the inversional levels in each individual state. The inversional potential function for the Hamiltonian is

$$V(\theta) = \tfrac{1}{2}V_1(1-\cos\theta) + \tfrac{1}{2}V_2(1-\cos 2\theta)$$

in which V_1 and V_2 are potential term constants and θ is inversional angle of the NH_2 plane from the ring plane. A sin and cos basis set was used in VNCOS for the wavefunction. The resulting potential constants then were used in the INROT program (using a particle in a ring basis set) to fit the observed transitions and intensities of the inversion mode in both states. By referring to our calculated results we found a previously unassigned inversion peak, I_4, at 1082 cm^{-1} in the emission spectra of the origin and I_0^2 which is missing in the emission spectra of I_1^1 and I_1^3. The calculated potential barriers

for the inversion mode of aniline are 517 cm^{-1} in S_0 and 0 cm^{-1} in S_1. All the observed and calculated results agree well with work published by others.

Aniline-ND_2 and Aniline-NHD

In Figure 6 a hot band appears at 239.0 cm^{-1} in the warmer spectrum which is missing in the jet-cooled spectrum. By analogy with aniline this peak can be assigned as I_1^1. The I_1^1 band for deuterated aniline is shifted by factor of 0.758 which is close to the expected factor of $1/\sqrt{2}$ (or 0.707) mentioned previously. Another hot band for aniline-ND_2 is found at 859 cm^{-1} and is assigned as I_1^3. It is partially overlapped by a weak transition which can be found in the jet-cooled spectrum, but the cold transition appears on the blue edge of the hot band so that it is possible to identify these as two separate transitions. The most intense peak at 546 cm^{-1} of the three that appear at ~ 550 cm^{-1} is assigned as I_0^2. The weakest one in this group is not a inversion transition and will be discussed later. The identification of the one in the middle is hard to determine. A lot of extra peaks in the excitation spectra of aniline-ND_2 come from a different species, aniline-NHD, even though the aniline-ND_2 sample (purchased from CIL) was claimed to have 99 atom percent purity of deuterium. NMR analysis revealed an N-H proton absorption at 3.5 ppm with 25% the intensity of a single proton (ND_2/NHD=3).

Figure 8 shows the dispersed emission spectra of aniline-ND_2. It is clear that the peak at 337 cm^{-1} shows up in both the origin and I_0^2 emission spectra but is missing in the hot band spectra I_1^1 and I_1^3. This band can be assigned as

I_2 for aniline-ND_2. Conversely, the peak at 444 cm^{-1} in the hot band spectra is missing in the spectra of the origin and I_0^2. Since the peak at 444 cm^{-1} has very high intensity in the I_1^3 spectrum, it must be the I_3 band. Calculated fits of the assigned inversion levels in both ground and excited states allows identification of I_4 and I_5. The I_4 band can be found at 707 cm^{-1} in the I_0^2 emission spectrum and is missing in the hot band spectra. And the I_5 (954 cm^{-1}) is found in both the emission spectra of I_1^1 and I_1^3 but is absent in those of the origin and I_0^2.

The peak at -8.2 cm^{-1} in the excitation spectra of aniline-ND_2 (Figure 6) is due to the aniline-NHD species. It can be assigned as the origin because it is close to the origin of aniline-ND_2 and the intensity ratio of NHD to ND_2 species in the spectra is consistent with that observed in NMR spectrum. By selectively exciting the possible inversion bands of aniline-NHD in the spectrum of aniline-ND_2 and dispersing their emission, one can identify the inversion bands of aniline-NHD in both the excitation and emission spectra. However, the assignments of the inversional transitions cannot completely be accomplished due to the influence of ND_2 species. The peaks from 618.0 cm^{-1} to 771.4 cm^{-1} may contribute to aniline-NHD. Figure 9 shows the dispersed emission spectra from peaks which may be attributed to aniline-NHD. We suspect the hot band I_1^1 of aniline-NHD overlaps with that of aniline-ND_2 since the band I_1^1 of NHD is not found as a individual peak in the excitation spectrum at warmer conditions. The actual I^1 of the NHD is estimated to be

Figure 8. Dispersed emission spectra of the inversion transitions in deuterated aniline. The condition for the top trace was 0.2 bar backing pressure and those of the others were 7 bar.

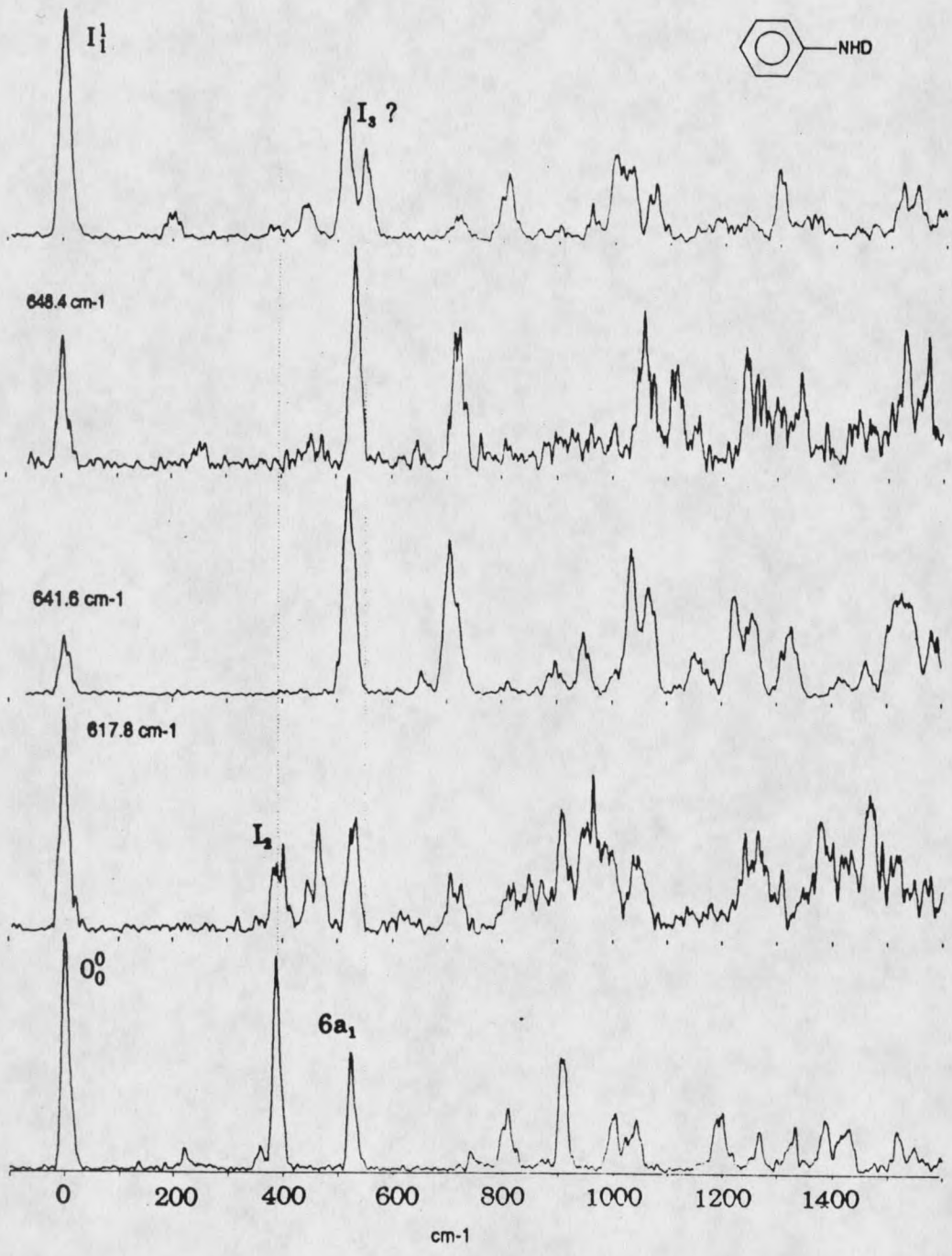

Figure 9. Dispersed emission spectra of the transitions attributed to aniline-NHD.

239 + 7 + 24 - 13 = 257 cm^{-1} if the I_1 for both NHD and ND_2 plus the frequency difference from the ND_2 origin are taken into account. In the I_1^1 emission spectrum of aniline-ND_2 the peak at 551 cm^{-1} cannot be found in all the cold spectra. We are not sure the band at 551 cm^{-1} to be I_3 for aniline-NHD because it seems to be too far from the published frequency 562.6 cm^{-1} for I_3.[6] The peak at 390 cm^{-1} in the origin emission spectrum is absent in the I_1^1 spectrum and is assigned as I_2. The emission spectrum from 618 cm^{-1} also displays a 395 cm^{-1} peak and we assign the 618 as I_0^2 for aniline-NHD. The peaks at 641.6 and 648.4 cm^{-1} in the jet-cooled excitation spectrum were thought to involve some inversion of aniline-NHD. However, the emission spectra demonstrate no transition at 390 cm^{-1} in the emission spectra refuting this possibility. The higher quanta inversion band I_4 of aniline-NHD at ground state is not found. The peak at 910 cm^{-1} in both origin and I_0^2 (618 cm^{-1}) spectra can be attributed to the combination of $I_2 6a_1$ by frequency.

<u>p-Toluidine and p-Toluidine-ND_2</u>

Para-methyl substitution of aniline gives p-toluidine. Even though the methyl group and the amine group are five bond lengths apart, the interaction between the two groups may still affect the internal motion of the NH_2 group via coupling through the conjugated π system. Nevertheless, the ring modes are not significantly affected by the methyl substitution. Figure 10 shows the excitation spectra at jet-hot and jet-cooled conditions. The hot band I_1^1 is found in the warmer spectrum at 291.8 cm^{-1}. I_1^3 is calculated to be about 1186 cm^{-1},

unfortunately this area is covered by the combinations of $6a_0^1$ plus numerous peaks from 700 cm^{-1} to 740 cm^{-1} so that there is no way to identify the weak I_1^3 band in this region.

A significant difference of the I_0^2 band in this spectra from that of aniline is that it is split into a quartet from 729 to 742 cm^{-1} instead of appearing as an individual peak as in aniline. The mechanism for the splitting will be discussed in next chapter. In order to validate the I_0^2 assignment, deuterated p-toluidine was investigated. Figure 11 shows the excitation spectra of deuterated p-toluidine. The most significant difference of the p-toluidine-ND_2 spectrum from that of p-toluidine is that three groups of split peaks show up from 440 cm^{-1} to 570 cm^{-1}. In this region there are two groups of triplet split peaks and one group with a doublet splitting. Such a large band shift means that at least one of them is due to the inversion mode. The NMR spectrum of the sample indicates that the NHD compound is also present at ~ 15%, consistent with the second origin seen at -8.2 cm^{-1} in the cold spectrum. As a result many more transitions appear in the deuterated cold spectrum than in protonated p-toluidine. Changing the relative ratio of NHD and ND_2 enables identification of the transitions due to the NHD species in the excitation spectrum. This is illustrated in Figure 12 in which the top trace has a much higher NHD to ND_2 ratio. Comparison of the two excitation spectra reveals that the three groups of split peaks in the 440-570 cm^{-1} region that were mentioned above are all transitions of p-toluidine-ND_2 because their intensities

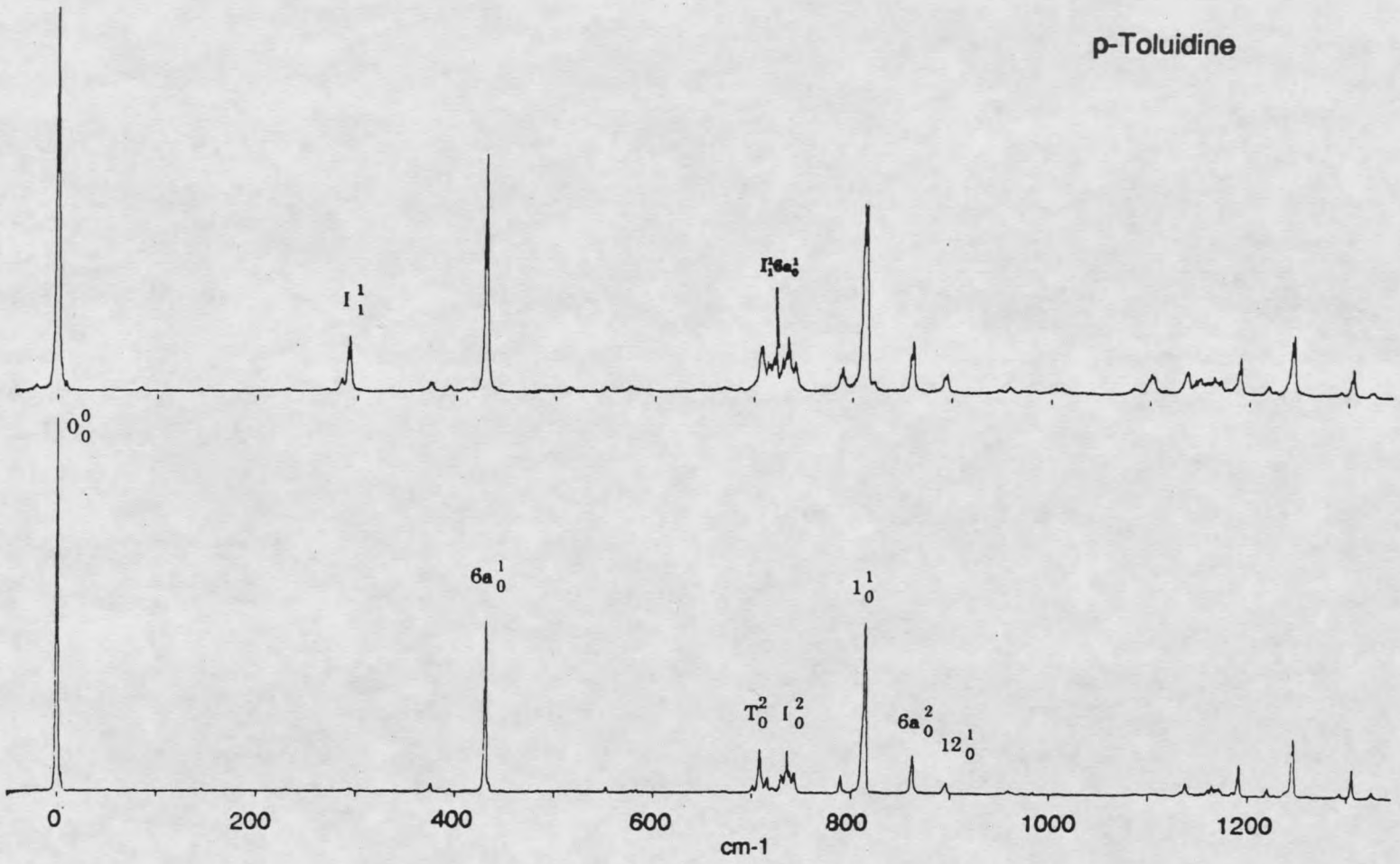

Figure 10. Excitation spectra of p-toluidine. The jet condition for the top trace was 0.2 bar and that for the bottom one was 7 bar.

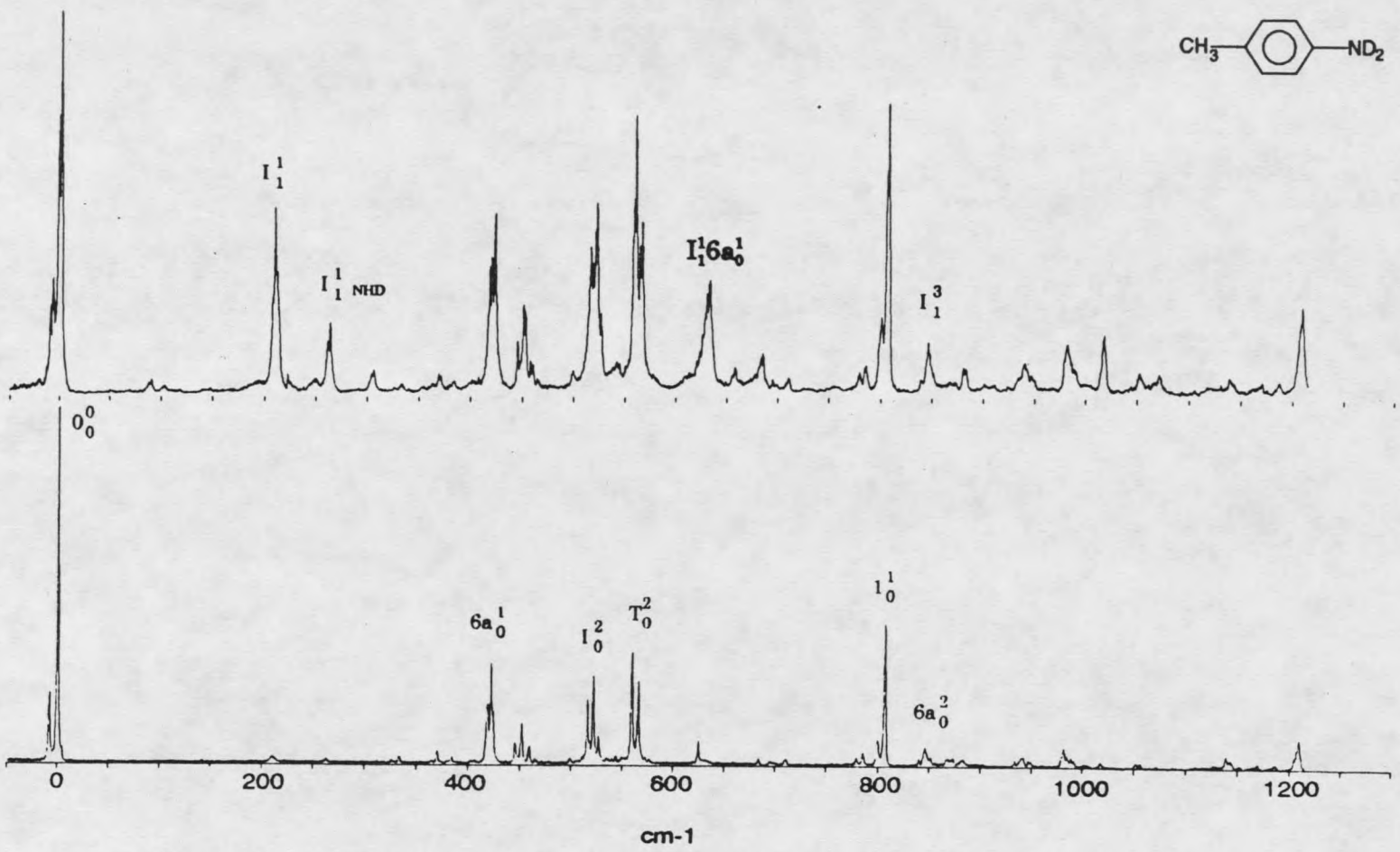

Figure 11. Excitation spectra of p-toluidine-ND_2. The top spectrum and the bottom one were taken under 0.2 bar and 7 bar respectively for the He backing pressure.

do not correlate with the NHD origin intensity. We surmise the I_0^2 band must exist in this region, and can estimate the frequency based on the deuterium effect. For p-toluidine I_0^2 is at 734 cm^{-1}, which yields an estimated frequency of $734 \times \sqrt{2} = 519$ cm^{-1} for the I_0^2 band of ND_2. The triplet peak centered at 521 cm^{-1} from the ND_2 origin is very close to this frequency.

Figure 13 shows the dispersed emission spectra of protonated p-toluidine for the origin, hot band, and the second of the split bands (729.4-742.4 cm^{-1}). The peak at 435 cm^{-1} in the origin spectrum is of very high intensity and overlaps a second, weaker peak which has the frequency 463 cm^{-1}. These two peaks overlap more in the emission spectrum of the 734.4 cm^{-1} band because we had to sacrifice resolution in order to get adequate signal intensity for the weaker excitation transition. Similar structure can be seen in Figure 12 for the other bands, 737.2 cm^{-1} and 742.4 cm^{-1}. In the spectrum of the 729.4 cm^{-1} band, the peak at 435 cm^{-1} is down to the noise level but the peak at 463 cm^{-1} keeps the same relative intensity as in other spectra. The 435 cm^{-1} band is present in all the spectra in Figure 12 except the I_1^1. Based on this evidence, the 435 cm^{-1} peak can be assigned as I_2 and all the quartet splitting peaks in the excitation spectrum can be assigned as I_0^2. The 463 cm^{-1} band appears in all the spectra including the hot band spectrum and is assigned as $6a_1$, consistent with other para-disubstituted benzenes. In the hot band spectrum the peak at 651 cm^{-1} is assigned as I_3. It is absent in the other spectra in the figure and the assignments consistent with Kydd and Krueger's result for the IR transition

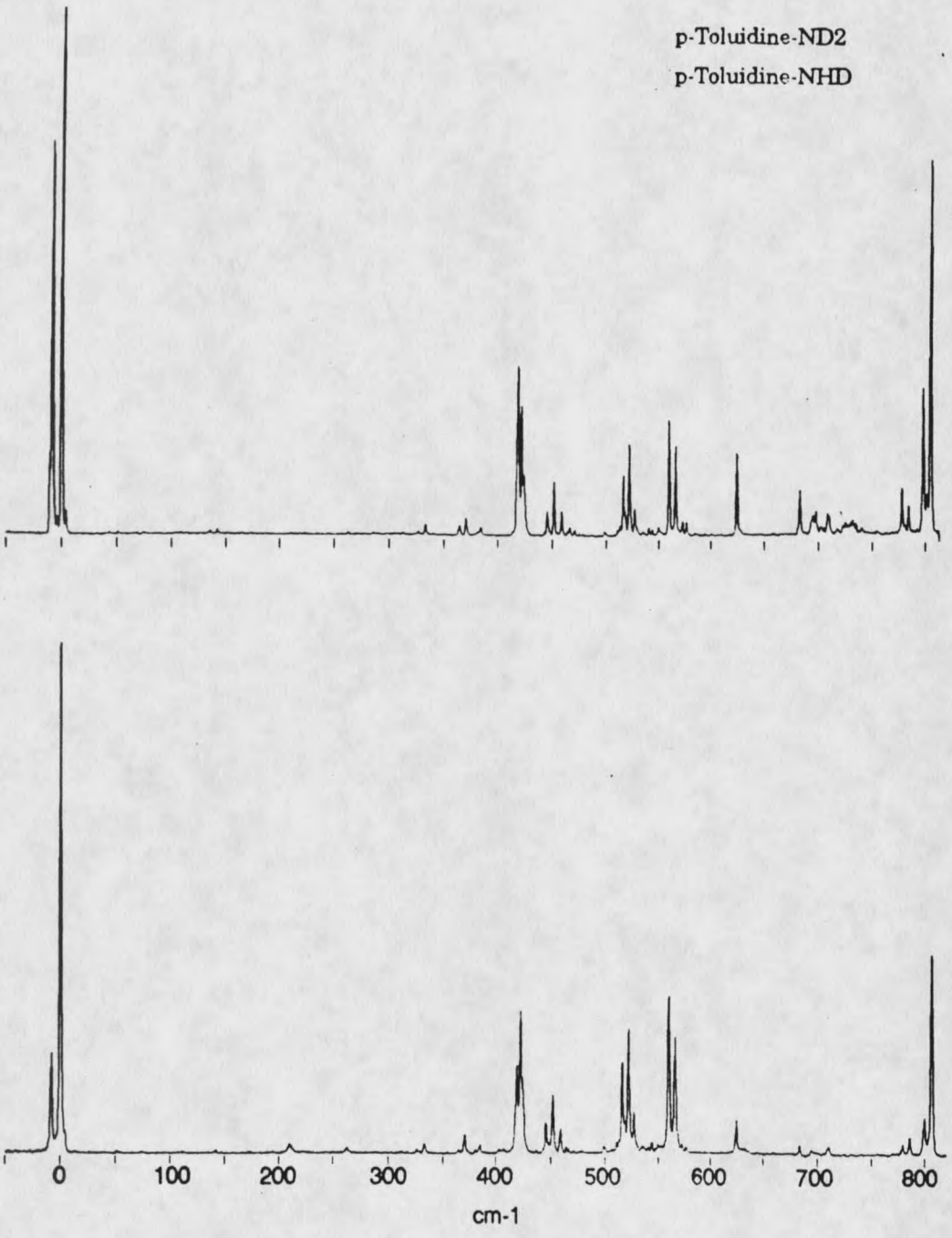

Figure 12. Excitation spectra of p-toluidine-ND_2 taken with different NHD/ND_2 ratios. The intensities of the split transitions in the region between 440 and 570 cm^{-1} do not increase with the intensity of the NHD origin peak (top trace).

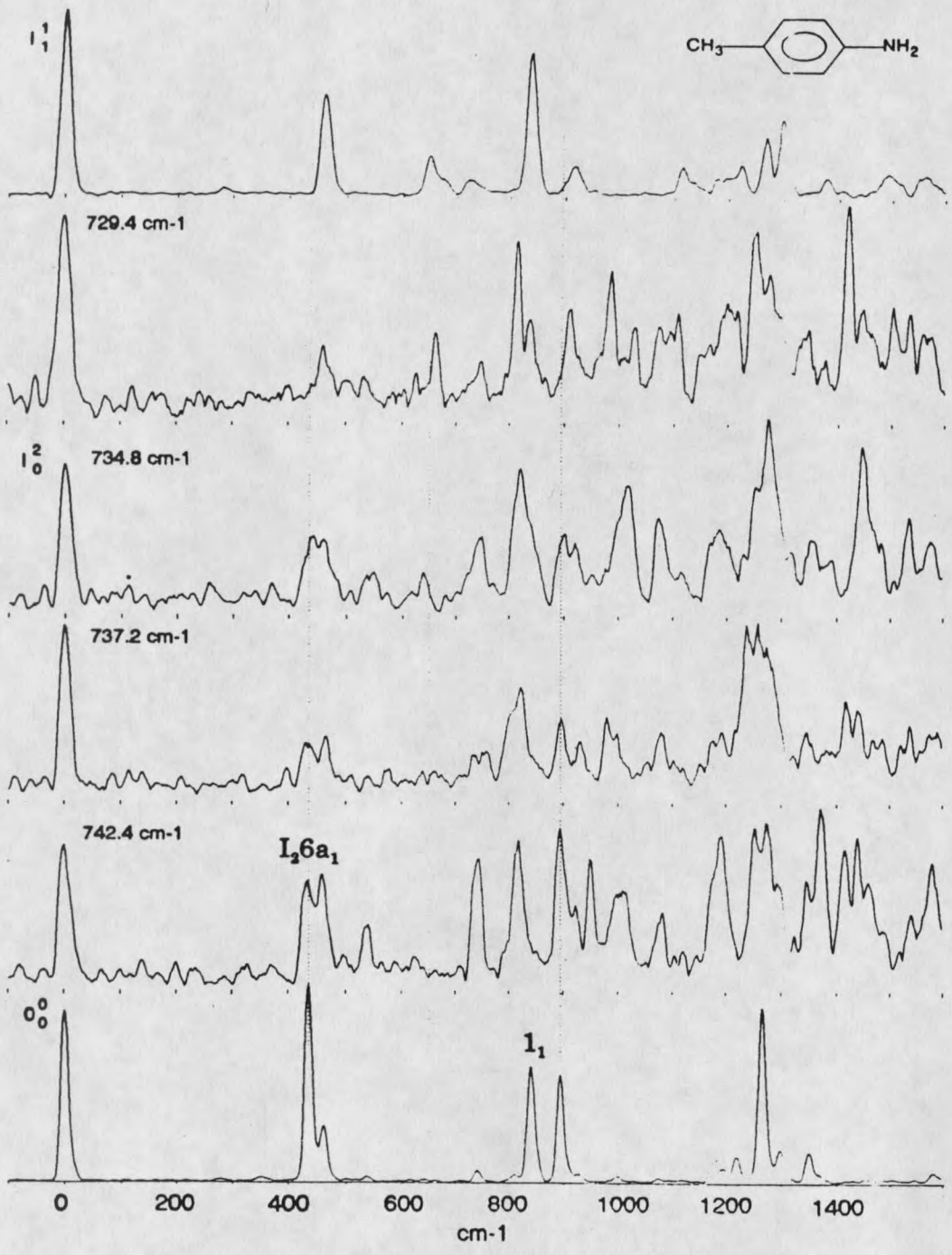

Figure 13. Dispersed emission spectra of p-toluidine for the inversional transitions. The dispersed spectra of split peaks centered at 736 cm-1 in the excitation spectrum are presented together in order for easy comparison.

between I_1 and I_3 as having a 651.3 cm^{-1} frequency.[16]

Further proof of the assignments of I_2 comes from comparing the emission spectra of p-toluidine with p-toluidine-ND_2. Figure 14 gives the emission spectra of the triplet split peaks around 521 cm^{-1} and the inversion hot bands. In the origin spectrum the I_2 band is identified at 310 cm^{-1} which is close to the frequency predicted by the $\sqrt{2}$ rule from 435 cm^{-1} frequency in the protonated molecule. The same peak appears weakly in all the other spectra in Figure 14 including the hot band spectra. This appears to violate the even quanta selection rules, but could conceivably be due to an accidentally degenerate transition. Therefore the peak at 310 cm^{-1} can be tentatively assigned as I_2 for p-toluidine-ND_2.

In the hot band spectra the I_3 band overlaps with $6a_1$. There is no reasonable individual peak that can be found to correspond to the I_3 frequency in the hot band spectra. Just as in aniline and deuterated aniline, we anticipate the I_3 transition to be weak in DE from I_1^1 but strong in the I_1^3 spectrum. That is why there is only a shoulder at 444 cm^{-1} in I_1^1 spectrum but a dominant band at the same frequency in I_1^3 spectrum.

When the above assignments are used for fits, the calculated I_4 and I_5 frequencies are 707 and 976.3 cm^{-1} respectively. However there is no significant transition that can be found to match the calculated frequency for I_4. It is possible that I_5 is the 973 cm^{-1} peak in the hot band spectrum.

In jet-hot excitation spectrum of p-toluidine-ND_2 (Figure 11) a second band

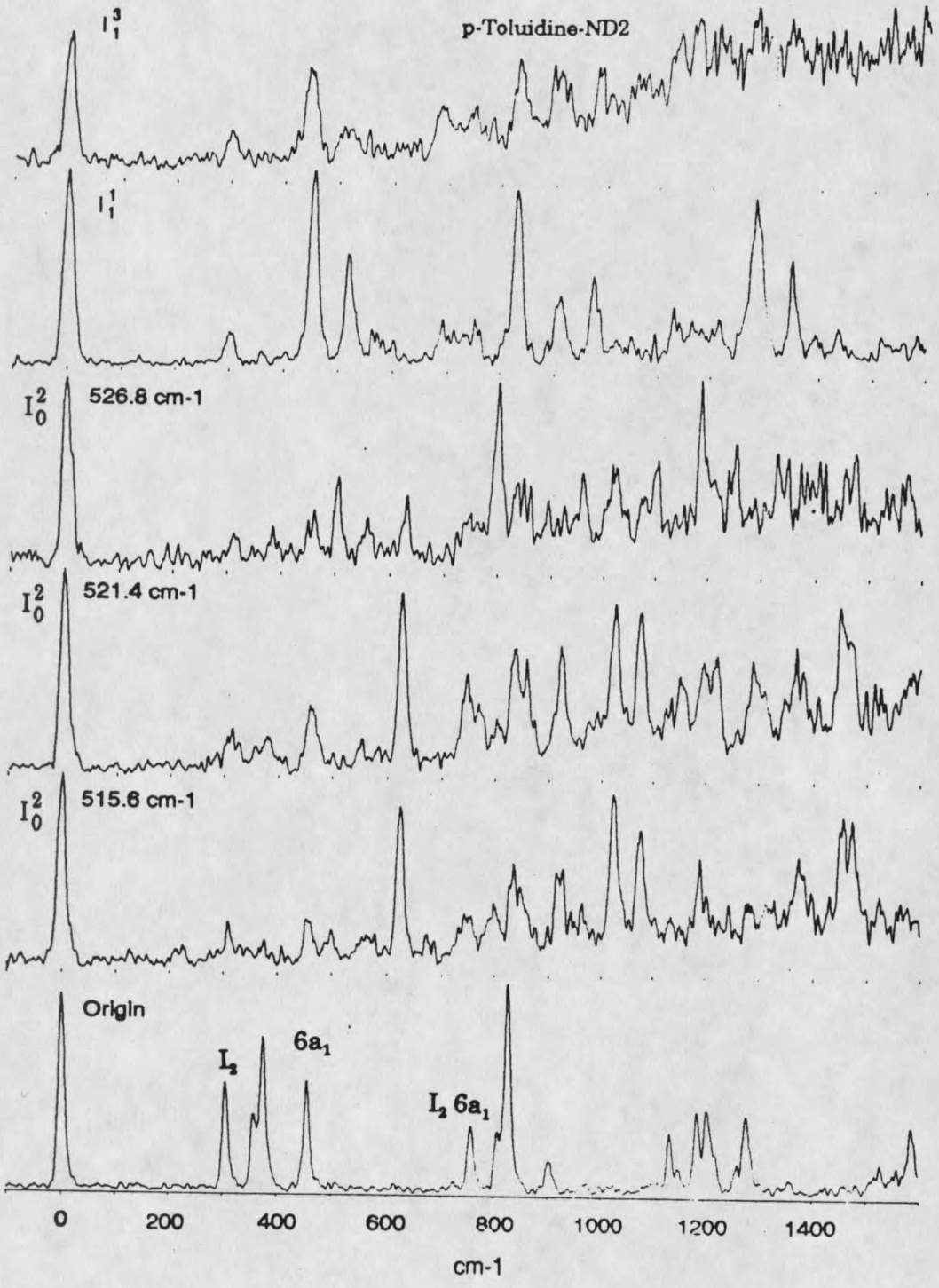

Figure 14. Dispersed emission spectra of p-toluidine-ND_2 for the inversional transitions.

appears at 262.4 cm^{-1} which is I_1^1 for the second species, p-toluidine-NHD. Referring to the assignment of aniline-NHD, the peak at 624.6 cm^{-1} in the jet-cooled excitation spectrum of p-toluidine-NHD can be assigned as I_0^2. In the ground state the I_2 band for NHD species shows up at 403 cm^{-1}. If we consider that the origin peak for p-toluidine-NHD has an 8.2 cm^{-1} blue shift from the origin of p-toluidine-ND_2, the I_2, I_1^1, and I_0^2 bands are 403 cm^{-1} in the ground state, and 270.4, and 632.8 cm^{-1} in the excited state respectively. The I_3 band of p-toluidine-NHD is found at 520 cm^{-1} in the emission spectrum of the I_1^1 262.4 cm^{-1} band.

P-Fluoroaniline and p-Toluidine-CD_3

P-fluoroaniline and p-toluidine-CD_3 were chosen for the study because both of them are isoelectronic with p-toluidine. As mentioned above, the I_0^2 band splitting is thought to be due to the interaction between amine and methyl groups, so changes in the para substituent should affect the splitting significantly but have a very minor effect on skeletal modes. The p-fluoroaniline excitation spectrum is shown in Figure 15 and bears a strong resemblance to the p-toluidine spectrum with the exception that the quartet splitting is absent. This indicates that the splitting observed in p-toluidine is associated with internal motion of the methyl group. If this is the case then the splitting should also be affected in the CD_3 compound (Figure 16). The I_0^2 band center is virtually unchanged (734.8 in CH_3 and 736.8 in CD_3) but the splitting is gone. A possible mechanism for this splitting is discussed

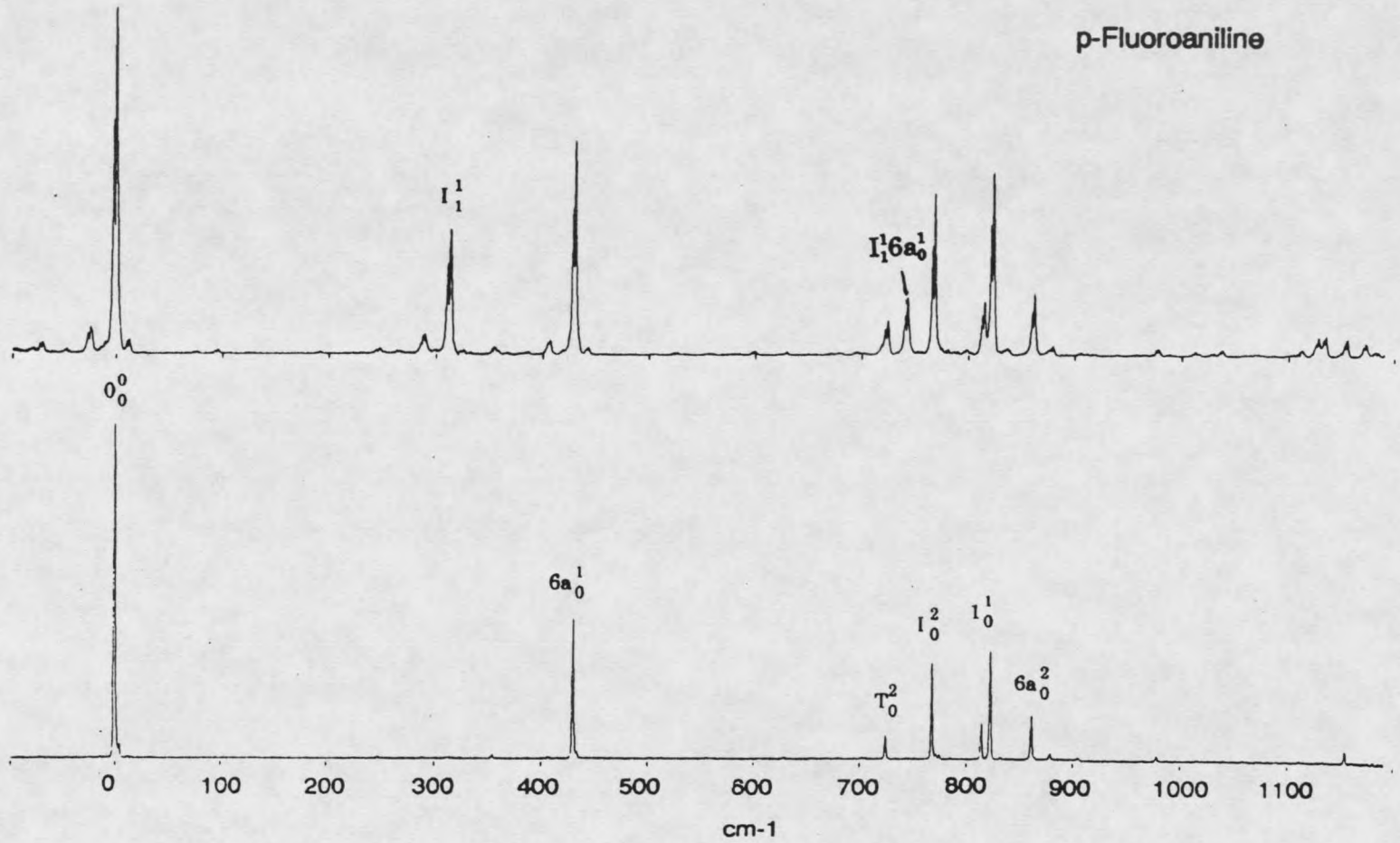

Figure 15. Excitation spectra of p-fluoroaniline. The jet condition was 0.2 bar for the top trace and 7 bar for the bottom one.

elsewhere.

In the warmer p-fluoroaniline spectrum (Figure 15, top) it is obvious that the I_1^1 band appears at 314 cm^{-1}. Use of this and the I_0^2 assignment leads to a calculated frequency for I_1^3 of 1201 cm^{-1}. Unfortunately no hot band appears in this region. We were unable to assign I_1^3 in p-toluidine-CD_3 as well.

The dispersed emission spectra for p-fluoroaniline are shown in Figure 17. The I_2 band shows up at 437 cm^{-1} in the origin spectrum and partially overlaps the $6a_1$ band at 455 cm^{-1}. The relative intensity pattern for I_2 and $6a_1$ looks very similar to that of p-toluidine which may be due to the similarity in both isoelectronic and mass properties of F and CH_3. Careful inspection of the $6a_1$ band in the emission spectra of p-fluoroaniline and p-toluidine reveals that the shift of the $6a_1$ band in p-fluoroaniline is more than that of p-toluidine. The shift of the $6a_1$ band in p-toluidine-CD_3 causes it to overlap with I_2 in the origin spectrum. Therefore, the $6a_1$ shift is a function of the mass of the para-substituted group. The greater the mass of the para substitution the larger the shift of $6a_1$ in the excitation spectrum because this mode involves the motions of the two para-substituents on the ring.

In the I_0^2 emission spectrum of p-toluidine-CD_3, the left shoulder of the 434 cm^{-1} band is I_2. This assignment should be convincing according to the analysis of other molecules presented above.

The frequencies of the nitrogen inversion transitions in the excitation spectra for all the anilines are listed in Table 2. The frequencies marked with

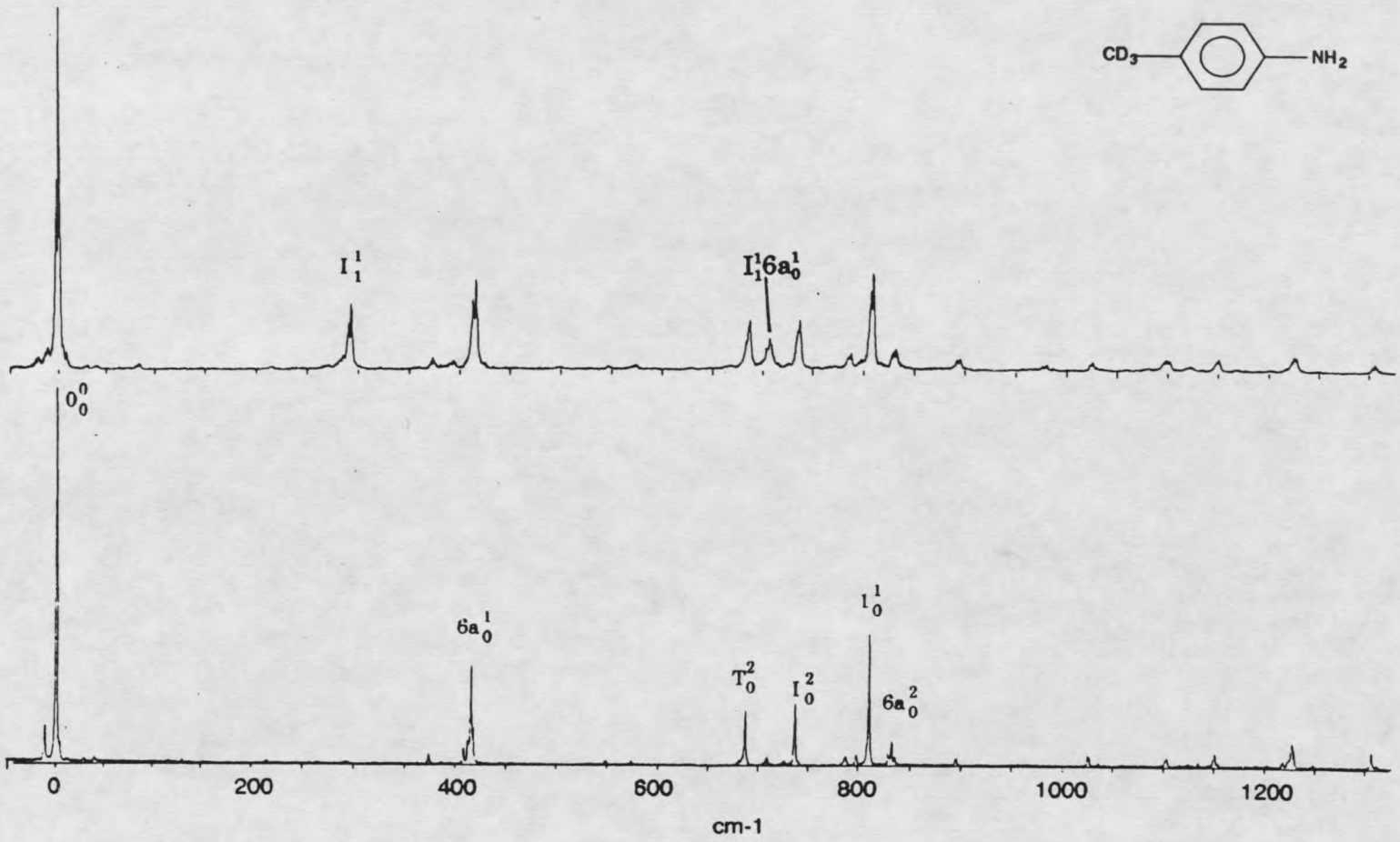

Figure 16. Excitation spectra of p-toluidine-CD_3. The jet condition was 0.2 bar for the top trace and 7 bar for the bottom one.

Figure 17. Dispersed emission spectra of p-fluoroaniline for the NH_2 inversional and torsional transitions.

the superscript * were not observed and are taken from calculations. The assignments, frequencies, and potential parameters for nitrogen inversion are listed in Table 3. For previously studied molecules, the calculated results are close to those published by others.

Table 2. The Frequencies of Inversional Transitions in the Excited State.

Excited State	I_1^1	I_0^0	I_1^0	V_1	V_2	Barr.
C_6H_5-NH_2	292.2	759.6	1183.8	23073	-5575	0
C_6H_5-ND_2	239.0	546.4	859.0	24826	-5683	0
C_6H_5-NHD	246 ?	617.8	959 ?	24234	-5715	0
F-C_6H_4-NH_2	314.0	768.0	1203*	23497	-5562	0
CH_3-C_6H_4-NH_2	291.8	734.8	1159*	22542	-5455	0
CH_3-C_6H_4-ND_2	209.6	521.4	845.2	27865	-7010	0
CD_3-C_6H_4-NH_2	219.8	736.8	1164*	23352	-5684	0

Assignment of the NH_2 Torsion for Aniline and para-Substituted Anilines

The amino torsion is the motion of the NH_2 group twisting about the N-C bond. One of the features of this mode is that there is a double minimum potential in both the ground and excited electronic states. Since NH_2 torsion is an out-plane mode, the selection rules should be even quanta transition allowed. The only transitions that can be observed in the spectra are even to even quanta. This property causes difficulty in fitting the torsional levels and is one reason that the torsional mode has not been assigned previously. A possible exception is the work of Larsen et at[12] who assigned a 236.5 cm^{-1} transition in the IR spectrum of aniline as the combination T_1-I_1. In this work

the methods to be used to identify NH_2 torsional transitions include deuterium substitution, dispersed emission, and computer modeling for all the aniline molecules.

Table 3. The Inversional Levels of the Anilines in the Ground State.

Ground State	I_1	I_2	I_3	I_4	I_5	V_1	V_2	Barr.
C_6H_5-NH_2	40.8*	421	706	1082		40230	-12600	515
C_6H_5-ND_2	13.5*	337	457	707	969	54058	-15539	551
C_6H_5-NHD	22.4*	395	587 ?	909*		45025	-14151	592
C_6H_4-NH_2	31.7[b]	439	707	1089*		41949	-13292	592
CH_3-C_6H_4-NH_2	33.2[b]	437	684	1076		40014	-12766	595
CH_3-C_6H_4-ND_2	11.9*	314	457	708 ?	962	48901	-14922	486
CD_3-C_6H_4-NH_2	31.5*	436	694*	1075*		40459	-12877	593

a. From Ref. 5;
b. From Ref. 7;
*. From calculation only;
?. Not for certain.

The transition at 700.2 cm^{-1} in the excitation spectra of aniline (Figure 5) is most likely a torsional band for NH_2 group because it shows a large deuterium shift.(Figure 6) Its dispersed emission spectrum (Figure 7) shows a unique peak at 729 cm^{-1} which is not observed in any of the other emission spectra. Thus, we assign it as a torsional band in the ground state. The torsional transitions mentioned above can be noted as T_0^2 and T_2 in the excitation and emission spectra, respectively. Further evidence for this assignment comes from a more careful consideration of the ND_2 data. In the excitation spectra of aniline-ND_2, the only possible band for ND_2 torsion is one

of the three close lying peaks around 550 cm^{-1}. Since the inversion band has already been assigned, the torsion band has to be one of the remaining two. In Figure 18, the dispersed emission spectra from the bands near 550 cm^{-1} and the origin are plotted. The 552 cm^{-1} band spectrum has a peak at 658 cm^{-1} and the 559 cm^{-1} band spectrum has a band at 600 cm^{-1}. The frequency of the former seems too large compared to the expected $\sqrt{2}$ change from the NH_2 molecule. We tentatively assign the 559 cm^{-1} transition in the aniline-ND_2 excitation spectrum as T_0^2 and the 600 cm^{-1} frequency as T_2. Higher quanta torsional bands are not easily identified. The computer estimated frequencies for T_4 are 1206 cm^{-1} for aniline-ND_2 and 1490 cm^{-1} for aniline-NH_2. Some transition can be found close to the above frequencies in the emission spectra for the two anilines. In the emission spectrum of 700 cm^{-1} band of aniline-NH_2 (Figure 7) there is a peak at 1488 cm^{-1} which cannot be attributed to a combination band and may be the fourth quanta torsional band of aniline. In the emission spectrum of 559 cm^{-1} band of aniline-ND_2 (Figure 18) there is a transition at 1213 cm^{-1} with similar intensity as the 600 cm^{-1} band which might be T_4. P-fluoroaniline has a very similar feature for the torsion mode as that of aniline. The peak at 724 cm^{-1} in the excitation spectra of p-fluoroaniline looks like it is analogous to the 700.2 cm^{-1} in the aniline spectrum. The dispersed emission spectrum of the 724 cm^{-1} band of p-fluoroaniline shows a intense band at 752 cm^{-1} which is missing in the spectra of the origin and I_1^1 bands.(Figure 17) However, the same band appears at the same frequency in

Figure 18. Dispersed emission spectra of aniline-ND_2 for the three near transitions around 552 cm-1.

I_0^2 emission spectrum with large intensity in p-fluoroaniline but weakly in the I_2 spectrum for aniline. So we tentatively assign the 752 cm^{-1} band as T_2 for p-fluoroaniline. The fourth quanta is calculated at 1522 cm^{-1} but the only peak around this frequency not attributed to a combination band is found at 1538 cm^{-1} in the T_0^2 emission spectrum for p-fluoroaniline.

In the excitation spectra of p-toluidine (Figure 10) the quartet band around 707 cm^{-1} is assigned as T_0^2 because it is shifted significantly by deuterium substitution in the amine group. In the emission spectra of T_0^2 (Figure 19), a strong transition at 746 cm^{-1} can be found in the spectra of 715 cm^{-1} band and is also present with medium intensity in the spectrum of the 707.6 cm^{-1} band. The frequency and intensity closely compares with T_2 of p-fluoroaniline.

It is difficult to identify the T_0^2 in the excitation spectra of deuterated p-toluidine because of the splitting and large number of transitions present. It is possible that T_0^2 may be the doublet at 562 cm^{-1} since the frequency is very close to that of deuterated aniline. In Figure 20, the emission spectra for the transitions from 515.6 cm^{-1} to 565.6 cm^{-1} are presented. In the emission spectra of the 559.4 and 565.6 cm^{-1} bands, a weak peak shows up at 624 cm^{-1}. This band also appears in the emission spectra of I_0^2 from 515.6 to 526.8 cm^{-1} with higher intensity. This behavior in the I_0^2 spectra is similar to that of p-fluoroaniline but the intensity ratio for the band in the I_0^2 and T_0^2 emission spectra are different for the two molecules. Calculated frequencies of the four quanta transition for p-toluidine and deuterated p-toluidine are 1523 cm^{-1} and

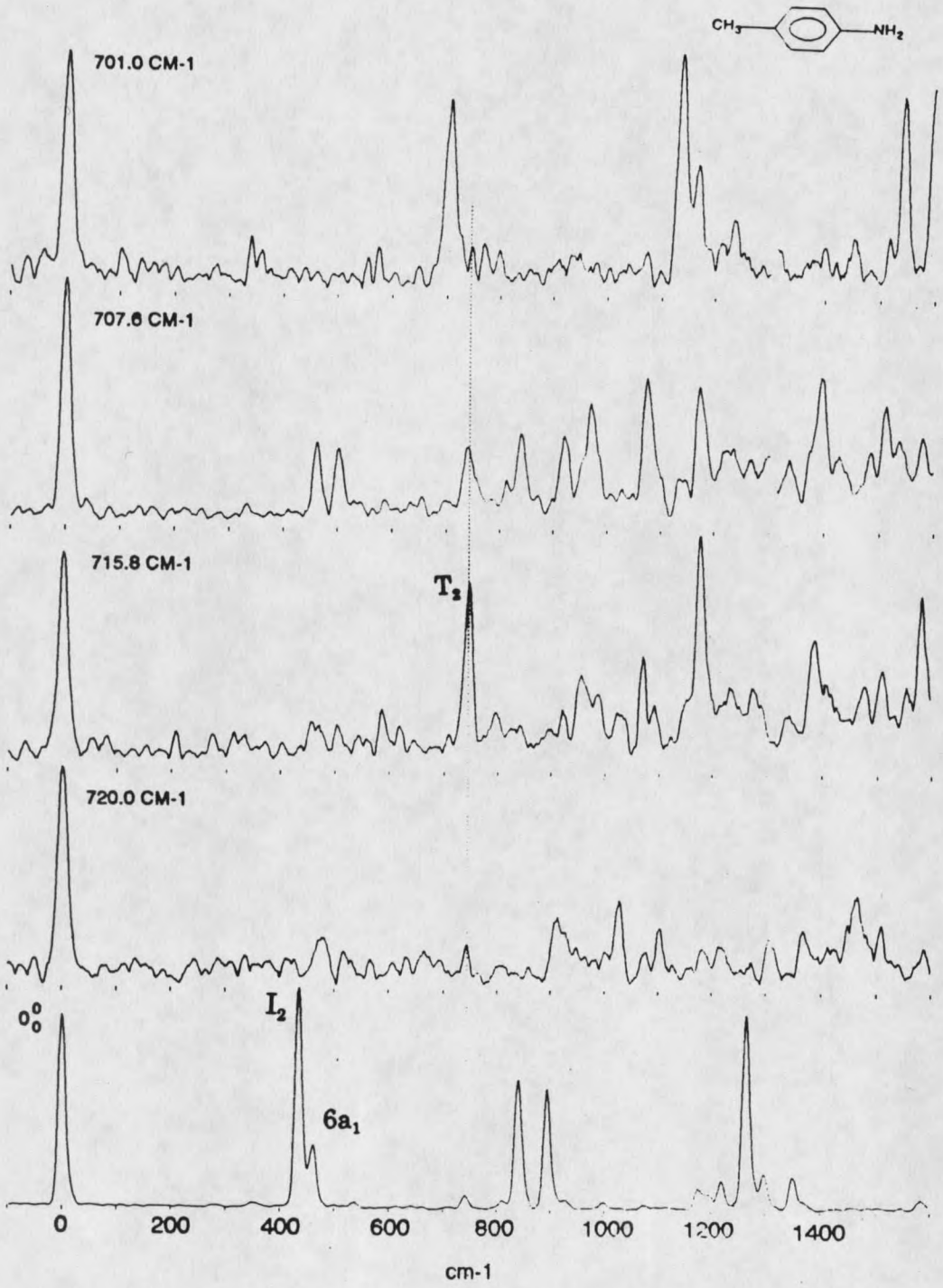

Figure 19. Dispersed emission spectra of p-toluidine for T^2_0 which has a quartet splitting in the excitation spectrum.

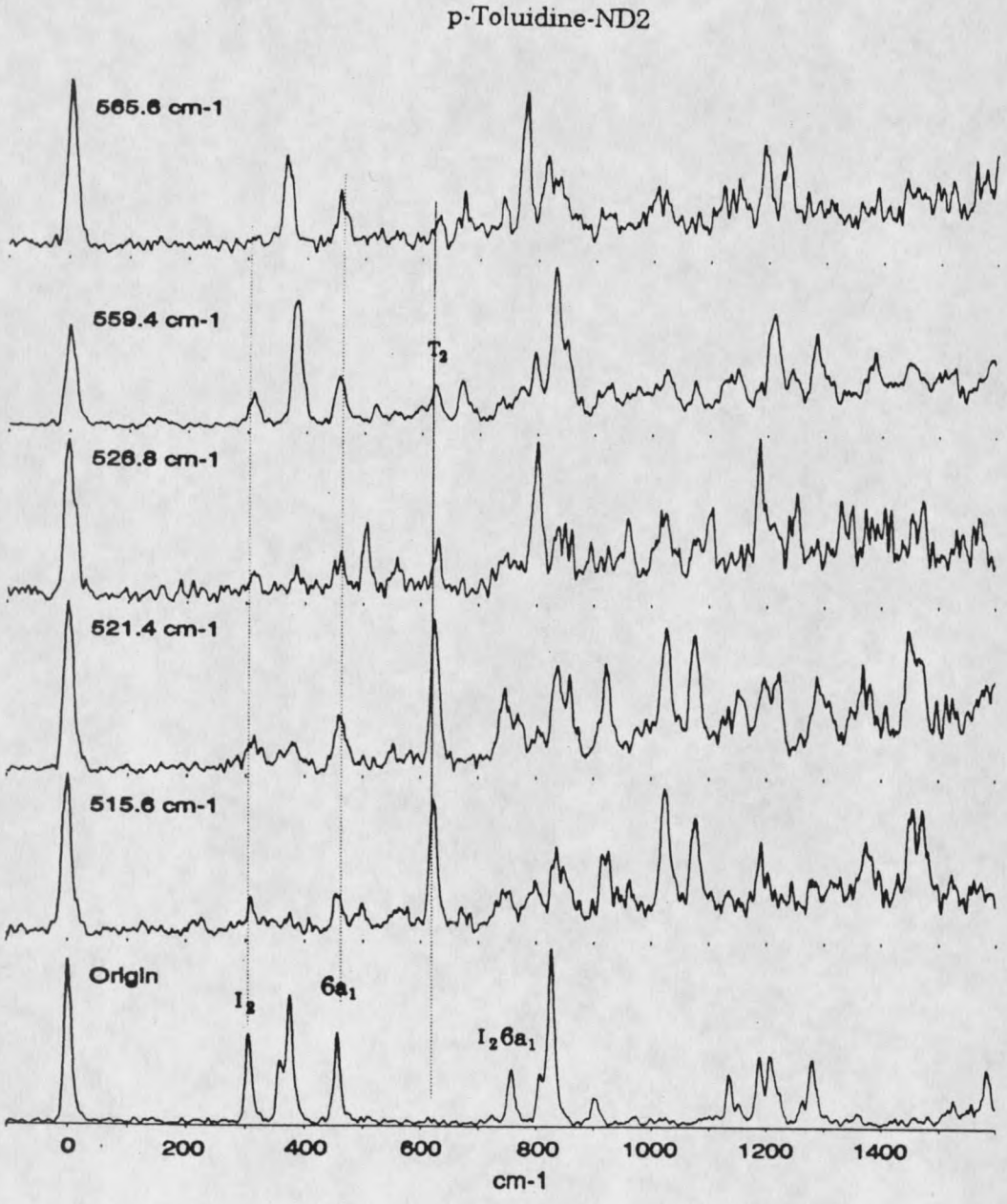

Figure 20. Dispersed emission spectra of deuterated p-toluidine. All the spectra were taken with high backing pressure at 7 bar. The top two spectra are for the doublet peaks and the following three spectra are for the triplet peaks in the excitation spectrum of p-toluidine-ND_2.

1253 cm^{-1}, respectively. The closest peaks that can be found to these frequencies are at 1512 cm^{-1} and 1254 cm^{-1}, respectively.

The T_0^2 of p-toluidine-CD_3 in the excitation spectra is easy to identify as the peak at 687 cm^{-1} by analogy with p-toluidine and p-fluoroaniline. The T_2 peak in the emission spectrum of p-toluidine-CD_3 (Figure 21) is clearly the single band at 713 cm^{-1} which is a reasonable frequency when compared to the other molecules. No band can be identified as the T_4 transition near the calculated frequency of 1465 cm^{-1} because of the spectral congestion in that region.

Table 4 presents the calculated results for modelling the amine group torsion. The potential function used in fitting the observed frequencies is the cosine series

$$V_{tor} = V_2[1-\cos(2\alpha)] + V_4[1-\cos(4\alpha)]$$

in which V_2 and V_4 are potential constants contributing to the barrier height and well shape, respectively. A particle in a ring basis set is used. Since the calculation involves an only single experimental level for each molecule, actual fitting could not be performed. Nevertheless, exploration of the parameter space coupled with experimental observation still yield useful information. For example, there is no splitting observed in the origin or in T^2 for aniline or p-fluoroaniline which would indicate either high barrier or a very low barrier. The high barrier would prevent tunneling and give rise to exactly degenerate levels in the double well. A very low barrier would cause a tunneling splitting

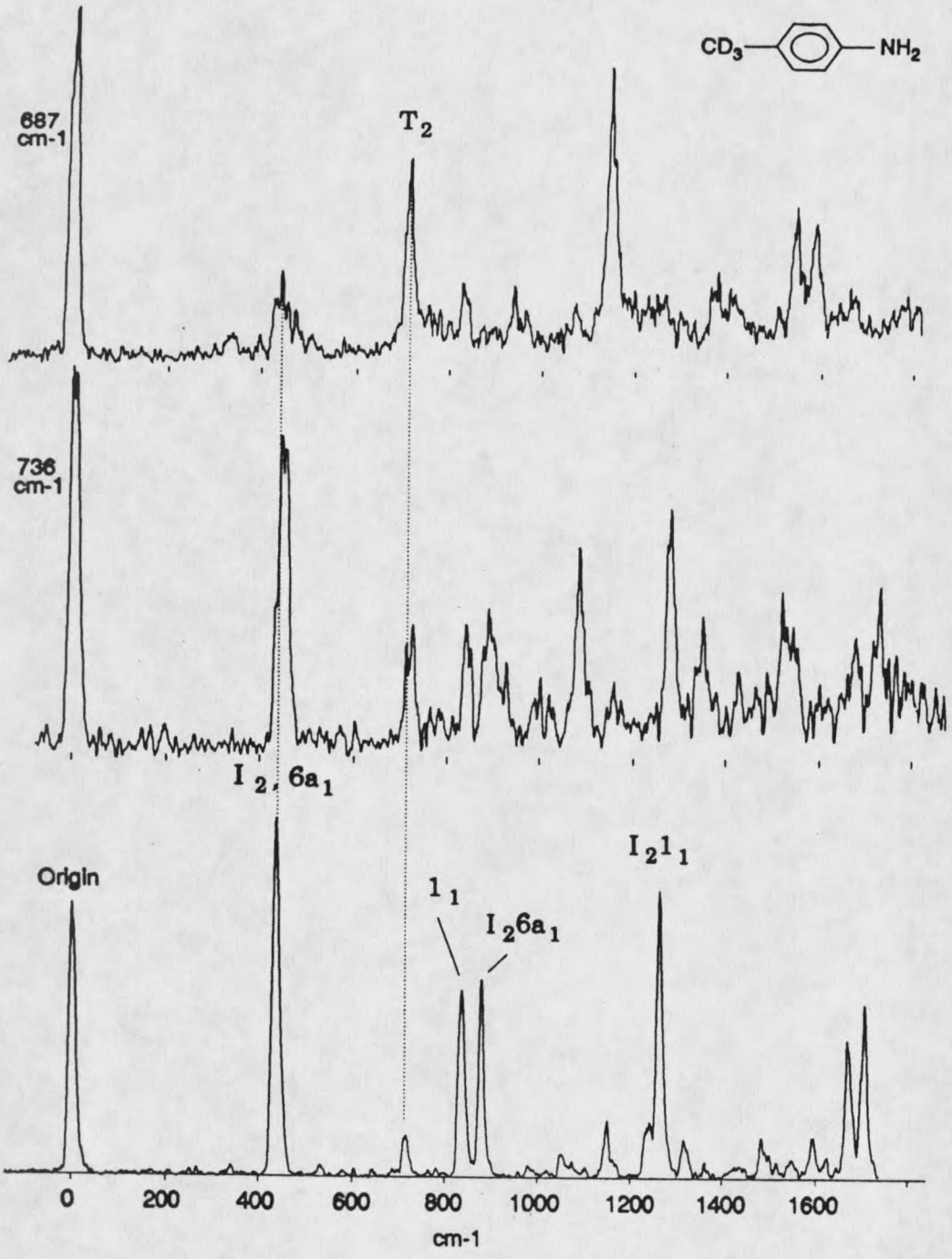

Figure 21. Dispersed emission spectra of p-toluidine-CD_3. Notice that the I_2 and the $6a_1$ bands are overlapped in the spectrum from the origin. All spectra were taken at high backing pressure (7 bar).

but would separate the transitions to such a large degree that they would be perceived as individual peaks rather than as a splitting (as occurs in the inversion in the ground state of aniline which has a 40 cm^{-1} splitting). Chemical intuition and spectroscopic data favor the high barrier. With a low barrier we would expect to observe a hot band originating from T_1 but this did not occur. Calculations required a value for the reduced internal rotational constant, B, which we determined using typical values for N-H bond lengths and angles. Use of this value allowed exploration of the V_2, V_4 parameter space. While a variety of values for these potential term and the barrier height gave acceptable values for the T_0^2 frequency, barrier heights > 14000 cm^{-1} would not fit this frequency and the barrier cannot be lower than 3000 cm-1 even V_4 = 0 cm-1. The best frequency for all species were found with barriers in the 6000-7500 cm^{-1} region. These barriers yielded levels which were doubly degenerate for low quanta and which had a 30-50 cm^{-1} anharmonicity.

Table 4. The Calculated Torsional Levels and Potential Parameters for Anilines

Transition	ϕ-NH_2	ϕ-ND_2	F-ϕ-NH_2	CH_3-ϕ-NH_2	CH_3-ϕ-ND_2	CD_3-ϕ-NH_2
Ground State						
T_1	358	298	368	369	311	349
T_2	728*	599*	747*	747*	624*	712*
T_3	1106	902	1132	1133	938	1085
T_4	1149 (1488)[a]	1206 (1213)[a]	1522 (1538)[a]	1524 (1512)[a]	1252 (1254)[a]	1464
V_2 [b]	6610	7375	6735	6745	7595	6635
V_4	-840	-685	-815	-815	-635	-905
Excited State						
T^1	337	305	351	342	277	329
T^2	700*	559*	724*	707*	562*	685*
T^3	1080	848	1112	1089	853	1059
T^4	1470 (1137)	1143	1511	1481 (1140)	1148	1445
V_2 [b]	6125	6505	6250	6105	6545	6045
V_4	-1015	-835	-980	-985	-835	-1035

* The level is used for computer fitting.
a The number in the bracket can be found in the spectrum.
b The barrier height is equal to V_2.

P-amino-p'-methyl-trans-Stilbene

P-amino-p'-methyl-trans-stilbene (PPTS) is a molecule with an amine and a methyl substituted on the two para positions of trans-stilbene. Our interest in this molecule comes from the presence of two non-rigid substituents, large amplitude motions in the chromophore, and the possibility of substituent interaction over the conjugated π system. The low frequency modes of PPTS

are generated not only by the substituted groups, but also by relative motions of the two phenyl rings. In trans-stilbene (no substitutions) there are three such low frequency modes, the in-plane phenyl wag, the out-plane phenyl flap, and the phenyl torsion. The notation for the three modes are ν_{25}, ν_{36}, and ν_{37} respectively, after Warshel's calculation[41] and they are pictured in Figure 22. Additional low frequency modes of PPTS come from the internal modes of the two para-substituents which are the methyl group torsion, and the amino group inversion and torsion.

The fluorescence excitation spectra of PPTS are shown in Figure 23 (the top trace is a warm spectrum and the bottom trace is a cold one). In the jet-cooled excitation spectrum of PPTS, there is a significant difference from the excitation spectrum of trans-stilbene.[35,37,42,44] However, the excitation spectrum of PPTS is similar to that of p-methyl-trans-stilbene (PMTS).[30] A doublet splitting appears at the origin and the other strong skeletal transitions in the spectra of both methylated molecules. A number of transitions dominate the low frequency region in the two spectra and it is obvious from the similar behavior of the two spectra that the very low frequency structure can be attributed to the substituent, CH_3. Thus, the methyl torsion transitions in the excitation spectrum of PPTS are expected to possess some similarities to those of p-methyl-trans-stilbene.

Methyl torsion can be treated as a hindered rotation around a symmetric axis. According to the selection rules of methyl torsion, the allowed transitions

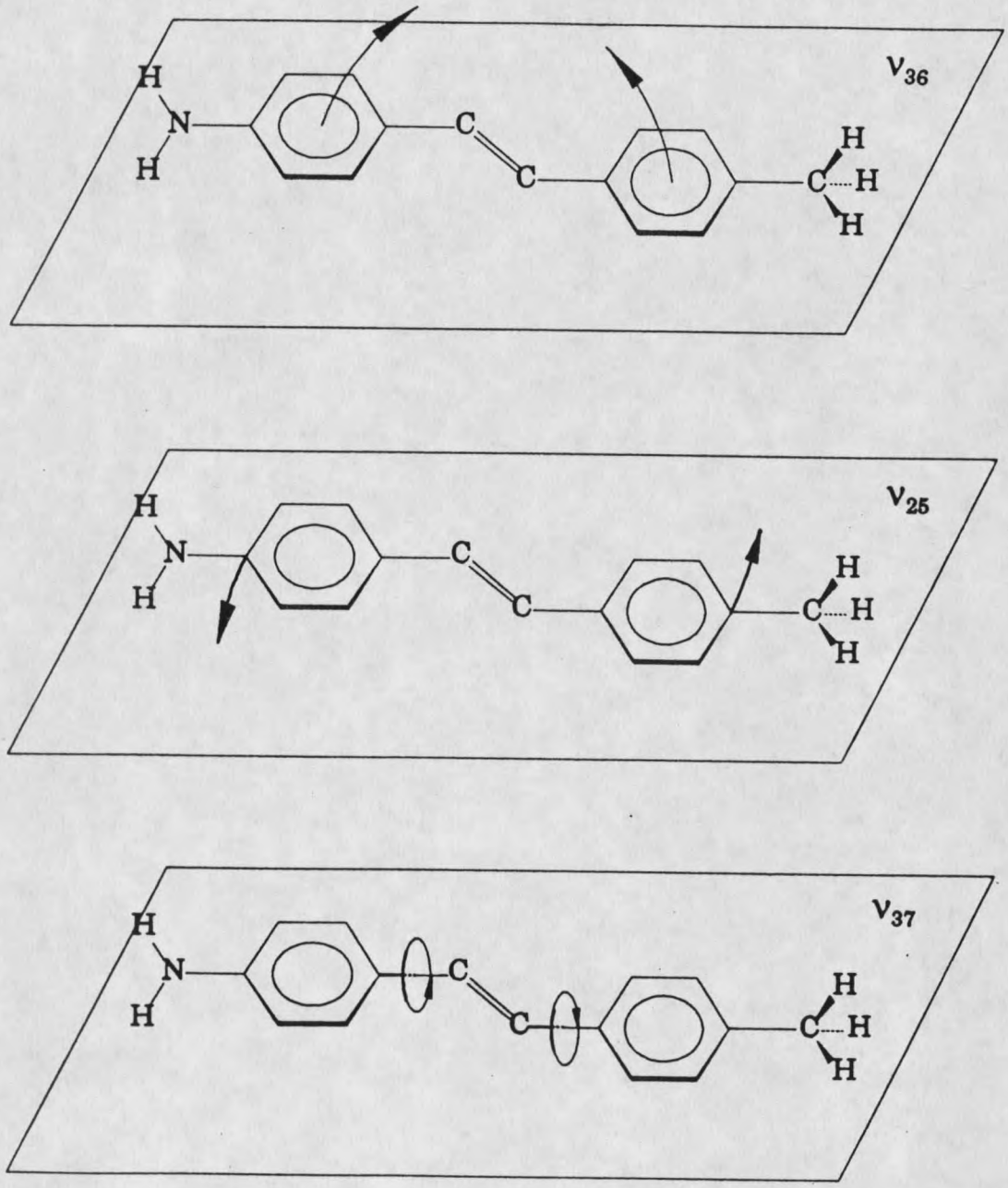

Figure 22. The low frequency skeletal modes of p-amino-p'-methyl-trans-stilbene.

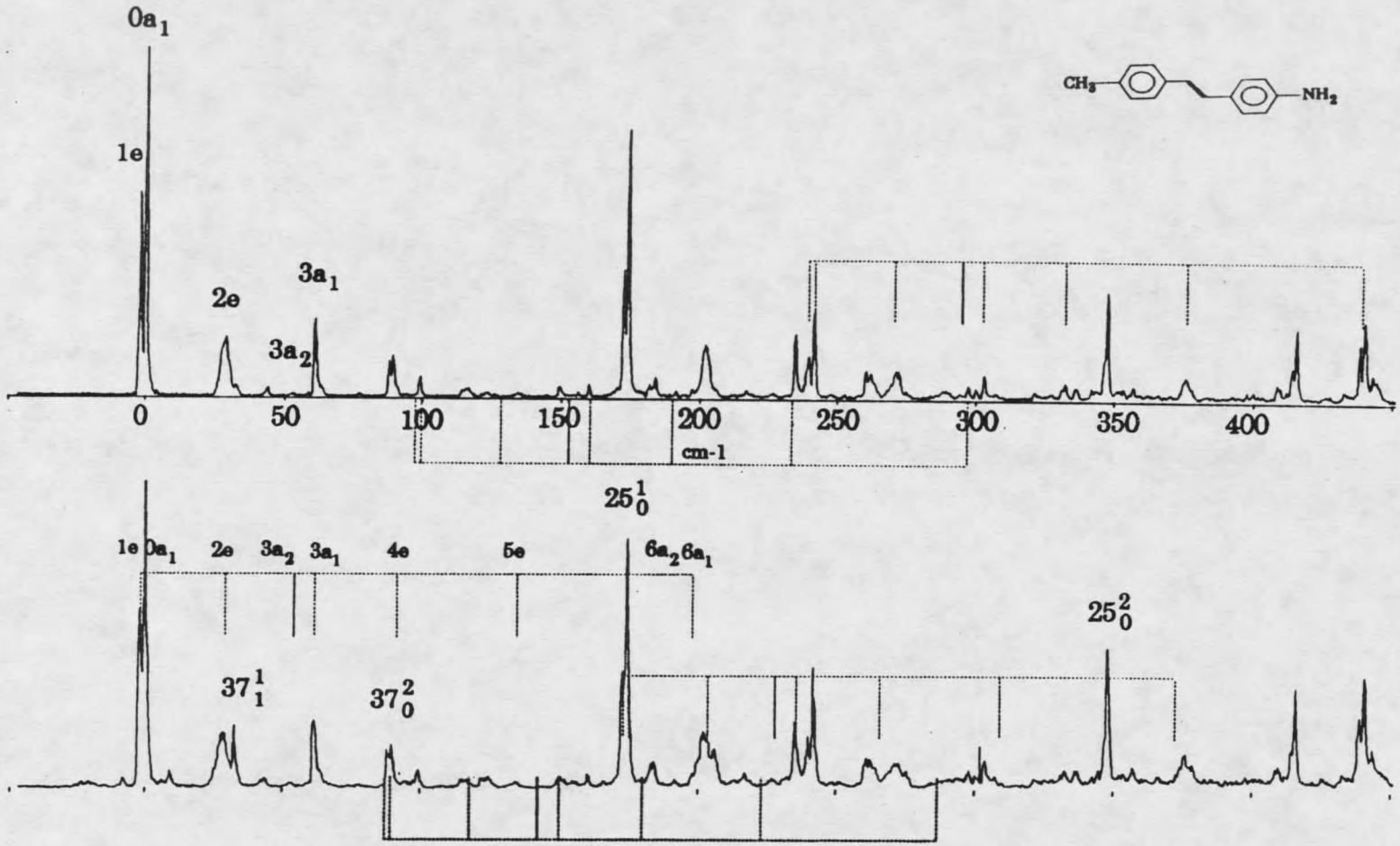

Figure 23. Excitation spectra of PPTS. The top trace was taken under high backing pressure (7 bar) and the bottom one at 0.2 bar.

can only happen for a to a or e to e levels between ground and excited states. The torsional levels have the order $0a_1$, 1e, 2e, $3a_2$, $3a_1$, 4e, 5e, $6a_2$, $6a_1$, ··· (with increasing energy) for both ground and excited states. The special intensity pattern of the low frequency transitions in the region from the origin to 61 cm^{-1} will be referred to as methyl rotor structure. This structure is repeated in combination with every strong transition in the excitation spectrum of PPTS. The split origin peak in the excitation spectrum of PPTS (Figure 23) results from the a and e tunneling splitting. We assign the more intense peak of the origin as $0a_1$ and the weaker one, at lower frequency as 1e. The splitting of the origin is 1.8 cm^{-1}, which means that the transition frequency of $0a_1 \leftarrow 0a_1$ is higher than that of 1e ← 1e. The 1e level in the ground state is predicted to have slightly larger spacing from the $0a_1$ level than exists for $0a_1$ in the excited state counterparts. The very broad band at 29.1 cm^{-1} is assigned as the 2e band which comes from the 2e ← 1e transition. There are actually two transitions contributing to any e to e transition band due to the double degeneracy of e levels. If the barrier for the methyl torsion is not very high, a slight splitting of the degenerate e levels will be expected. If the e level were completely degenerate in both states, the band width of the 2e would be the same as that of the $0a_1$ in the excitation spectrum. This difference in width aids in making assignments.

A sharp peak at 61.1 cm^{-1} in the spectrum is assigned as the $3a_1 \leftarrow 0a_1$ transition. Higher level transitions for the methyl rotor are not obvious in the

excitation spectrum because of their low intensities and their overlap with other bands.

Dispersing each individual peak in the excitation spectrum provides the evidence for the assignments for the methyl torsion transitions in the excitation spectrum. The dispersed emission spectra of a′ and e′ bands in the excitation spectra are plotted with the same scale in Figure 24. The peak at 20 cm^{-1} is present in both 1e′ and 2e′ emission spectra but is missing in the $3a_1'$ spectrum. There is a weak peak at 24.3 cm^{-1} in $0a_1'$ emission spectrum but its frequency is 4 cm^{-1} different from the peak at 20 cm^{-1}. The 24.3 cm^{-1} frequency can be attributed to another transition which will be discussed in detail later. Therefore the peak at 20 cm^{-1} can be assigned as 2e″ in the emission spectra. The 2e″ band partially overlaps the one at 24 cm^{-1} due to the low resolution of the monochromator. The $3a_1''$ band appears as a very strong transition at 52 cm^{-1} in the $3a_1'$ emission spectrum. This band is missing in the 2e′ spectrum.

The assignments of methyl torsion bands are strongly supported by the evidence of correlating the transitions in both excitation and emission spectra, the band widths, and the presence of combination bands. Unfortunately we cannot determine absolute frequencies for the 1e levels in our experiments. We can measure the $0a_1$, 1e transition splitting which is dependent on the level splitting in both electronic states. Selection rules prevent measurement of 1e″ relative to $0a_1''$ so the second parameter needed for this determination is absent. The splitting, however, can be calculated with high confidence.

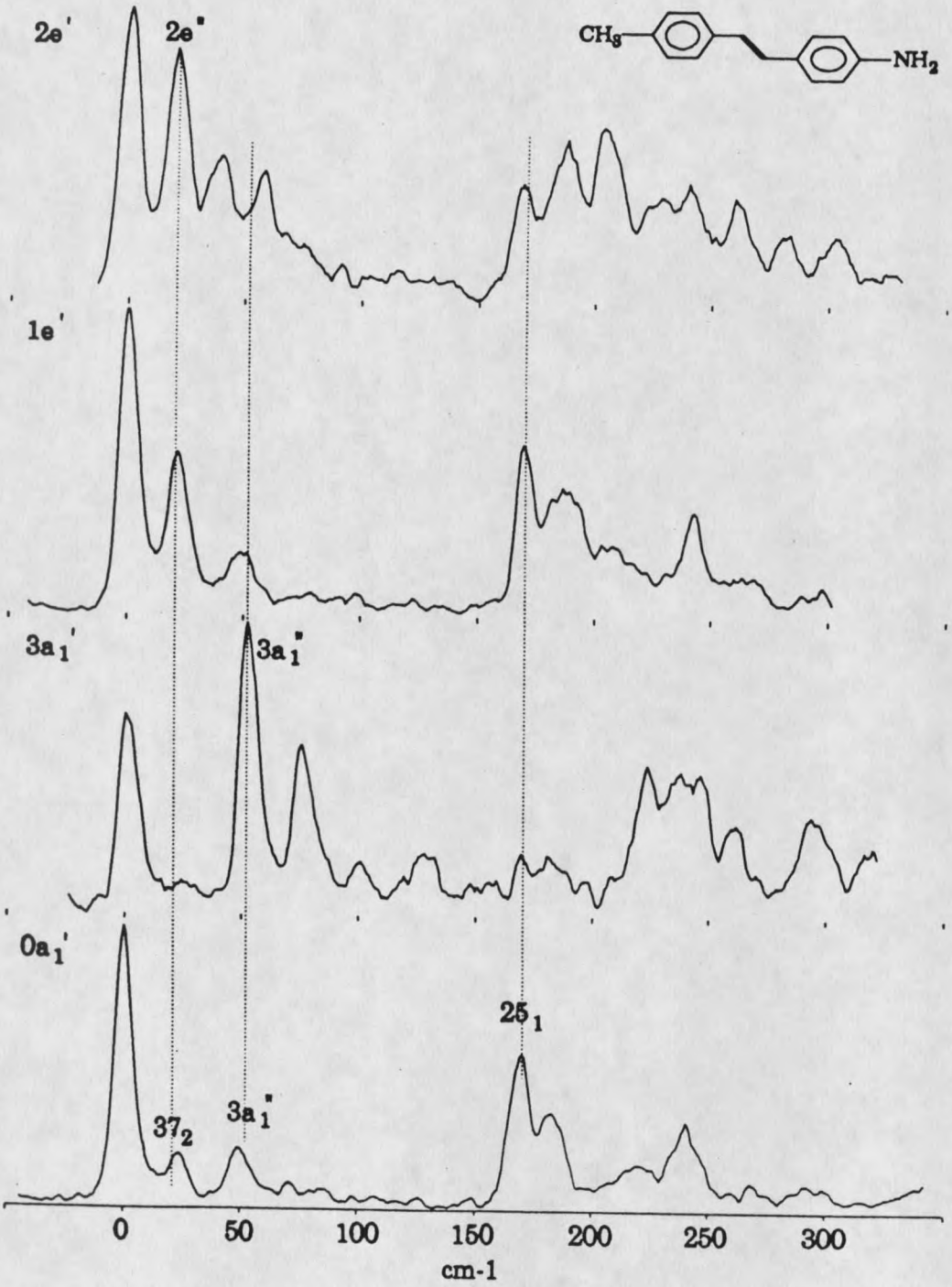

Figure 24. Dispersed emission spectra of PPTS for methyl torsional transitions. The top two are for the "e" levels and the bottom two are for the "a" levels.

Calculation for the methyl torsion levels was performed with the same programs used in the calculations for inversion levels. The potential term used in the perturbation Hamiltonian is

$$V(\alpha) = \frac{1}{2}V_3(1-\cos 3\alpha) + \frac{1}{2}V6(1-\cos 6\alpha)$$

in which V_3 and V_6 are potential term constants and α is the coordinate corresponding to the conformation of the methyl rotor. A particle in a ring basis set is used for the wavefunction of the methyl rotor. The internal rotation constant B, is estimated by using tetrahedral structure and the typical C-H bond length of methane. The observed methyl torsion levels were first fit for $0a_1$, 1e, 2e, and $3a_1$ in each electronic state by adjusting the B value during the preliminary calculation in VNCOS program. The VNCOS calculation yields the barrier height and the potential term constant for each individual electronic state. These least fit parameters are then used in INROT, which is capable of calculating energy levels for two states simultaneously and transition intensities between them.

The calculated 1e level in the ground state is 4.5 cm^{-1} with ± 0.5 cm^{-1} accuracy. The 1e level in the excited state can be determined to be 2.7 cm^{-1} according to red shift of the 1e transition by 1.8 cm^{-1} relative to the $0a_1$ band in the excitation spectrum. The 4e, 5e, and $6a_1$ levels in both states can be identified in the spectrum by referring to the calculation. Both observed and calculated frequencies for methyl torsional levels of PPTS are listed in Table 5.

Table 5. The Frequencies and Potential Term Constants of Methyl Torsion for PPTS in the Ground and the Excited State.

Energy Level	Frequency (cm^{-1})		Max
Observed	Calculated	Error	%
Ground State B = 5.1 cm^{-1}			
$0a_1$	0	0.0	± 5.6
1e	-	4.5	
2e	22	22.3	
$3a_2$	45	45.4	
$3a_1$	52	51.5	
4e	82	82.7	
5e	125	128.5	
$6a_1$	183	184.6	
V_3		18.9	
V_6		-5.2	
Excited State B = 5.3 cm^{-1}			
$0a_1$	0.0	0.0	± 0.4
1e	-	2.7	
2e	31.8	33.0	
$3a_2$	53.1	51.6	
$3a_1$	61.1	61.0	
4e	91.0	92.7	
5e	137.8	139.9	
$6a_1$	197.3	197.9	
V_3		54.1	
V_6		-5.9	

The transitions of the low frequency modes of trans-stilbene and p-methyl-

trans-stilbene have been identified in both their fluorescence excitation and dispersed emission spectra.[35,37,44,45] The mode of the phenyl ring in-plane wag of the two stilbenes is denoted ν_{25} which is totally symmetric and harmonic. The observed frequency of the fundamental in the excitation spectrum is 198 cm^{-1} in trans-stilbene and 183 cm^{-1} in PMTS.[42,30] The selection rule for ν_{25} is any quanta allowed. The overtones of the ν_{25} mode of trans-stilbene are intense enough to observe a progression up to the fourth quanta in the excitation spectrum.[42] There is only slight change for the ν_{25} frequency in the dispersed emission spectrum compared with that in the excitation spectrum.

Figure 25 shows a larger range excitation spectrum of PPTS and the strong transition at 174 cm^{-1} can be assigned by analogy as 25_0^1. This is in good agreement with the 25_0^1 frequency of 198 cm^{-1} in trans-stilbene and 183 cm^{-1} in PMTS.

The second overtone of ν_{25} in PPTS appears at 347.7 cm^{-1}. The first quanta of ν_{25} in ground state is measured at 170 cm^{-1} in the dispersed emission spectra of PPTS (Figure 26). This band is prominent in the dispersed emission from all S_1 levels we investigated.

In the out-plane mode ν_{37}, each phenyl ring twists about the C_{ph}-C_e axis distorting the molecule into a propeller like geometry. The selection rules for mode ν_{37} are even quanta transitions allowed because it is not totally symmetric. We assign the 89.7 cm^{-1} peak as 37_0^2, similar to the 90.2 cm^{-1} frequency for this transition in PMTS. The similarity of 37_0^2 in the two

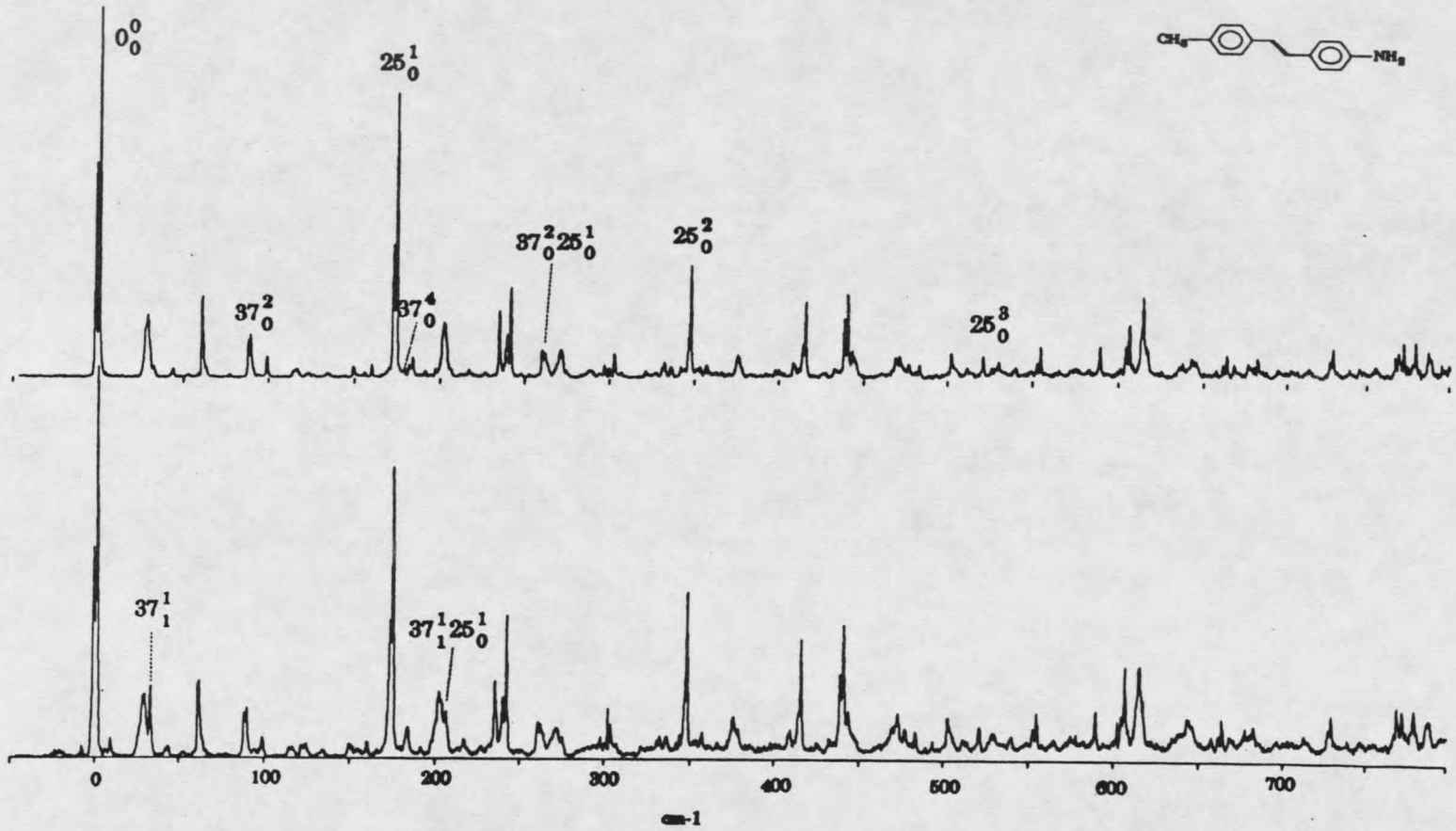

Figure 25. Excitation spectra of PPTS with larger frequency range. The top trace was taken under a high backing pressure at 7 bar and the bottom one at 0.2 bar.

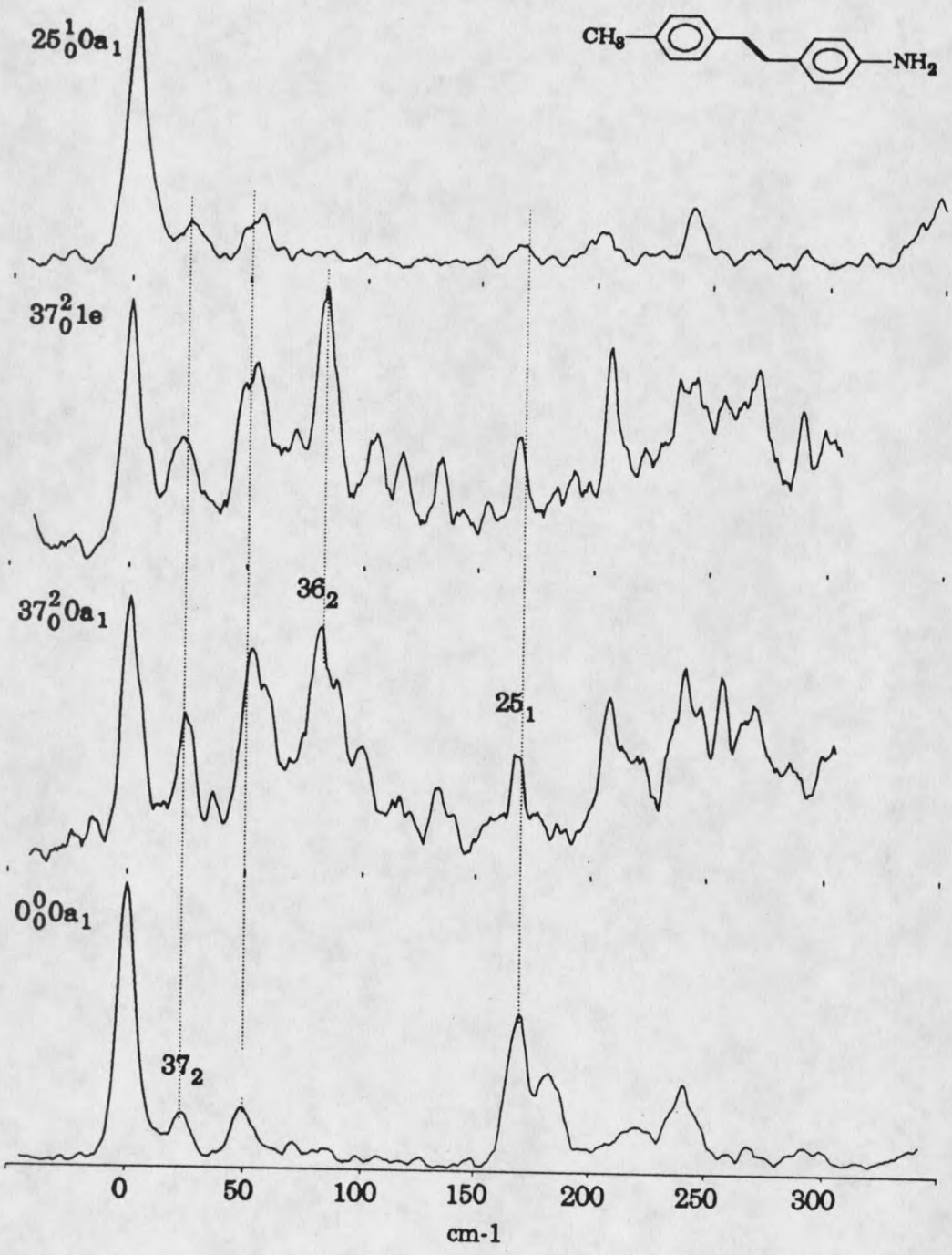

Figure 26. Dispersed emission spectra of PPTS for the transitions involving mode ν_{37} and mode ν_{25}.

molecules is reasonable given that the heavy atoms of the substituents lie on the torsional axis and will have little effect on the moment of inertia. The higher quanta transition 37_0^4 cannot be identified conclusively in the excitation spectrum due to its low intensity and overlap with other bands, however, the band at 178.9 cm^{-1} is a possibility.

The dispersed emission spectra of PPTS for the origin, 37_0^2, 37_0^21e, and 25_0^1 are shown in Figure 26. All display a peak at 24 cm^{-1} in the emission spectra. Transitions at similar frequencies are observed in stilbene and PMTS. The fact that the frequency changes little with para substitution, and that the frequency is present in the unsubstituted stilbene, indicates that this transition is due to the ν_{37} mode and we assign it as 37_2. The 37_4 transition is submerged by the $3a_1$ band in the emission spectra. However a transition at 48 cm^{-1} can still be distinguished from the $3a_1''$ band in the 37_0^21e spectrum.

There is a strong hot band that appears at 32.7 cm^{-1} in the excitation spectrum with slightly warmer conditions for the jet.(the lower trace in Figure 25) Compared with the transitions in the jet-cooled spectrum, the band widths of all the transitions in the warm spectrum are nearly the same. This similarity means that the jet conditions for the two spectra were actually not greatly changed. Therefore, the intensity of the hot band in the warm spectrum must come from a very low, non-zero level in the ground state. For non-totally symmetric modes the strongest hot band must be the transition from the first quanta in the ground state to the first quanta in the excited

state. Referred to the assignments of 37_1^1 for trans-stilbene and PMTS,[29,11] we assign the hot band at 32.7 cm^{-1} in the warm spectrum as 37_1^1 for PPTS. The out-plane mode ν_{36} of PPTS has the same selection rules as ν_{37}. The transition of 36_0^2 is unidentified in the excitation spectrum. This band appears at 68.9 cm^{-1} and 35.9 cm^{-1} in the excitation spectra of trans-stilbene and PMTS respectively.[11,43] Hence, the frequency of 36_0^2 for PPTS has to be below 35.9 cm^{-1} in the excitation spectrum of PPTS. Maybe it is completely submerged the broad 2e band in the spectrum.

In the emission spectrum of $37_0^2$2e (Figure 26) a strong transition appears at 83 cm^{-1}. Another transition shows at 54 cm^{-1} in the same spectrum. Referring the 36_2 frequency of 116 cm^{-1} in PMTS we tentatively assign the peak at 83 cm^{-1} as 36_2. In considering the possible combination of ν_{36} and ν_{37}, the frequency of 36_1+37_1 will be 53.5 cm^{-1} if the vibrational spacing under the second quanta is close to harmonic for each individual mode. The peak at 54 cm^{-1} may then be the $36_1 37_1$ band. Some of the observed vibrational levels for the ν_{25}, ν_{36}, and ν_{37} modes are listed in Table 6.

Combinations of methyl torsion and the skeletal modes in PPTS can be seen clearly in the excitation spectrum. Following the 25_0^1 band there is methyl rotor structure which matches the frequency of 25_0^1 plus 1e, $0a_1$, 2e, $3a_2$, and $3a_1$. The same methyl rotor structure can also be seen in combination with 37_0^2, even though the transitions are weak.

Table 6. The Vibration Levels of ν_{25}, ν_{36}, and ν_{37} Modes

Mode & Level	Frequency (cm^{-1}) Ground State	Mode & Level	Frequency (cm^{-1}) Excited State
25_1	170	25^1	174.0
25_2	341	25^2	347.7
	25^3	522.0	
36_1 [a]	41	36^1	---
36_2	82	36^2	---
37_1 [a]	12	37^1 [a]	44.9
37_2	24	37^2	89.7

a. The frequency taken a half of its second quanta is not an observed value.

Nitrogen inversion transitions were not found in the excitation spectra of PPTS, not even the hot band I_1^1. The possible reason will be discussed later.

DISCUSSION

Nitrogen Inversion

The nitrogen inversion transitions in aniline and substituted aniline have been assigned. The evidence from the deuterium labeling, fluorescence excitation, and dispersed emission spectra have given strong support for the assignments. Some special features of the I_0^2 and T_0^2 transitions, however, are very interesting such as the strong transition of I_0^2 in all the anilines and the splitting of I_0^2 and T_0^2 in p-toluidine. The discussion will concentrate on these two issues in this section.

In the excitation spectra of all the anilines presented, the strong inversion transition I_0^2 have intensity competitive with the totally symmetric ring mode transitions. The intensity of the transition results from the net overlap integral, of the two inversion wave functions in the two electronic states. The greater the overlap, the stronger the intensity of the transition. The degree of overlap is dependent on the potential surfaces. The proper potentials for maximum overlap of inversion transition I_0^2 can be determined from potential analysis, but even qualitative consideration of the surfaces is instructive.

There are four possible combinations for the potential surfaces in the two

electronic states. These are drawn in Figure 27. The transition is assumed to obey the Born-Oppenheimer approximation. Based on this assumption, there are three areas separated by two vertical dashed lines in each graph corresponding to the I_0^2 transition. The overlap integral ($\langle\psi'/\psi''\rangle$) of the two wave functions in the ground and excited states will be negative between the two dashed lines, and positive otherwise. The net overlap is a summation of the three partial overlaps between and beside the two dashed lines.

The net overlap in graphs (a) and (b) is nearly zero. On the other hand, the remaining two cases have significant net overlaps. The relative ratio of the positive to the negative integral is 2.7 for (d) and 2.2 for (c). Thus, we see that a strong I_0^2 band indicates a change in potential shape (and amino geometry) between the two electronic transitions. However, the strong hot band shown in the excitation spectrum indicates that the first quanta must be very low but easily occurs when the ground state has a double minimum potential due to the tunneling splitting. So taken together, a strong I_0^2 band and an easily observed hot band, I_1^1, are generally indicative of a pyramidal amino geometry in S_0 and a planar geometry in the excited state.

The Splitting of I_0^2 and T_0^2 in the Excitation Spectrum of p-Toluidine†

The jet-cooled fluorescence excitation spectrum of p-toluidine is shown in Figure 28 (top trace) and agrees well with similar spectra published by

† Most of the ideas expressed in the section originated from Lee Spangler and have already appeared in the literature. Since the experimental work presented in this thesis led to the following analysis and since these ideas provided the motivation for further experiments (e.g. PPTS), it is appropriate to present the material here.

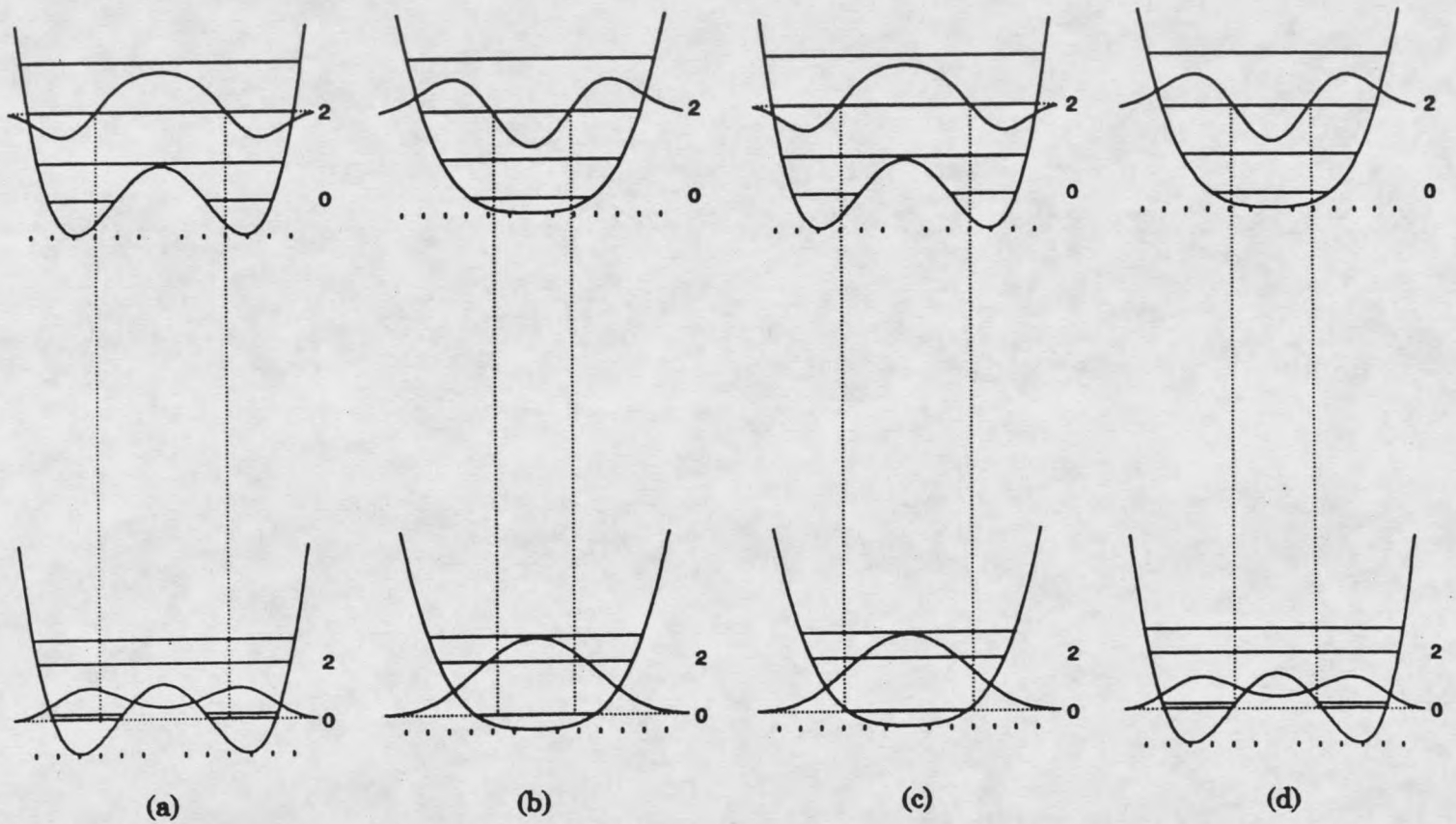

Figure 27. The qualitatively different possible combinations for the inversion potentials in the ground and excited states. The maximum overlap for the I_0^2 transition comes from the combination of a double minimum potential in the ground state and a single minimum potential in the excited state as shown in (d).

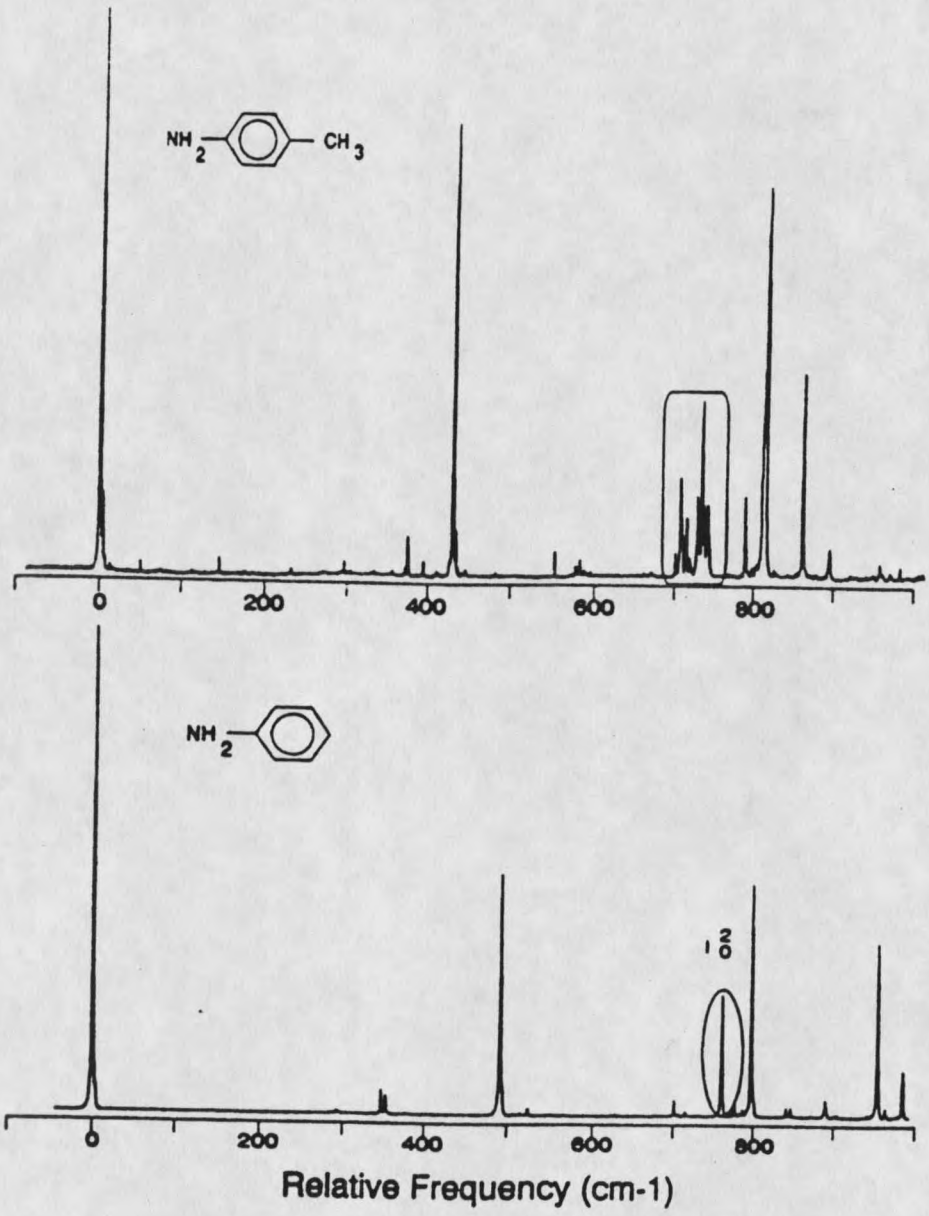

Figure 28. The fluorescence excitation spectrum of p-toluidine (top) showing the split transitions in the 700 cm-1 region. This spectrum is slightly saturated to make the weak , low frequency transitions more visible. The bottom trace is the spectrum of aniline with the two quanta transition of the nitrogen inversion mode indicated.

Smalley and co-workers and Lubman et al.[20] A notable feature of this spectrum is the two transitions centered at 709 and 736 cm^{-1}, each of which show an apparent quartet splitting. These appear in the same region of the spectrum as the nitrogen inversion mode appears in the parent molecule, aniline (see Figure 28, bottom for comparison). Deuteration of the amino group causes a large shift in the split transitions as shown in Figure 29. It is clear that the split peaks do shift and by more than 30 cm^{-1}. This > 18% shift indicates that the split peaks are vibrational modes which involve almost exclusive motion of the amino protons and are likely to be overtones of the one quantum forbidden nitrogen inversion mode or amino torsional mode which fit this description. We assigned the 709 cm^{-1} transition as two quanta of the amino torsion (T_0^2) and the 736 cm^{-1} transition as two quanta of the inversion (I_0^2) by analogy with aniline. We now address the cause of the splitting. The deuterium shifts in the ND_2 spectrum implicate the large amplitude amine motions as the transitions which are being split, yet the splitting is absent in the I_0^2 transition in aniline. The lack of splitting in aniline would seem to indicate that the methyl group also plays a role in causing the spectral splitting in p-toluidine.

This hypothesis can be tested by substituting fluorine for the CH_3. Fluorine is isoelectronic with CH_3 and has nearly the same mass but it has no internal degrees of freedom. Comparison of the two fluorescence excitation spectra (Figure 30) reveals a one - to - one correspondence of the major spectral

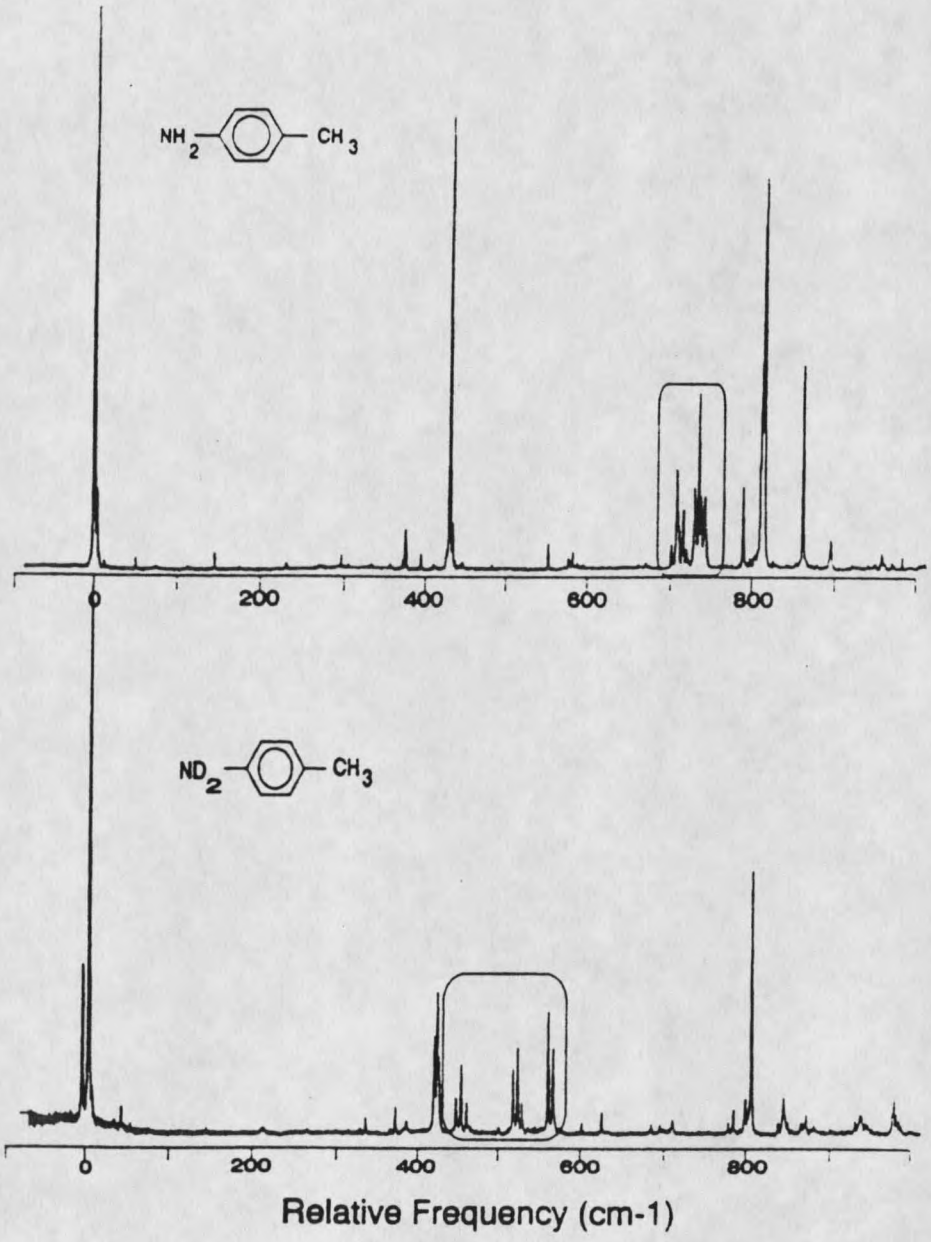

Figure 29. Comparison of the p-toluidine and p-toluidine-ND_2 spectra showing the large deuterium shift transitions. This indicates that the vibrational mode that is being split must involve almost exclusive motion of the amino protons.

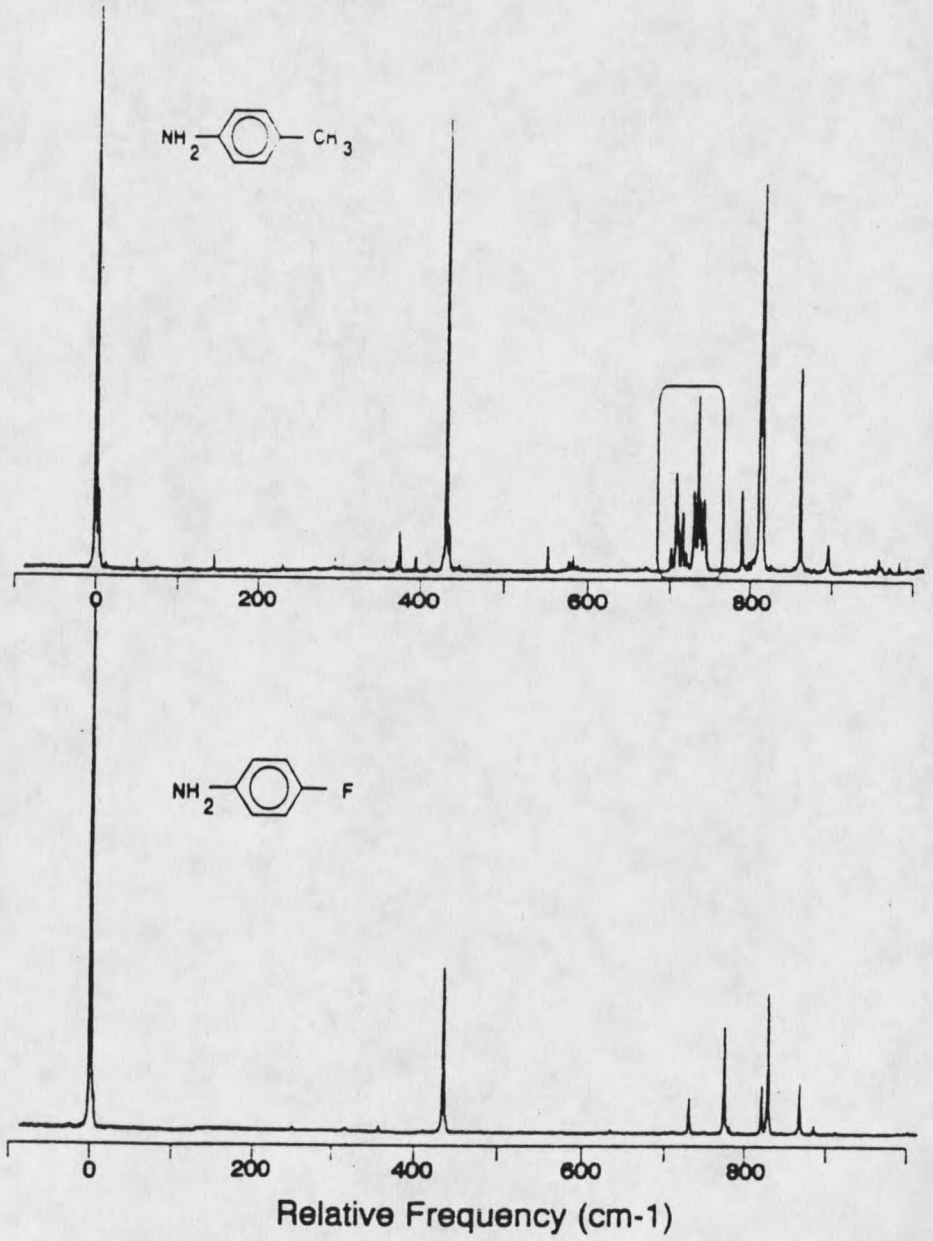

Figure 30. Comparison of the p-toluidine and p-fluoroaniline excitation spectra. There is a strong correspondence in the two spectra with exception of the absence of transitions below 200 cm-1 and lack of splitting in the 700 cm-1 region in the p-fluoroaniline.

features for these two molecules with the exception that single peaks appear in the p-fluoroaniline spectrum at approximately the correct frequency for the center of mass for the quartets in p-toluidine. The disappearance of the splitting with fluoro substitution provides compelling evidence that the internal rotation of the methyl group is involved in the interaction that causes the quartet splitting.

A quartet splitting requires four quasidegenerate levels to give rise to the four transitions. These nearly degenerate levels are most likely caused by vibrations which have multiple minima and tunnelling interaction. Three such vibrations exist in p-toluidine, the N inversion, the amino torsion, and the methyl torsion. The lowest levels of the inversion are known and have large enough level separations that an inversion doublet cannot contribute to the quartet of transitions. The methyl torsion, however, has a well known tunneling splitting which gives rise to a nondegenerate "a" symmetry level and a doubly degenerate "e" symmetry level. These two levels become degenerate in the infinite barrier case and can have a maximum splitting of ~5.3 cm^{-1} in the free rotor case ($E=m^2B$ for a particle in a ring and B~5.3 cm^{-1} for a methyl attached to a para substituted benzene). The a and e torsional levels have different nuclear spin wave functions so they cannot cool into each other and thus will always give rise to two transitions (that are sometimes unresolvable). The excitation spectrum has a$\leftrightarrow$a and e$\leftrightarrow$e selection rules so degenerate transitions can result even when the splitting in each electronic state is large.

The two equivalent hydrogens in the amino group dictate a double minimum potential for the amino torsion. We anticipate a high barrier in the excited state because the planarity of the group indicates that the nitrogen lone pair is shared with the π system and that the N-phenyl bond order is greater than one. The tunneling interaction in this case might be expected to be small, but nonzero, and will give rise to a twofold splitting.

Thus it appears that the source of the four transitions in the quartets is the twofold splitting of the amino torsion combined with the twofold splitting due to the methyl torsion. These four quasidegenerate levels should give rise to four transitions at the origin and for all of the vibronic bands in the spectrum However, a splitting is observed in only two of the prominent transitions. The point to be made here is that all the vibronic peaks in the spectrum are comprised of four torsional components but in most cases these components are not resolved in our experiment because they are very nearly degenerate. When the amino group is involved in some large amplitude motion (as determined from the ND_2 experiment), this degeneracy splits and the four torsional transitions become separated by several wavenumbers. It is not necessarily surprising that the nitrogen inversion would perturb the amine torsion to this extent because both motions are localized at the same portion of the molecule. It is surprising that the methyl torsional levels are so strongly affected, given the local nature of the inversion and CH_3 torsion and the separation between the groups.

Group Theory

At this point it would be desirable to determine the selection rules, assign the spectrum, and use the experimental frequencies to determine the potential surface along the nonrigid coordinates. The selection rules can be determined from a proper group theoretical treatment and requires use of the molecular symmetry (MS) group.[1,2] The nonrigid motions can cause exchange of identical nuclei—an operation not properly accounted for in point groups. The MS group can be constructed from the complete nuclear permutation and inversion (CNPI) group by eliminating "unfeasible" operations. The CNPI group is constructed by considering all permutations of identical nuclei (note that the Hamiltonian must be invariant to such operations) and inversion of coordinates for all particles in the molecule fixed axis system. This creates an unwieldy group with a large number of symmetry operations. Most of them can be discarded as unfeasible because they would require the breaking and reforming of bonds to perform the permutation. While the Hamiltonian would be invariant to such an operation, the energetics make such a permutation highly unlikely to occur spontaneously or during the course of our experiments, therefore such operations can be excluded from the group. Permutations for large amplitude motions that involve tunneling are feasible and must be retained. Thus we must have permutations that correspond to the CH_3 torsion and the NH_2 torsion and inversion. The relevant operations are E, (123), $(23)^*$, (45), and (67) (89) where 1, 2, and 3 are the methyl protons, 4 and 5 are the

amino protons, and 6, 7, 8, and 9 are the ring protons. All other classes can be constructed from products of these operations. Permutations are labeled by their effect on the hydrogens but in the case of the ring hydrogens, the carbons to which they are attached are permuted as well. The classes of symmetry operations, the class size, and their effect on the molecule are shown in Figure 31. There are 24 operations in 12 classes. The molecular symmetry group, G_{24} was then constructed by use of the group criteria that the number of classes equals the number of irreducible representations and

$$\Sigma l^2_1 = h, \tag{1}$$

where h is the order of the group and l_i is the dimension of the irreducible representation i. From these conditions it can be seen that there must be eight singly degenerate and four doubly degenerate representations. The representations were then simply written down such that they were orthogonal and met the group criterion

$$\sum_R [X_i(R)]^2 = h, \tag{2}$$

where $X_i(R)$ is the character of the irreducible representation i under the operation R. The resulting group (Table 7) was then checked explicitly for closure under the direct product operation and was found to be isomorphic with D_{6h}. The irreducible representations were labeled according to their

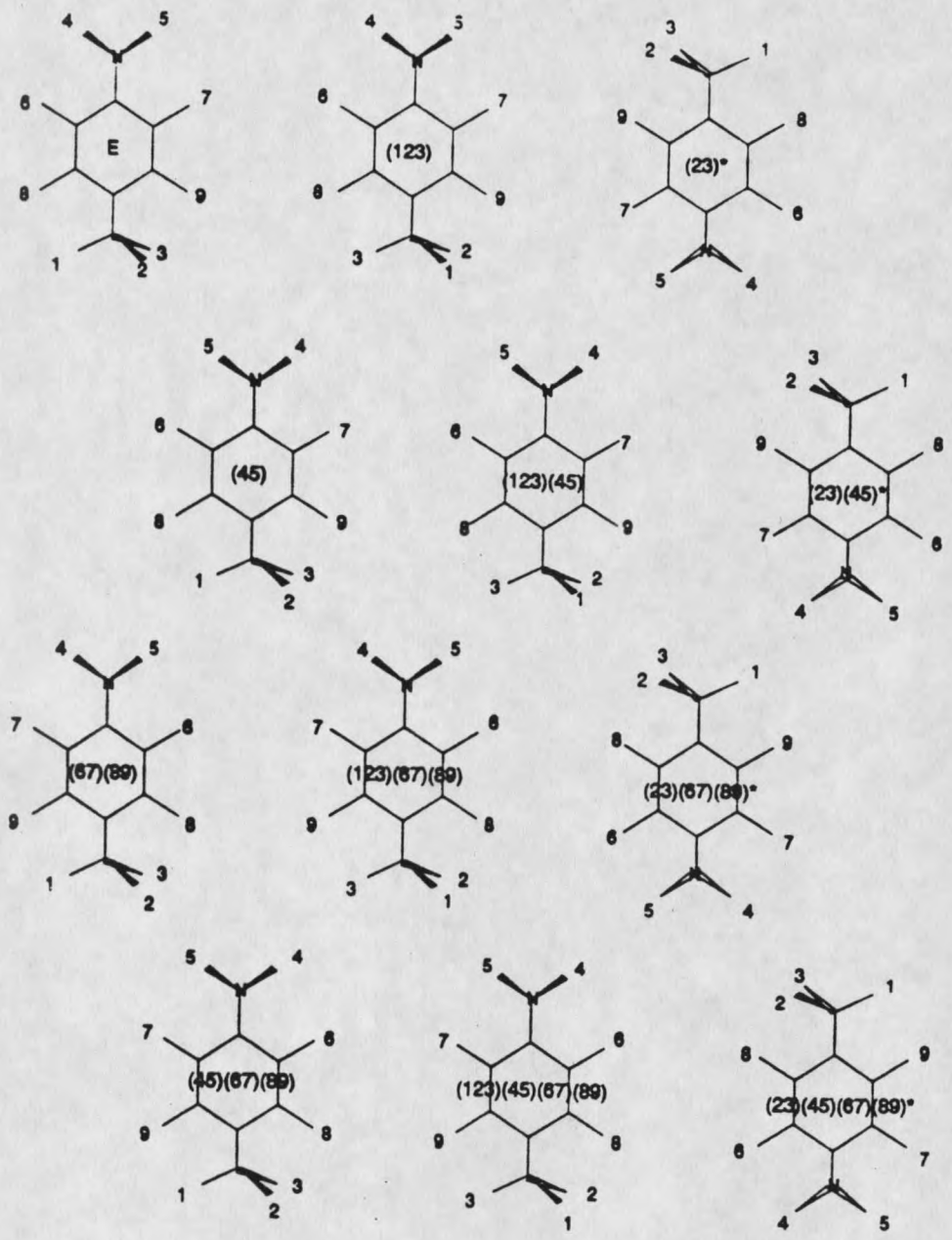

Figure 31. The symmetry operations given in the class headings for the G_{24} molecular symmetry group.

Table 7. Character Table for G_{24}.

s	E	(123)	(23)*	(45)	(123)(45)	(23)(45)*	(67)(89)	(123)(67)(89)	(23)(67)(89)*	(45)(67)(89)	(123)(45)(67)(89)	(23)(45)(67)(89)*	
c	1	2	3	1	2	3	1	2	3	1	2	3	
			R_c^π			R_c^π	R_a^π	R_a^π	R_b^π	R_a^π	R_a^π	R_b^π	
A_{1g}^+	1	1	1	1	1	1	1	1	1	1	1	1	$T_a, \Gamma_1(ND_2)$
A_{1g}^-	1	1	1	1	1	1	−1	−1	−1	−1	−1	−1	T_b
A_{2g}^+	1	1	−1	1	1	−1	1	1	−1	1	1	−1	$\Gamma_2(ND_2)$
A_{2g}^-	1	1	−1	1	1	−1	−1	−1	1	−1	−1	1	T_c
A_{1u}^+	1	1	−1	−1	−1	1	1	1	−1	−1	−1	1	Γ_{tot}
A_{1u}^-	1	1	−1	−1	−1	1	−1	−1	1	1	1	−1	
A_{2u}^+	1	1	1	−1	−1	−1	1	1	1	−1	−1	−1	Γ_{tot}
A_{2u}^-	1	1	1	−1	−1	−1	−1	−1	−1	1	1	1	
E_g^+	2	−1	0	−2	1	0	2	−1	0	−2	1	0	
E_g^-	2	−1	0	−2	1	0	−2	1	0	2	−1	0	
E_u^+	2	−1	0	2	−1	0	2	−1	0	2	−1	0	
E_u^-	2	−1	0	2	−1	0	−2	1	0	−2	1	0	

Table G_{24}, isomorphic with D_{6h}. This is the appropriate symmetry group for p-toluidine if the amino group can torsionally tunnel. Operations such as (67)(89) mean interchange nucleus 6 with 7 and 8 with 9 and (123) is a cyclic permutation. The * indicates inversion of all coordinates in the space fixed axis system in addition to the permutation. Notes: T_a indicates a transitional symmetry and these representations have the same symmetry as the components of the dipole moment operator. R_a^π labels are used to help determine rotational symmetries. Γ_{rot} indicates the two Pauli allowed total symmetries for both p-toluidine and p-toluidine-CD_3. $\Gamma_t(ND_2)$ indicates the Pauli allowed symmetries for p-toluidine-ND_2.

behavior under the generating operators mentioned above. The A and E labels denote symmetric and antisymmetric with respect to (123) (as well as the degeneracy of the representation), 1 and 2, s and a and ′ and ″ denote symmetric and antisymmetric behavior under (23)*, (45), and (67) (89), respectively. Because the group can be generated from products of these operations, the direct product rules for the irreducible representation labels will work in the standard way. For example s⊗s=s, s⊗a=a, and a⊗a=s.

The nonrigid vibrations were then classified using the techniques of Longuet-Higgins[1] and Bunker[2]. The methyl torsional levels have the symmetries (in order of increasing energy) a_{1s}', e_s'', e_s', a_{2s}'', a_{1s}'', e_s', e_s'', a_{2s}', a_{1s}', ···. The N inversion has a_{2s}'' symmetry, regardless of whether the harmonic oscillator basis or the particle in a ring basis set is used for the classification. This indicates that the perturbed internal rotor calculation is a reasonable model for the amino inversion. The amino torsion was classified using a particle in a ring basis set and has symmetry a_{1s}' for n=0, $a_{1a}'+a_{2a}'$ for n=± odd and $a_{1a}'+a_{2a}'$ for n=± even. The levels that are doubly degenerate in the free rotor limit do not have a degenerate symmetry classification. This is because these levels must split to correlate properly to the infinite barrier limit. The degeneracies in the free rotor limit go as (in order of increasing energy) 1, 2, 2, 2, ···. In the infinite barrier case, two identical wells exist with no tunneling interaction giving rise to levels of identical energy in each well and no mechanism to split them. Therefore, all levels are doubly degenerate in the

infinite barrier limit and the correlation with the nondegenerate lowest level in the free rotor limit causes all of the degenerate pairs in the free rotor limit to split as indicated in the correlation diagram in Figure 32. One consequence of this correlation is that the amino torsion can contribute a different number of transitions to the multiplet depending on the barrier height. With zero barrier, there will be two low lying amino torsional levels, the nondegenerate n=0 level and the doubly degenerate n=±1 level. With a nearly infinite barrier there will also be only two low lying levels, the n=0 and one of the n=|1| levels and the statistical weighting will be different because the second level will be nondegenerate. At small but nonzero barriers, the n=±1 degeneracy may start to split and give three levels of slightly different energies.

The rotational and nuclear spin functions were also determined using Bunker's methods and the resulting total Pauli allowed symmetries for the ground state as shown in Table 8. This treatment does explain some features of the spectrum. For example, in the high NH_2 torsional barrier case, the four levels due to the amino torsional tunneling splitting and the methyl torsional tunneling splitting cannot cool into each other because they must have different nuclear spin symmetries to be Pauli allowed. This indicates that four nearly degenerate transitions are expected because collisional cooling cannot depopulate the levels caused by the tunneling splittings. Also the nuclear spin statistical weighting factors predict a 3 to 1 ratio for the NH_2 torsional splitting if the weights for the rotational levels are averaged. A 2 to 1 spin

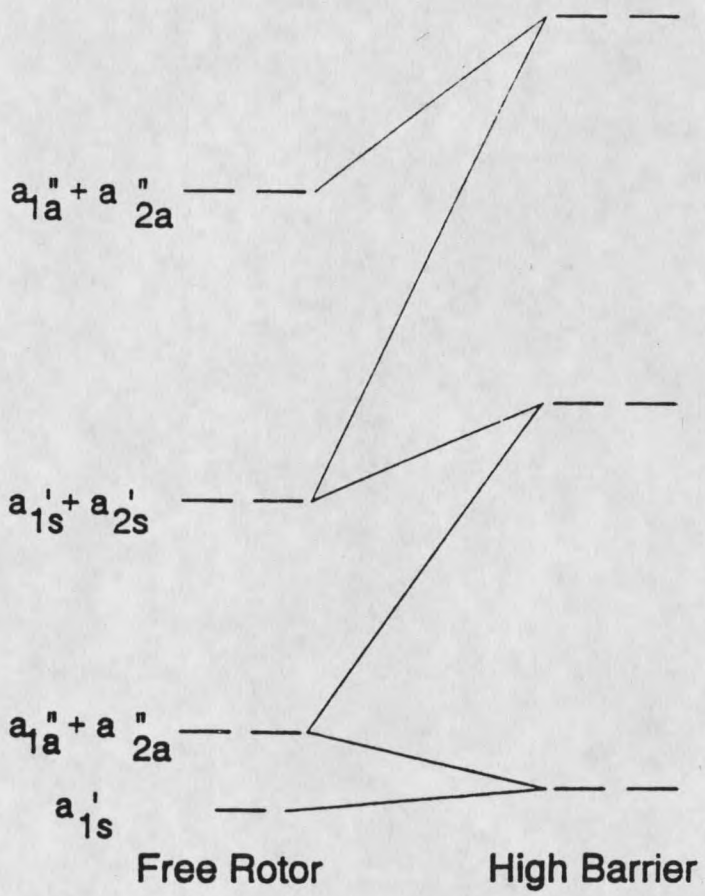

Figure 32. A correlation diagram for the NH_2 torsion. The left side is the limiting case of a zero barrier to internal rotation, the right side is the high barrier case corresponding to two equivalent wells and no tunneling interaction. The vertical energy spacings in the right side are not shown to scale compared to those on the left side for asthetic reasons. Note that the doubly degenerate levels in the free rotor case do not have a doubly degenerate symmetry representation. This because all of the doubly degenerate levels must split to properly correlate with the high barrier case. This diagram also illustrates three possible cases for the splitting caused by the NH_2 torsion. (1) Near the high barrier limit two nondegenerate levels are expected. (2) At, or very near free rotor limit, a nondegenerate and a doubly degenerate level are expected. (3) A little above the free rotor limit, three nondegenerate levels are expected.

Table 8. Symmetries for p-Toluidine Wavefunctions Under G_{24}.

Γ_{ns}	NH_2CH_3	NH_2CD_3	ND_2CH_3		Γ_{rot}	m	$\Gamma_{CH3\ tor}$
A_{1s}'	120	300	240	ee	A_{1s}'	0	a_{1s}'
A_{1s}''	72	180	144	eo	A_{2s}'	± 1	e_s''
A_{2s}'	0	30	0	oe	A_{1s}''	± 2	e_s'
A_{2s}''	0	18	0	oo	A_{2s}''	± 3	$a_{1s}'' + a_{2s}''$
A_{1a}'	40	100	120			± 4	e_s'
A_{1a}''	24	60	72	n	$\Gamma_{N\ tors}$	± 5	e_s''
A_{2a}'	0	10	0	0	a_{1s}'	± 6	$a_{1s}' + a_{2s}'$
A_{2a}''	0	6	0	± 1	$a_{1a}'' + a_{2a}''$		
E_s'	60	240	120	± 2	$a_{1s}' + a_{2s}'$		
E_s''	36	144	72	± 3	$a_{1a}'' + a_{2a}''$		
E_a'	20	80	60	± 4	$a_{1s}' + a_{2s}'$		
E_a''	12	48	36				

$\Gamma_{N\ tor}$ ⊗	$\Gamma_{CH3\ tor}$ ⊗	Γ_{rot} ⊗	Γ_{ns} ⊗	$= a_{2a}', a_{1a}'$	NH_2–Ph–CH_3 wt	NH_2–Ph–CD_3 wt
A_{1s}'	A_{1s}'	A_{1s}'	A_{1a}'	A_{1a}'	40	100 + 10
		A_{2s}'	A_{1a}'	A_{2a}'	40	100 + 10
		A_{1s}''	A_{1a}''	A_{1a}'	24	60 + 6
		A_{2s}''	A_{1a}''	A_{2a}'	24	60 + 6
A_{1s}'	E_s''	$A_{1s}' = E_s''$ ⊗	E_a''	$A_{2a}' + A_{1a}'$	2×12	2×48
		$A_{2s}' = E_s''$ ⊗	E_a''	$A_{2a}' + A_{1a}'$	2×12	2×48
		$A_{1s}'' = E_s'$ ⊗	E_a'	$A_{2a}' + A_{1a}'$	2×20	2×80
		$A_{2s}'' = E_s'$ ⊗	E_a'	$A_{2a}' + A_{1a}'$	2×20	2×80
$A_{2a}'' + A_{1a}''$	A_{1s}'	A_{1s}''	A_{1s}''	etc.	2×72	2×(180 + 18)
		A_{2s}'	A_{1s}''		2×72	2×(180 + 18)
		A_{1s}''	A_{1s}'		2×120	2×(300 + 30)
		A_{2s}''	A_{1s}'		2×120	2×(300 + 30)
$A_{2a}'' + A_{1a}''$	E_s''	A_{1s}'	E_s'		2×2×60	2×2×240
		A_{2s}'	E_s'		2×2×60	2×2×240
		A_{1s}''	E_s''		2×2×36	2×2×144
		A_{2s}''	E_s''		2×2×36	2×2×144
Γ_{inv} ⊗	Γ_{CH3tor} ⊗	Γ_{rot} ⊗	Γ_{ns} ⊗	$= a_{2a}', a_{1a}'$	NH_2–Ph–CH_3 wt	NH_2–Ph–CD_3 wt
A_{1s}'	A_{1s}'	A_{1s}'	A_{1a}'	A_{1a}'	40	100 + 10
		A_{2s}'	A_{1a}'	A_{2a}'	40	100 + 10
		A_{1s}''	A_{1a}''	A_{1a}'	24	60 + 6
		A_{2s}''	A_{1a}''	A_{2a}'	24	60 + 6
A_{1s}'	E_s''	$A_{1s}' = E_s''$ ⊗	E_a''	$A_{2a}' + A_{1a}'$	2×12	2×48
		$A_{2s}' = E_s''$ ⊗	E_a''	$A_{2a}' + A_{1a}'$	2×12	2×48
		$A_{1s}'' = E_s'$ ⊗	E_a'	$A_{2a}' + A_{1a}'$	2×20	2×80
		$A_{2s}'' = E_s'$ ⊗	E_a'	$A_{2a}' + A_{1a}'$	2×20	2×80
A_{2s}''	A_{1s}'	A_{1s}'	A_{1a}''	etc.	24	60 + 6
		A_{2s}'	A_{1a}''		24	60 + 6
		A_{1s}''	A_{1a}'		40	100 + 10
		A_{2s}''	A_{1a}'		40	100 + 10
A_{2s}''	E_s''	A_{1s}'	E_a'		2×20	2×80
		A_{2s}'	E_a'		2×20	2×80
		A_{1s}''	E_a''		2×12	2×48
		A_{2s}''	E_a''		2×12	2×48

weighting ratio is predicted for the CH_3 tunneling doublet but the double degeneracy of the e level should counteract this effect and give a 1 to 1 ratio in the spectrum. Even though we cannot resolve the rotational structure, averaging of the rotational weights should cause some error in the later case. The ee and eo symmetry rotational levels have the larger weighting for the a torsional levels, but the e torsional levels have their oe and oo rotational levels more heavily weighted. Since the ee is the lowest sublevel for any given even J value in an asymmetric top and the eo is the lowest sublevel for odd J values, the ee and eo levels will have significantly larger Boltzman factors under the extremely cold conditions of the spectrum. Given this fact, and that p-toluidine is a near prolate top with significantly courser K structure than J structure, the reversal of large and small rotational weights in the e torsional levels should cause deviation from the averaged weights and give the a levels greater relative intensity. This rotational issue, in addition to the NH_2 torsional degeneracy issue discussed above, makes it difficult to determine the appropriate statistical weighting factors when there is only vibronic resolution. It is useful to consider weights for the limiting cases as is shown in Table 9.

Table 9. Statisical Weight Ratios (Including Torsional Degeneracies) for Several Limiting Cases

		High NH_2 Torsional Barrier		Low NH_2 Torsional Barrier	
m_{CH3}	n_{NH2}	J=K=0 Rot. wts.	Averaged	J=K=0	Averaged Rot. wts.
0	0	5	1	5	1
1	0	3	1	3	1
0	1	9	3	18	6
1	1	15	3	30	6

The values reported are obtained by dividing the weights appearing in Table 8 by either 8 or 32 (depending on which column in the table) in order to achieve a ratio with lower numbers. The limiting cases are: weights with J=K=0, weights with rotational values averaged, a high amino torsional barrier, and a low torsional barrier. At our temperatures we anticipate the weights should be close to the high barrier, J=K=0 case. This table suggests an elegant way to assign the quartet components. If we raise the temperature, the integrated intensities should start to approach the high barrier, rotationally averaged weights. Unfortunately, the rotational broadening caused by the higher temperature and the appearance of the $6a_0^1I_1^1$ hot band in this region cause significant spectral overlap so that it is not possible to reach a definitive conclusion from this data (Figure 33). However, the ratios of the

peaks in the cold spectrum do not seem to change in the predicted manner which probably indicates that Franck-Condon factors, rather than statistical weights, dominate the relative intensities of the quartet.

It is interesting to note that the group theory does not appear to predict methyl torsional selection rules. The singly degenerate levels all have the same nuclear spin wave functions and so can cool into each other. The same is true for all doubly degenerate levels but the doubly degenerate levels cannot cool into the singly degenerate ones (see Table 8). Because of the like $\leftrightarrow$ like selection rules in the excitation spectrum and the cold temperatures in the jet, this should give a sparse spectrum for the methyl rotor compared to most CH_3 containing molecules that are of G_6 symmetry (and have a threefold potential). Inspection of the low frequency region of the spectrum reveals a large number of transitions, albeit weak ones, in the first 200 cm^{-1} of the spectrum. Empirically it appears likely that these are due to the methyl rotor because they are absent from the fluoroaniline spectrum, but it is not possible to generate this number of low frequency transitions using the selection rules derived from G_{24}. We assign the 12.8 cm^{-1} peak as $2e_s''$ and the 51.0 and 75.2 cm^{-1} peaks as $3a_{1s}''$ and $4e_s''$, respectively. All of these transitions should be symmetry forbidden. Similar results were obtained by Ito and co-workers.[54] for p-fluorotoluene, a close analog of G_{12} symmetry which should have the same CH_3 torsional selection rules. They observed torsional frequencies of 13.7 (2e), 52.9 (3a), 74.3 (4e), and 108.4 cm^{-1} (5e) in this molecule and confirmed their

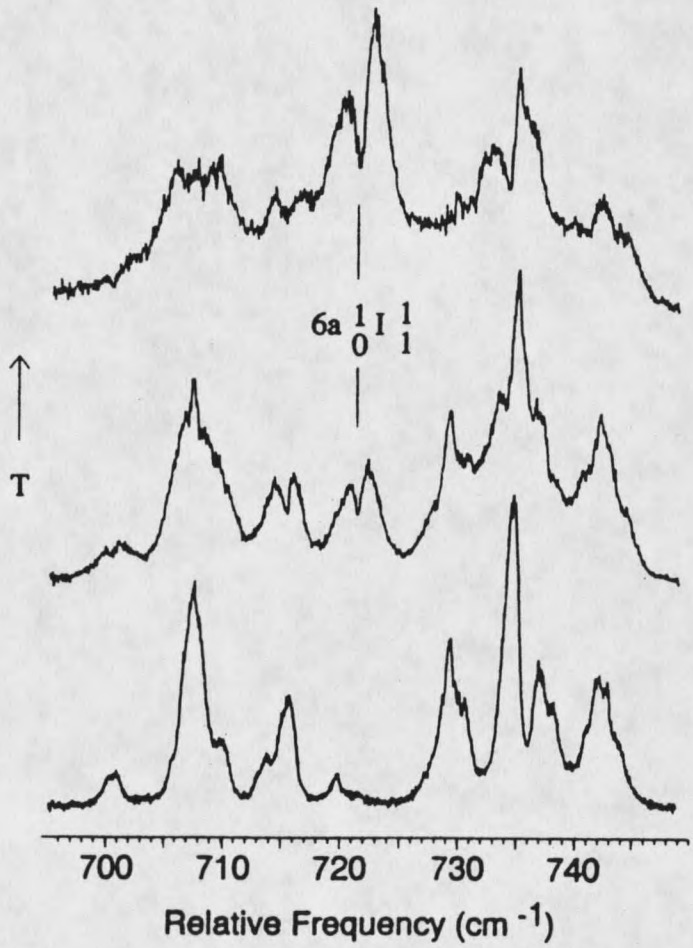

Figure 33. The two split transitions above 700 cm-1 in the p-toluidine spectrum. The spectra were taken under widely different expansion conditions. The top spectrum, taken under the highest temperature condition, was taken by sampling the very beginning of the nozzle pulse. The dominant transition under these conditions is the combination band $6a_0^1I_1^1$.

assignments by use of dispersed fluorescence. The internal rotation constant required to fit their data was B=4.9 cm^{-1}, and fits of our frequencies require a similar value. This value of B requires significant distortion of the methyl geometry ($B_{methane}$= 5.23 cm^{-1}) which does not seem to be physically reasonable. Given that transitions involved are expected to be forbidden, the unusual intensities and frequencies are probably both due to a perturbation. There are no terms in the rigid internal top-rigid rotor Hamiltonian that causes rotations to connect levels of different m quantum numbers for the CH_3 torsion. But when the rotations are involved in the direct products, the transitions do have allowed symmetry. This may indicate that rotations are involved in the mechanism but that some nonrigid body coupling (such as coriolis coupling) is required as well.

The Qualitative Appearance of the Potential Surface

Even though we cannot yet determine the potential surface from the observed spectrum, we can determine some of its essential feature and understand much of the spectral behavior by considering the "symmetry" of the surface along NH_2-CH_3 plane. This can be accomplished by drawing a reference configuration of the molecule on that plane and drawing new pictures at points on the plane where an equivalent (isoenergetic) conformation is reached. The drawing of the isoenergetic configurations will give the number of equivalent minima on that surface and their relative positions, even if the reference configuration is not the minimum energy configuration. This is true

because no matter what reference conformation is chosen, the "map" will have the symmetry, i.e., the same relative positions, for equivalent conformations. This is easily shown by starting with several different conformations and performing the exercise. Such a map is shown for the excited state in Figure 34. A planar geometry is used for the amine group based on the fit of the inversion frequencies discussed above (see Figure 4) and on the known planar geometry of aniline.[8] We see that equivalent conformations can be obtained by either of two operations, rotation of NH_2 by 180° or rotation of the CH_3 by 60°. This results in 12 minima arranged in a rectangular coordinate pattern, indicative of independent coordinates.

Mapping of the ground state surface results in an interesting difference because the NH_2 group is nonplanar, a 180° rotation of that group does not result in an isoenergetic conformation. The same is true of a 60° rotation of the CH_3 group because either operation will take the reference conformation from a staggered form to an eclipsed form (with respect to the NH_2 and CH_3) as seen in Figure 35. Thus equivalent conformations are reached by 360° rotation of the NH_2 or a 120° rotation of the CH_3. The nearest neighbor minimum, however, is reached by a combination of a 180° NH_2 rotation and a 60° CH_3 rotation. The resulting zig-zag potential is shown in Figure 36 and indicates a possible interdependence of the two modes in the ground state. The six "missing" conformations do not necessarily imply that there are maxima at these points. In fact, the maximum for the NH_2 torsion is expected

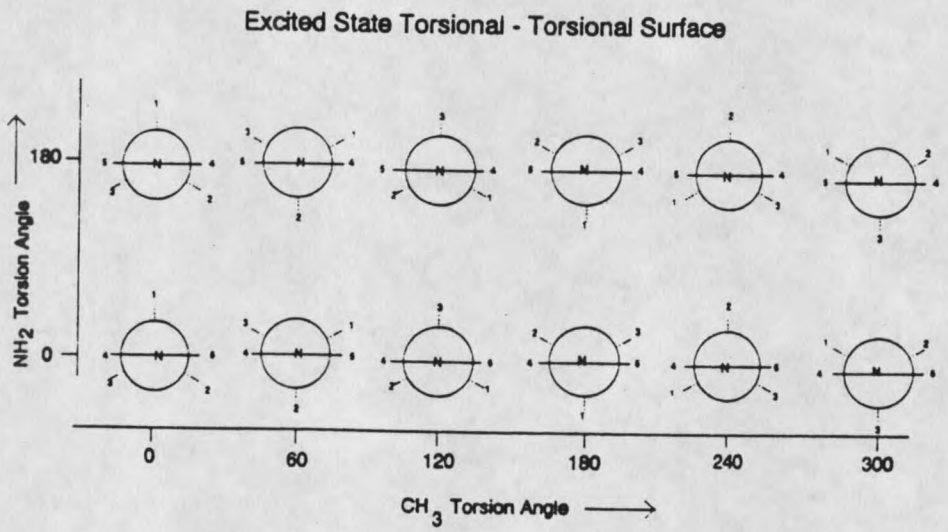

Figure 34. A diagram of the equivalent (isoenergetic) conformers of the excited state of p-toluidine obtained by rotation of the amino and methyl groups. The potential surface along the NH_2 and CH_3 torsional coordinates will have the same number of minima with the same spatial relationship as the drawings in this diagram.

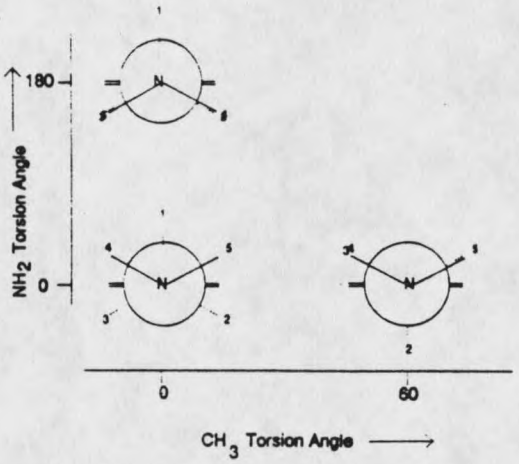

Figure 35. This diagram illustrates how 60° rotation of the CH_3 or 180° rotation of the NH_2 causes the methyl and amino groups to be eclipsed in the pyramidal ground state. Thus these two operations do not results in an isoenergetic conformation.

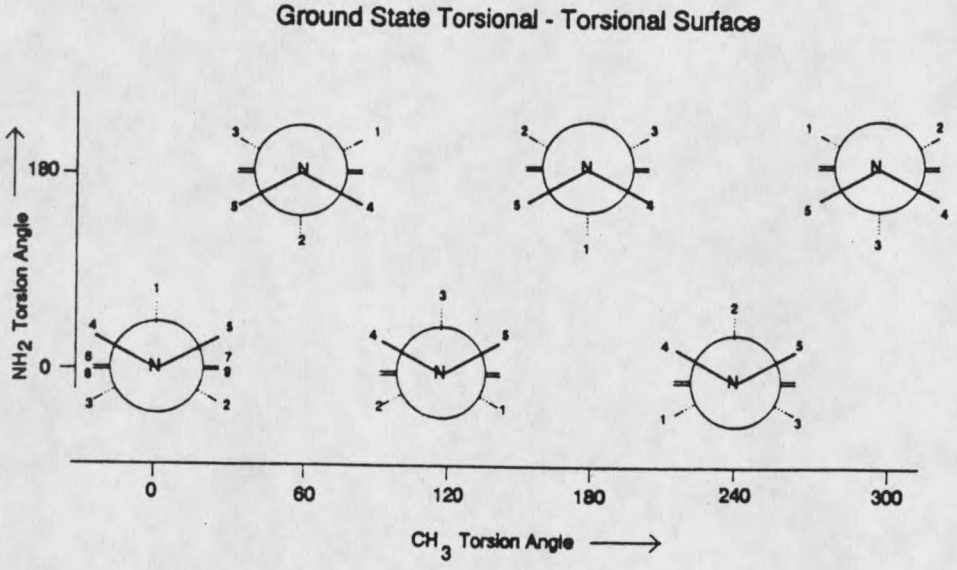

Figure 36. A diagram of the equivalent (isoenergetic) conformations of the ground state of p-toluidine obtained by rotation of the amino and methyl groups.

at 90° because this angle would not permit sharing the lone pair with the π system. Thus, in the ground state we expect six local minima at the missing positions and six global minima at the pictured positions. The unusual symmetry of this surface compared to that of the excited state may cause problems with the selection rules determined by the above symmetry treatment.

These qualitative surfaces can be employed to explain some of the unusual features of the large amplitude inversion of the amino on the excited state torsion-torsion map. Distortion of the NH_2 away from planar geometry will cause configurations related by a 180° amino group twist to become inequivalent, and the excited state surface will start to resemble that of the ground state. Since the amino group is planar in the excited state, the inversion mode will oscillate the NH_2 group out of the plane on both sides of the molecule causing a conversion between staggered and eclipsed geometries depending on the phase of the oscillation. Thus the inversion converts the molecule between conformations of two different energies and should be expected to affect the energies of levels for the other moieties which can cause conversion between the two conformations. The magnitude of this effect should have some dependence on the magnitude of the out plane distortion. This probably explains the lack of observed splitting at the origin. Apparently the zero point motion is insufficient to cause splitting at our resolution.

This model also nicely accounts for the lack of splitting in the I_0^2 transitions

in aniline and p-fluoroaniline. We have attributed two peaks of the quartet in p-toluidine to the NH_2 torsion splitting. The NH_2 group is present in both aniline and p-fluoroaniline so one might expect to see a doublet splitting in the I_0^2 transition in these two molecules. The lack of amino torsion splitting can, however, be explained by the absence of the methyl group. The role of the CH_3 group in p-toluidine to make the "up" vs "down" NH_2 conformations have different energies in the ground state because they convert the molecule between an eclipsed vs staggered form as shown in Figure 35. If a hydrogen or a fluorine is substituted for the methyl, the asymmetry caused by the CH_3 is removed and the up and down conformations have identical energies. This gives rise to a rectangular surface map for the ground state in aniline and p-fluoroaniline just as the excited state surface has. Furthermore, an amino group out of plane distortion will not lower the symmetry of the excited state surface as occurs in p-toluidine.

The Structure of p-amino-p′-methyl-trans-Stilbene

The QCFF-π calculation of the equilibrium conformation of trans-stilbene showed the structure of the molecule was planar in the ground and the excited states.[41] Vibronic spectral analysis by Zweir and coworkers confirmed these geometries.[44] A single para-substituted methyl does not change the planarity for the parent molecule, trans-stilbene.[30] Based on above evidence, it might be expected that the structure of the p-amino-p′-methyl-trans-stilbene (PPTS) will

have co-planar rings and ethylenic bond. It is intriguing to consider the structure of the molecule for three reasons. First, if the behavior of the amino group in PPTS were the same as it in aniline, the strong nitrogen inversion hot band I_1^1 and overtone I_0^2 would be found in the excitation spectra of PPTS. Furthermore, if the methyl group in PPTS had the same effect as it does in p-toluidine, one would expect a similar splitting for the inversion and torsion bands in the excitation spectrum of PPTS. Additionally, the methyl torsion levels of PPTS are lowered by almost factor two compared with those of p-methyl-trans-stilbene, indicating a significant amino influence on the methyl behavior even though the two groups are separated by eleven bond lengths. The third issue concerns the phenyl ring torsional mode. If the phenyl ring can tunnel through the torsional barrier (turn over by 180°), the motion will also have to be treated with non-rigid group theoretical techniques.

To address the first issue, we have to compare the PPTS molecule with aniline and p-toluidine. The very low frequency of the first quantum of inversion of the amino group in the ground state is the precondition to have a strong hot band in the excitation spectrum. Such a low frequency typically only happens in a motion that has a multiple minimum potential. If the first quantum is too high to be populated by changing the jet condition, there will not be a significant hot band in the jet excitation spectrum. It should be noted that there is no hot band in the expected I_1^1 region for PPTS. If the methyl group of PPTS functions as the one in p-toluidine, splitting in I_0^2 and T_0^2 would

be expected. No splitting peaks are observed and no peaks of similar intensity to I_0^2 for the anilines are observed in the 700-800 cm^{-1} region. The inversion mode of the amino group has to exist in PPTS but does not have significant intensity in the excitation spectrum. Since all the features of nitrogen inversion of p-toluidine are absent in the PPTS molecule, one must conclude that the Franck-Condon factor (FCF) must be significantly different than in the single ring aniline. If the geometry in both states is the same, a significantly weaker I_0^2 transition is expected from the previous arguments. If this is true I_1^1 would still have appreciable FCF's, but the spectral intensity would also depend on the population of I_1. If both states were pyramidal I_1^1 would have high intensity due to the low I_1 energy. Thus, we conclude from the absence of I_1^1 and I_0^2 intensity that PPTS has a planar amino group in both electronic states. In order to further investigate the amino group structure, an X-ray diffraction experiment of a PPTS crystal was performed at room temperature. The unit cell of the crystal is composed of eight molecules and is presented in Figure 37(a). There are four hydrogen bonded asymmetric pairs per unit cell. The proton donor molecule is almost completely planar as shown in Figure 37(b). The two protons on the amino group stay in the symmetry plane of the PPTS. The structure of the proton accepter molecule is not planar Figure 37(c). The double bond and the methyl containing ring (toluene ring) lie in the same plane. The plane of the amino containing ring (aniline ring) is twisted by ~17° relative to the other ring plane. The amine

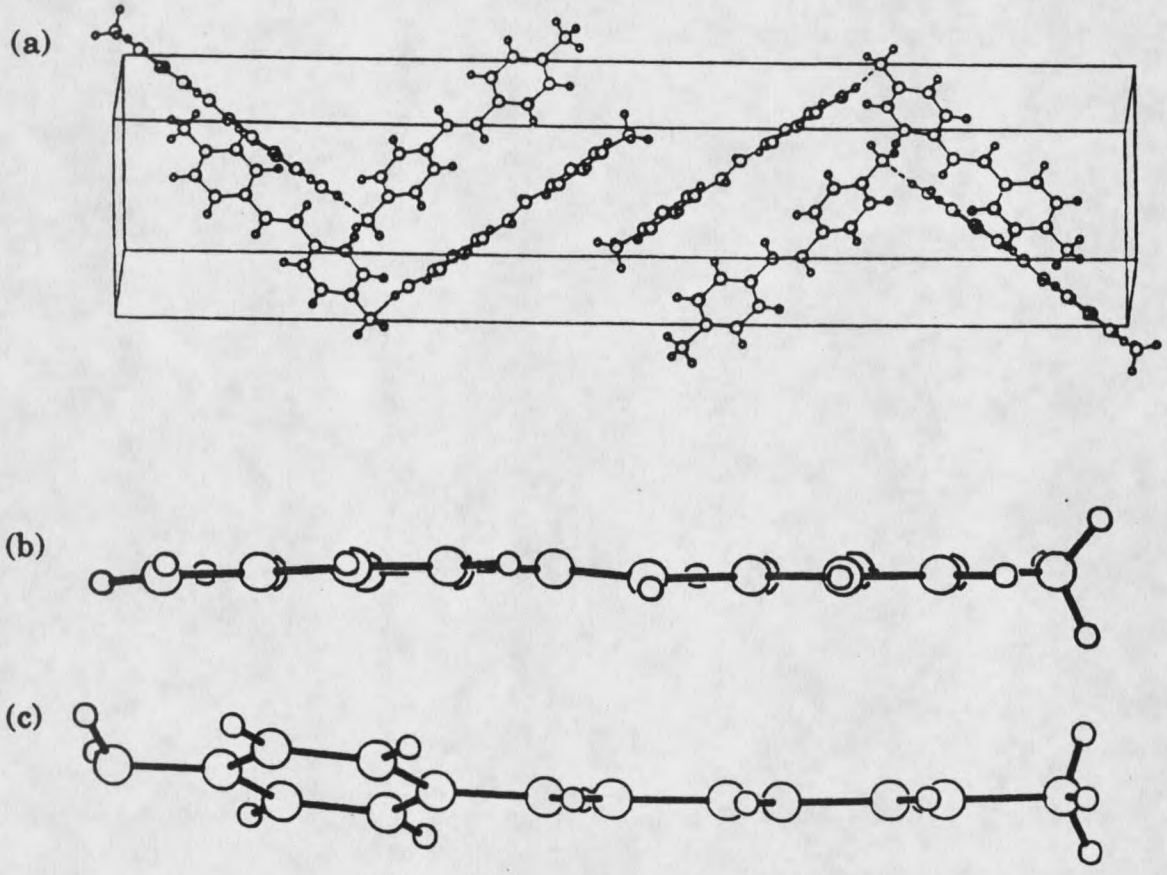

Figure 37. The structures of the p-amino-p'-methyl-trans-stilbene (PPTS) crystal measured by X-ray diffraction. (a) The unit cell of the crystal is composed of four dimers formed by hydrogen bonding. (b) The proton donor in each dimer is planar. (c) the proton accepter has a pyramidal structure on the amino group and the phenyl ring with the amino group is twisted by ~17° relative to the rest of the molecule.

group is pyramidal in the accepter molecule, and also twisted by the same angle as the aniline ring. That is to say the bisector to the amino N-H bonds is perpendicular to the attached ring plane. The important evidence from this result is that the pyramidal structure for the amino group happens only when the lone pair on nitrogen is used to bond with a proton in another PPTS. If there is no proton bonded to the nitrogen, the amine group will keep a planar structure and the entire molecule is planar also.

Because we attribute the pyramidal nature of the one NH_2 and the twisting of the aniline ring in PPTS to structural changes included by the H-bond, we suspect the donor geometry to more closely resemble that of the isolated molecule. This is consistent with the fact that no hot band or I_0^2 appears in the excitation spectrum of PPTS. The donor isolated molecule geometry relationship is supported by the X-ray structure of aniline at 252 K which was reported by Fukuyo et al[55]. Here too, a dimer is formed by hydrogen bonding in the crystal, however, both amino groups in the aniline dimer are pyramidal. Thus the donor has the same amino geometry as the gas phase molecule in the ground state. Furthermore, since this is a pyramidal geometry, an intense I_1^1 band appears in the excitation spectrum. While not absolutely conclusive, the evidence provided gives rise to a compelling argument for a planar amino group in both electronic states of PPTS.

The strong interaction between the amino and the methyl groups in PPTS causes the methyl torsion frequencies to be lowered by about a factor of two

compared with those of p-methyl, trans-stilbene. It is surprising that the coupling between the two groups is so strong even though they are separated by ten atoms. A possible mechanism for this interaction involves the electron donating nature of the amino group. When the lone pair on the nitrogen is involved in the conjugated π system, the electron density of the π orbital will go up and the withdrawing tendency of the p_z-orbital on the carbon atom in the methyl will go down. In this case the methyl rotor has more "freedom" to twist, in other words, the barrier of methyl torsion is lowered. The calculated barriers for the methyl torsion of PPTS are 18.9 cm^{-1} and 54.1 cm^{-1} in the ground and the excited states respectively. However, the barriers in p-methyl, trans-stilbene are 28 cm^{-1} in the ground state and 150 cm^{-1} in the excited state. If the amine group in PPTS is substituted by a nitro group, the electronic withdrawing group is expected to cause the methyl torsion frequencies to shift even higher than those of p-methyl-trans-stilbene. Other workers will undertake these experiments.

To address the question of tunneling in the phenyl ring torsion, we have to investigate the selection rules by using molecular symmetry theory. Owing to the non-rigid nature of the CH_3 and NH_2 groups, the molecular symmetry group of PPTS should be G_{12} if the phenyl rings cannot torsionally tunnel. However, if they can tunnel, there are four more equivalent conformations accessible which will generate a larger group. Referring to the numbered atoms in PPTS (Figure 38), the irreducible representations are labeled

according to their behavior under the generating operators in the same method discussed for creating the G_{24} table for p-toluidine. The molecular symmetry group G_{48} is generated when the permutations of the atoms on the phenyl rings due to tunneling are considered.(Figure 38) Both G_{12} and G_{48} character tables are shown in Table 10 and 11. The A and E labels denote symmetric and antisymmetric with respect to (345) or (543). The subscript "s" and "a" denote symmetric and antisymmetric behavior under (12) in both G_{12} and G_{48} symmetry groups. The symmetric and antisymmetric characters under $(34)^*$, (45), or $(53)^*$ are denoted as the subscripts 1 and 2 in the G_{12} group and the

Table 10. Character Table for G_{12}.

G_{12}	E	(345)	$(34)^*$	(12)	(12)(345)	$(12)(34)^*$
1	2	3	1	2	3	
$A_{s,1}$	1	1	1	1	1	1
$A_{a,1}$	1	1	1	-1	-1	-1
$A_{s,2}$	1	1	-1	1	1	-1
$A_{a,2}$	1	1	-1	-1	-1	1
E_s	2	-1	0	2	-1	0
E_a	2	-1	0	-2	1	0

capital letters A and B in the G_{48} group, respectively. In the G_{48} table, the subscript 1 and 2 denote symmetric and antisymmetric under (CD), and 3 and

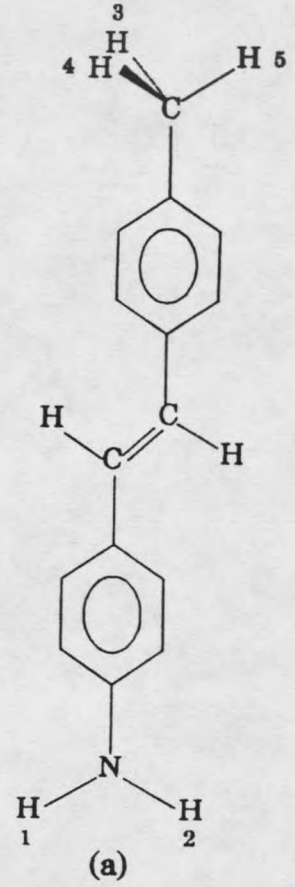

(a)

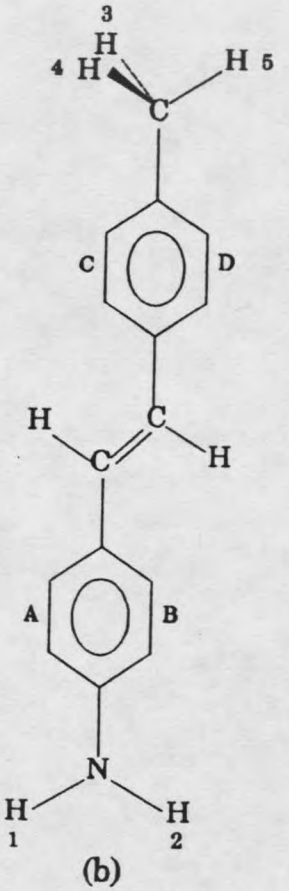

(b)

Figure 38. The numbering in p-amino-p'-methyl-trans-stilbene for molecular symmetry operations. (a) and (b) are used for the symmetry groups G_{12} and G_{48}, respectively. The permutation (AB) or (CD) means that all the atoms on the individual ring must switch their positions symmetrically as mirror images.

4 denote symmetric and antisymmetric under (AB)(CD), respectively.

If the phenyl rings cannot tunnel in the ring torsion, the molecular symmetry of PPTS belongs to G_{12}. The symmetries of the methyl torsional levels are denoted to be

$\Gamma_{\text{me-tor}} =$	$A_{s,1}$	$m = 0$
	E_s	$\|m\| = 1$
	E_s	$\|m\| = 2$
	$A_{s,1} + A_{s,2}$	$\|m\| = 3$
	E_s	$\|m\| = 4$
	E_s	$\|m\| = 5$
	$A_{s,1} + A_{s,2}$	$\|m\| = 6$

in which m represents the quantum number for methyl torsion and the symmetry labels are the same as the irreducible representations in the character table of G_{12}. As labeled above, the torsion levels 1e and 2e have the same symmetry E_s. Therefore the transition from 1e to 2e is allowed in the symmetry G_{12}. Furthermore since both 0a and 3a have the total symmetry $A_{s,1}$, the transition from 0a to 3a will be allowed also.

If the protons on the phenyl ring bonded to the methyl group are allowed to permute (CD), (that is ring tunneling can occur), the methyl torsion levels have the following symmetry in G_{48}

$\Gamma_{\text{me-tor}} =$	$A_{s,1}$	$m = 0$
	$E_{s,2}$	$\|m\| = 1$
	$E_{s,1}$	$\|m\| = 2$
	$A_{s,2} + B_{s,3}$	$\|m\| = 3$
	$E_{s,1}$	$\|m\| = 4$
	$E_{s,2}$	$\|m\| = 5$
	$A_{s,1} + B_{s,1}$	$\|m\| = 6$

Now the 1e and 2e methyl torsion levels have different symmetries. The direct product $E_{s,2} \otimes E_{s,1} = A_{s,2} + B_{s,2} + E_{s,2} \neq A_{s,1}$, so that the methyl torsion transition from 1e to 2e is not allowed. The methyl torsion transition from $0a_1''$ to $3a_1'$ is also forbidden since they have different symmetries. Thus we conclude that the rings cannot torsionally tunnel and the proper Hamiltonian for the molecule does not require a term for that possibility.

The symmetries for the methyl torsional levels will not change in different electronic states. Thus, the observed transitions of $2e' \leftarrow 1e''$ and $3a_1' \leftarrow 0a_1''$ are allowed in the G_{12} but forbidden in G_{48} groups, according to the different symmetry labels of the methyl torsional levels in the two symmetry groups. The G_{48} symmetry does not properly give the labels to the methyl torsional levels. Therefore the correct symmetry for PPTS is G_{12} and the phenyl rings cannot tunnel.

Another interesting thing is the a and e methyl torsion splitting change with different quanta of the skeleton mode transitions in the excitation

spectrum of PPTS. The "a" and "e" splittings on the origin, 25_0^1, and 25_0^2 are 1.8 cm^{-1}, 1.5 cm^{-1}, and 1.1 cm^{-1} respectively. This is very unusual for the coupling change of the 1e level of a methyl rotor with different quanta of a skeleton mode in the excited state.

Table 11. Character Table for G_{48}

G_{48}	E	(345) (543)	(34)* (45)* (53)*	(12)	(12)(345) (12)(543)	(12)(34)* (12)(45)* (12)(53)*	(AB)	(AB)(345) (AB)(543)	(AB)(34)* (AB)(45)* (AB)(53)*	(AB)(12)	(AB)(12)(345) (AB)(12)(543)	(AB)(12)(34)* (AB)(12)(45)* (AB)(12)(53)*
	1	2	3	1	2	3	1	2	3	1	2	3
$A_{s,1}$	1	1	1	1	1	1	1	1	1	1	1	1
$A_{s,2}$	1	1	1	1	1	1	1	1	1	1	1	1
$A_{s,3}$	1	1	1	1	1	1	-1	-1	-1	-1	-1	-1
$A_{s,4}$	1	1	1	1	1	1	-1	-1	-1	-1	-1	-1
$A_{a,1}$	1	1	1	-1	-1	-1	1	1	1	-1	-1	-1
$A_{a,2}$	1	1	1	-1	-1	-1	1	1	1	-1	-1	-1
$A_{a,3}$	1	1	1	-1	-1	-1	-1	-1	-1	1	1	1
$A_{a,4}$	1	1	1	-1	-1	-1	-1	-1	-1	1	1	1
$B_{s,1}$	1	1	-1	1	1	-1	1	1	-1	1	1	-1
$B_{s,2}$	1	1	-1	1	1	-1	1	1	-1	1	1	-1
$B_{s,3}$	1	1	-1	1	1	-1	-1	-1	1	-1	-1	1
$B_{s,4}$	1	1	-1	1	1	-1	-1	-1	1	-1	-1	1
$B_{a,1}$	1	1	-1	-1	-1	1	1	1	-1	-1	-1	1
$B_{a,2}$	1	1	-1	-1	-1	1	1	1	-1	-1	-1	1
$B_{a,3}$	1	1	-1	-1	-1	1	-1	-1	1	1	1	-1
$B_{a,4}$	1	1	-1	-1	-1	1	-1	-1	1	1	1	-1
$E_{s,1}$	2	-1	0	2	-1	0	2	-1	0	2	-1	0
$E_{s,2}$	2	-1	0	2	-1	0	2	-1	0	2	-1	0
$E_{s,3}$	2	-1	0	2	-1	0	-2	1	0	-2	1	0
$E_{s,4}$	2	-1	0	2	-1	0	-2	1	0	-2	1	0
$E_{a,1}$	2	-1	0	-2	1	0	2	-1	0	-2	1	0
$E_{a,2}$	2	-1	0	-2	1	0	2	-1	0	-2	1	0
$E_{a,3}$	2	-1	0	-2	1	0	-2	1	0	2	-1	0
$E_{a,4}$	2	-1	0	-2	1	0	-2	1	0	2	-1	0

Table 11. Character Table for G_{48} (continued)

G_{48}	(CD)	(CD)(345) (CD)(543)	(CD)(34)* (CD)(45)* (CD)(53)*	(CD)(12)	(CD)(12)(345) (CD)(12)(543)	(CD)(12)(34)* (CD)(12)(45)* (CD)(12)(53)*	(AB)(CD)	(AB)(CD)(345) (AB)(CD)(543)	(AB)(CD)(34)* (AB)(CD)(45)* (AB)(CD)(53)*	(AB)(CD)(12)	(AB)(CD)(12)(345) (AB)(12)(CD)(543)	(AB)(CD)(12)(34)* (AB)(CD)(12)(45)* (AB)(CD)(12)(53)*
	1	2	3	1	2	3	1	2	3	1	2	3
$A_{s,1}$	1	1	1	1	1	1	1	1	1	1	1	1
$A_{s,2}$	-1	-1	-1	-1	-1	-1	-1	-1	-1	-1	-1	-1
$A_{s,3}$	-1	-1	-1	-1	-1	-1	1	1	1	1	1	1
$A_{s,4}$	1	1	1	1	1	1	-1	-1	-1	-1	-1	-1
$A_{a,1}$	1	1	1	-1	-1	-1	1	1	1	-1	-1	-1
$A_{a,2}$	-1	-1	-1	1	1	1	-1	-1	-1	1	1	1
$A_{a,3}$	-1	-1	-1	1	1	1	1	1	1	-1	-1	-1
$A_{a,4}$	1	1	1	-1	-1	-1	-1	-1	-1	1	1	1
$B_{s,1}$	1	1	-1	1	1	-1	1	1	-1	1	1	-1
$B_{s,2}$	-1	-1	1	-1	-1	1	-1	-1	1	-1	-1	1
$B_{s,3}$	-1	-1	1	-1	-1	1	1	1	-1	1	1	-1
$B_{s,4}$	1	1	-1	1	1	-1	-1	-1	1	-1	-1	1
$B_{a,1}$	1	1	-1	-1	-1	1	1	1	-1	-1	-1	1
$B_{a,2}$	-1	-1	1	1	1	-1	-1	-1	1	1	1	-1
$B_{a,3}$	-1	-1	1	1	1	-1	1	1	-1	-1	-1	1
$B_{a,4}$	1	1	-1	-1	-1	1	-1	-1	1	1	1	-1
$E_{s,1}$	2	-1	0	2	-1	0	2	-1	0	2	-1	0
$E_{s,2}$	-2	1	0	-2	1	0	-2	1	0	-2	1	0
$E_{s,3}$	-2	1	0	-2	1	0	2	-1	0	2	-1	0
$E_{s,4}$	2	-1	0	2	-1	0	-2	1	0	-2	1	0
$E_{a,1}$	2	-1	0	-2	1	0	2	-1	0	-2	1	0
$E_{a,2}$	-2	1	0	2	-1	0	-2	1	0	2	-1	0
$E_{a,3}$	-2	1	0	2	-1	0	2	-1	0	-2	1	0
$E_{a,4}$	2	-1	0	-2	1	0	-2	1	0	2	-1	0

CONCLUSIONS

The transitions of the nitrogen inversion mode in aniline and para substituted anilines have been assigned in both the fluorescence excitation and dispersed emission spectra. These assignments are firmly supported by the large deuterium shift, the strong hot band, and the intense second overtone transition of the amino inversion in the excitation spectra of all the aniline molecules. Furthermore, assigned inversional transitions in the excitation spectra are consistent to the even quanta selection rules in the dispersed emission spectra. The potential surfaces of each aniline have been fit using the observed and assigned inversional levels, which have double minima in the ground state and a single minimum in the excited states. This spectroscopic study indicates that the structures of all the aniline molecules are pyramidal in the ground state and planar in the excited state. The inversional levels are very anharmonic in both states.

The NH_2 torsional transition is assigned in the excitation spectrum of each aniline molecule for the first time based on the large deuterium shift observed for this mode. The expectations of the high level of the first quanta and high

barrier in both states are supported by the absence of a strong NH_2 torsional hot band and no resolved tunneling splitting in the NH_2 torsional mode, respectively. The calculated first torsional level in the ground state is above 300 cm-1 for any aniline-like molecule investigated.

The I^2_0 and T^2_0 splittings in the excitation spectrum of p-toluidine are caused by the interaction between the NH_2 and CH_3 groups. The mechanisms of the splittings are explained as the torsion (NH_2) and torsion (CH_3) coupling according to molecular symmetry theory.

The structure of p-amino-p'-methyl-trans-stilbene (PPTS) has been studied by the spectroscopic methods and X-ray diffraction. The nearly planar geometry of the proton donor in the PPTS crystal dimer provides the important fact to predict the structure of gas phase PPTS to be planar in the ground state. The absence of the hot band and I^2_0 in the excitation spectrum of PPTS indicates that the potential surface of PPTS must be a single well in both states, which is consistent with the X-ray result. Methyl torsional levels are affected by the para substitution of NH_2 group in PPTS. The coupling between the methyl and the amino groups is so strong that this occurs even though the groups are separated by ten atoms. The strength of the coupling does not cause them to be separated by ten atoms. The conjugated π-cloud is believed to mediate the interaction. The frequencies of the methyl torsional transitions in PPTS are reduced by over a factor of 2 compared with those in PMTS. It is explained that the electron donating nature of the amino group and the lone

pair in the amino group involving the π-conjugated system makes the methyl rotor released more so that the barrier of the hindered rotation of the methyl group is lowered down.

REFERENCES CITED

1. H. C. longuet-Higgins, Mol. Phys. 6, 445 (1963).

2. P. R. Bunker, "Molecular Symmetry and Spectroscopy" (Academic, New York, 1979).

3. J. T. Hougen and B. M. Dekoven, J. Mol. Spectrosc. 98, 375 (1983).

4. J. C. D. Brand, D. R. Williams, and T. J. Cook, J. Mol. Spectrosc. 20, 359 (1966).

5. M. Quack and M. Stockburger, J. Mol. Spectrosc. 43, 87 (1972).

6. R. A. Kydd and P. J. Krueger, Chem. Phys. Letters 49, 539 (1977).

7. J. C. Evans, Spectrochim. Acta 16, 428 (1960).

8. J. M. Hollas, M. R. Howson, T. Ridley, and L. Halonen, Chem. Phys. Letters 98, 611 (1983).

9. J. Lemaire, I. Dimicoli, F. Piuzzi, and R. Botter, Chem. Phys. 115, 119 (1987) (Noth-Holland).

10. M. A. Smith, J. W. Hager, and S. C. Wallace, J. Chem. Phys. 80, 3097 (1984).

11. Z. Niu, K. M. Dunn, and J. E. Boggs, Mol. Phys. 55, 421 (1985).

12. N. W. Larsen, E. L. Hansen, and F. M. Nicolaisen, Chem. Phys. Letters 43, 584 (1976).

13. N. Mikami, A. Hiraya, I. Fujiwara, and M. Ito, Chem. Phys. Letters 74, 531 (1980).

14. J. G. Philis and L. Goodman, Spectrochim. Acta 45A, 561 (1989).

15. J. Murakami, K. Kaya, and M. Ito, Chem. Phys. Letters 91, 401 (1982).

16. A. R. Bacon and J. M. Hollas, Faraday Discuss. Chem. Soc. 86, 129 (1988).

17. R. A. Kydd and P. J. Krueger, J. Chem. Phys. 72, 280 (1980).

18. N. Alasbegovic, L. Colombo, and P. Bleckmann, J. Raman Spec. 6, 92 (1977).

19. D. E. Powers, J. B. Hopkins, and R. E. Smalley, J. Chem. Phys. 72, 5721 (1980).

20. R. A. Kydd and S. Mah, Spectrochim. Acta 38A, 1031 (1982).

21. R. Tembereull, T. M. Dunn, and D. M. Lubman, Spectrochim. Acta 42A, 899 (1986).

22. G. L. Carlson and W. G. Fateley, J. Phys. Chem. 81, 2308 (1977).

23. S. Yan and L. H. Spangler, J. Chem. Phys. 96, 4106 (1992).

24. J. Christoffersen, J. M. Hollas, and G. H. Kirby, Mol. Phys. 16, 441 (1969).

25. J. A. Draeger, Spectrochim. Acta 41A, 607 (1985).

26. J. B. Lambert, R. J, Nienhuls, and R. B. Finzel, J. Phys. Chem. 85, 1170 (1981).

27. M. Ito, J. Phys. Chem. 91, 517 (1987).

28. P. J. Breen, J. A. Warren, and E. R. Bernstein, J. Chem. Phys. 87, 1927 (1987).

29. W. J. Hehre, L. Radom, and J. A. Pople, J. Am. Chem. Soci. 94, 1496 (1972).

30. L. H. Spangler, W. B. Bosma, R. D. van Zee, and T. S. Zwier, J. Chem. Phys. 88, 6768 (1988).

31. Z. Q. Zhao, C. S. Parmenter, D. B. Moss, A. J. Bradley, A. E. W. Knight, and K. G. Owens, J. Chem. Phys. 96, 6362 (1992).

32. D. M. Sammeth, S. S. Siewert, P. R. Callis, and L. H. Spangler, J. Phys. Chem. 96, 5771 (1992).

33. P. J. Breen, E. R. Bernstein, and J. I. Seeman, J. Chem. Phys. 87, 3269 (1987).

34. A. E. Dorigo, D. W. Pratt, and K. N. Houk, J. Am. Chem. Soci. 109, 6591 (1987).

35. T. Urano, M. Maegawa, K. Yamanouchi, and S. Tsuchiya, J. Phys. Chem. 93, 3459 (1989).

36. Z. Meić and H. Güsten, Spectrochim. Acta 34A, 101 (1987).

37. T. Urano, H. Hamaguchi, M Tasumi, K. Yamanouchi, S. Tsuchiya, and T. L. Gustafson, J. Chem. Phys. 91, 3884 (1989).

38. J. A. Syage, W. R. Lambert, P. M. Felker, A. H. Zewail, and R. M. Hochstrasser, Chem. Phys. Letters 88, 266 (1982).

39. T. J. Majors, U. Even, and J. Jortner, J. Chem. Phys. 81, 2330 (1984).

40. T. Urano, H. Hamaguchi, M. Tasumi, K. Yamanouchi, and S. Tsuchiya, Chem. Phys. Letters. 137, 559 (1987).

41. A. Warshel, J. Chem. Phys. 62, 214 (1975).

42. J. A. Syage, P. M. Felker, and A. H. Zewail, J. Chem. Phys. 81, 4685 (1984).

43. J. A. Syage, P. M. Felker, and A. H. Zewail, J. Chem. Phys. 81, 4706 (1984).

44. L. H. Spangler, R. van Zee, and T. S. Zwier, J. Phys. Chem. 91, 2782 (1987).

45. T. Suzuki, N. Mikami, and M. Ito, J. Phys. Chem. 90, 6431 (1986).

46. C. A. Taatjes, W. B. Bosma, and T. S. Zwier, Chem. Phys. Letters 128, 127 (1986).

47. T. S. Zwier, E. Carrasquillo M, and D. H. Levy, J. Chem. Phys. 78, 5493 (1983).

48. D. O. Dehaan and T. S. Zwier, J. Chem. Phys. 90, 1460 (1989).

49. E. B. Wilson, J. C. Decius, and P. C. Cross, "Molecular Vibrations" (McGraw-Hill, New York, 1955).

50. G. Varsanyi D. Sc.," Assignments for Vibrational Spectra of Seven Hundred Benzene Derivatives" (John Wiley & Sons, New York, 1974).

51. J. T. Meek, E. Sekreta, W. Wilson, K. S. Viswanathan, and J. P. Reilly, J. Chem. Phys. 82, 1741 (1985).

52. H. D. Durst and G. W. Gokel, "Experimental Organic Chemistry" (McGraw-Hill Book Company,1980).

53. G. D. Hartman, W. Halczeko, and B. T. Phillips, J. Org. Chem. 51, 142 (1986).

54. J. D. Lewis, T. B. Malloy, Jr., T. H. Chao, and J. Laane, J. Mol. Struct. 12, 427 (1972).

55. M. Fukuyo, K. Hirotsu, and T. Higuchi, Acta Cryst. B38, 640 (1982).